
Chern-Simons Gravity and Fermions in Axion-SU(2) Gauge Field Models of Inflation

Leila Mirzagholi



München 2020

Chern-Simons Gravity and Fermions in Axion-SU(2) Gauge Field Models of Inflation

Leila Mirzagholi

Dissertation
an der Fakultät für Physik
der Ludwig-Maximilians-Universität
München

vorgelegt von
Leila Mirzagholi
aus Teheran, Iran

München, den 31 August 2020

Erstgutachter: Prof. Dr. Eiichiro Komatsu

Zweitgutachter: Prof. Dr. Stefan Hofmann

Tag der mündlichen Prüfung: 28 Oktober 2020

Contents

Zusammenfassung	xi
Abstract	xiii
Conventions	xv
1 Introduction	1
1.1 Single Scalar Field Inflation	2
1.1.1 Cosmological Perturbations	3
1.1.1.1 Perturbations in General Relativity	3
1.1.1.2 Quantum Fluctuations	6
1.2 Alternatives to Single Scalar Field Inflation	11
2 Axion-SU(2) Gauge Fields Models of Inflation	15
2.1 Historical Development	15
2.2 Chromo-Natural Inflation	16
2.2.1 Inflationary Dynamics	17
2.3 Perturbations of CNI	22
2.3.1 Degrees of Freedom of CNI	22
2.3.2 Quantization and Power Spectrum	24
2.3.3 Scalar Fluctuations	25
2.3.4 Tensor Fluctuations	27
2.3.5 Observational Constraints	28
2.4 Relation to Gauge-flation	30
2.5 The case with U(1)	30
2.6 Mimetic Chern-Simons SU(2)	33
2.7 Axion-SU(2) Gauge Field Spectator Sector	35
2.7.1 Perturbations of Axion-SU(2) Spectator Sector	37
2.8 Signatures and Bonuses	38
2.8.1 Chiral Gravitational Waves	39
2.8.2 Gravitational Leptogenesis	42
2.8.3 Tensor non-Gaussianity	44

3	Effects of Gravitational Chern-Simons during Axion-SU(2) Inflation	47
3.1	Introduction	47
3.2	Model Setup and Introduction	48
3.2.1	Action	48
3.2.2	Background Evolution	49
3.3	Tensor Perturbations	50
3.3.1	Without $F\tilde{F}$	53
3.3.2	With $F\tilde{F}$	53
3.4	Stability Analysis	54
3.5	Discussion	55
4	Fermions Production and Backreaction from Axion-SU(2) Gauge Fields	61
4.1	Introduction	61
4.2	Fermions in Axion-SU(2) Gauge Field Inflation	62
4.3	Fermion Production	66
4.3.1	Ψ^+ Spinors	66
4.3.2	Quantization of the S_+ fermions	68
4.3.3	S_+ Hamiltonian	69
4.3.4	Ψ^- Spinors	74
4.3.5	Quantization of the S_- fermions	75
4.3.6	S_- Hamiltonian	76
4.4	Backreactions	78
4.4.1	VEVs of Quadratic Fermionic Operators	79
4.4.2	Backreaction on the SU(2) Background	82
4.4.3	Backreaction on the Axion Background	84
4.4.4	Parameter Space of a Model	85
4.5	Discussion	86
5	Summary and Outlook	93
A	Spinor Covariant Derivative	95
B	Whittaker Functions	97
	Acknowledgement	109

List of Figures

1.1	The polarizations of gravitational waves	9
1.2	Current constraints on n_s and r	10
2.1	The region of field space over which the axion ranges during the inflationary period	21
2.2	The evolution of the gauge field during the inflationary period	22
2.3	The right- and left-handed helicity gauge tensor	28
2.4	Comparison of the tensor-to-scalar ratio, r and the spectral index, n_s in CNI	29
2.5	The trajectories of gauge-flation and CNI	31
2.6	The inflationary field configuration of mimetic Chern-Simons SU(2)	34
2.7	Various components of ϵ_H	38
2.8	The sourced right- and left-handed linear gravitational wave	41
2.9	The gravitational waves power spectrum	42
2.10	The integrand of (2.132)	44
2.11	Feynman diagrams of the tree-level contributions from the cubic interactions to the bispectrum of gravitational waves	45
3.1	The sourced right-handed helicity mode function of gravitational waves	52
3.2	The right- and left-handed helicity mode functions of gravitational waves for different values of ξ_2	57
3.3	Same as the right panel of Figure 3.1 but for $\xi_2 = 4.5 \times 10^{-3}$	58
3.4	The right-handed helicity mode functions for four different cases: $F\tilde{F}$ and $R\tilde{R}$, without $R\tilde{R}$, without $F\tilde{F}$, and without both terms for different values of ξ_2	59
4.1	The Bogoliubov coefficients $ \beta_{s,k}(\tau) ^2$	73
4.2	The expectation values of the backreaction currents of the + and -	82
4.3	The energy density fraction of the gauge field ϵ_B as a function of the effective mass of the gauge field	88
4.4	Same as Fig. 4.3, but for $m = 10H$ and $\xi_\varphi = 10$	89
4.5	Same as Fig. 4.3, but for $m = 10H$ and $\xi_\varphi = 1$	90
4.6	Same as Fig. 4.3, but for $m = H$ and $\xi_\varphi = 10$	91

List of Tables

2.1	U(1) gauge field versus SU(2) gauge field	32
2.2	Gravitational waves from vacuum versus axion-SU(2) gauge field	39

Zusammenfassung

Die vorliegende Dissertation präsentiert zwei wichtige Konsistenztests eines Modells für die kosmologische Inflation, nämlich das Axion-SU(2)-Eichfeldmodell. Dieses Modell umfasst besagtes Eichfeld, welches mittels seiner drei Komponenten einen homogenen und isotropen Hintergrund erzeugt, sowie via eines Chern-Simons-Terms an ein Axionfeld gekoppelt ist. Das SU(2)-Eichfeldmodell zeichnet sich durch drei charakteristische Vorhersagen für die Gravitationswellen aus, die während der Inflationsepoche erzeugt werden: sie können von der Skaleninvarianz abweichen, nicht-Gaussisch und zirkular polarisiert sein. Alle drei Eigenschaften treten in den kanonischen Inflationsmodellen, die nur ein aktives Feld enthalten, nicht auf.

Bevor dieses Szenario ernsthaft als eine mögliche Phase im frühen Universum in Betracht kommt, muss dessen theoretische Konsistenz bewiesen werden. Zu diesem Zweck untersuche ich zuerst Modelle, in denen das Axionfeld sowohl gravitativ als auch an die Eichfelder, durch jeweilige Chern-Simon Terme, gekoppelt ist. Beide Terme manifestieren dieselbe zugrundeliegende Physik, und sollten daher immer beide berücksichtigt werden. Darüberhinaus muss die Möglichkeit überprüft werden, dass der gravitative Chern-Simons Term *Ghost*-Instabilitäten erzeugt (d.h. Felder, die instabil sind). Neben der Existenz eines stabilen Bereichs im Parameterraum zeigen meine Resultate, dass diese Kopplungsterme die Amplitude der erzeugten Gravitationswellen um bis zu 50% ändern können. Sie zeigen weiterhin, wie der freie Kopplungsparameter des gravitativen Chern-Simons Terms durch Beobachtungen eingeschränkt werden kann.

Im zweiten Teil studiere ich die Teilchenproduktion, die durch eine Kopplung des SU(2)-Eichfeld mit einem massiven Dirac-Fermionen-Dublett erzeugt wird. Die Motivation dafür ist, dass eine Kopplung des Inflatonfeldes mit Materiefeldern im Allgemeinen zu Teilchenproduktion führt. Dies kann unter Umständen zu einer Rückreaktion führen, die den homogenen Hintergrund der Eichfeldkomponenten destabilisiert und damit zu einem frühen Ende der Inflationsepoche führt. Die Kopplung an Fermionen führt zu einer nichttrivialen Kopplung zwischen den verschiedenen Flavor- und Chiralitätskomponenten, und zu einer wesentlichen Komplizierung der zu lösenden Gleichungen. Um eine Lösung zu ermöglichen, habe ich die existierenden Lösungsansätze in zwei Punkten verbessert. Erstens werden die Operatoren antisymmetrisiert, was eine Gleichbehandlung von Teilchen und Antiteilchen ermöglicht. Zweitens habe ich das Konzept der instantanen Vakuumsabtraktion erweitert, um auftretende UV-Divergenzen zu behandeln.

Die hier präsentierten Studien zeigen, dass der kosmologische Hintergrund und somit

die Inflationsepoche im $SU(2)$ -Eichfeldmodell stabil bleibt, auch wenn beide Chern-Simons Kopplungsterme sowie eine Kopplung an massive Dirac-Fermionen zugelassen werden.

Abstract

In this thesis, we present two important consistency checks on axion-SU(2) gauge field model of inflation. Axion-SU(2) gauge field models of inflation consist of an SU(2) gauge field in an isotropic and homogeneous background, coupled to an axion field via a Chern-Simons term. This setup can source gravitational waves that come equipped with three distinctive features: they can be non-scale invariant, highly non-Gaussian, and circularly polarized. These features are unique and are not shared by canonical single scalar field inflation models.

However, before such models can be taken seriously as feasible description of the early universe evolution, their theoretical consistency within established empirically possible settings, need to be asserted.

With this goal in mind, we first examined the viability of inflation models with a spectator axion field coupled to both gravitational and SU(2) gauge fields via Chern-Simons couplings. Both parity-violating terms, i.e. gravitational Chern-Simons, and the other Chern-Simons term arise from the same underlying physics and exist simultaneously; hence they should be both treated on equal footing. Moreover, given that gravitational Chern-Simons terms may introduce ghost instabilities in the model, it is crucial to check the stability of the setup as well. As a result of this study, we found that the impact of these terms on the production and propagation of gravitational waves can be as large as a fifty percent enhancement. Moreover, using the phenomenological success of the axion-SU(2) sector, we can constrain the new free parameter, i.e. the coupling strength of the gravitational Chern-Simons term, in this setup.

In the second study, we examined the particle production by a SU(2) gauge field coupled to a massive Dirac doublet. The reason for coupling these fields is that usually, couplings to other matter species can lead to particle production, which in turn induces backreaction on and destabilization of the stable, isotropic, and homogeneous configuration that the non-Abelian and axion backgrounds have during inflation. This coupling leads to a nontrivial mixing between fermion components of different flavors and chirality, hence complicates the system of equations. To carry out the needed calculation we made two technical improvements compared to extant literature. First, we applied the antisymmetrization of the operators to treat particles and antiparticles on equal footing. Second, to deal with the UV divergences, we extended the idea of an existing instantaneous vacuum subtraction scheme.

On the basis of both of these investigations, we conclude that the background dynamics

of an axion-SU(2) sector remains unaffected and phenomenologically viable in the presence of the gravitational Chern-Simons term and massive fermions.

Conventions

- We use natural units in which $\hbar = c = k_B = \epsilon_0 = 1$ and the reduced Planck mass is given by $M_{pl} = 1/\sqrt{8\pi G}$.
- Greek indices μ, ν , etc. go over the four spacetime coordinates $x^\mu = [x^0, x^1, x^2, x^3]^T$ where x^0 represents the time coordinate. Latin indices i, j , etc. go over the three spatial coordinates.
- The Minkowski metric is given by the $\eta_{\mu\nu} = \text{diag}[-1, 1, 1, 1]$.
- Summation over repeated indices is assumed unless otherwise stated.

Chapter 1

Introduction

Inflation [1, 2, 3, 3, 4] provides us with a paradigm to explain the flatness and horizon problems of the early universe and it also explains the observations of the cosmic microwave background (CMB) to a great degree. In its original form, inflation utilized expansion of spacetime through a scalar field slowly rolling on a flat potential, following a graceful exit from the period of accelerated expansion.

A crucial aspect of inflation that makes it very successful, is that it provides a natural setup to create the initial conditions necessary for the Hot Big Bang model. More specifically, and from a physical point of view, the inflaton field that is responsible for the expansion of spacetime dominates the energy density content of the universe during this period and governs the end of inflation by setting how much expansion needs to happen. On the other hand, Heisenberg's uncertainty principle states that precise timing is not possible in quantum mechanics, hence the inflaton has to have spatially varying fluctuations that differ in expansion. The so-called quantum vacuum fluctuations during inflation generate the scalar and tensor perturbations. The scalar perturbations [5, 6, 7, 8] seed the observed large scale structure in the universe. The scalar fluctuations have been detected in the CMB experiments, while the tensor perturbations [9, 10] originating in the early universe have not yet been detected.

It is relatively easy to build phenomenological mechanisms that provide us with an early time accelerated expansion. Some properties of these models have been constrained by CMB experiments to some extent, but much remains to be done. The CMB experiments have constrained the properties of scalar fluctuations, but primordial tensor fluctuations, which are a common feature in all inflationary models, and therefore are bound to shed light on the microphysics of inflation and further constrain the models, remain to be detected. To see the importance and the difficulty of this task, note that it is very unlikely for the current colliders to reach the energy levels present at the very early stages of the universe. Consequently, detection of the stochastic background of gravitational waves may be our only chance currently to probe such high energies.

Before discussing the main contributions of this thesis, we first lay out the basics of single-field slow-roll inflation as a standard example, and point out the properties of scalar and tensor fluctuations in a general setup.

1.1 Single Scalar Field Inflation

Let us consider a scalar field $\varphi(t, \mathbf{x})$ as the inflaton. We can write this field as the background value and some perturbations around the background value: $\varphi(t, \mathbf{x}) = \bar{\varphi}(t) + \delta\varphi(t, \mathbf{x})$. Assuming a potential $V(\varphi)$ for the scalar field, we can write the inflation action as

$$S = \int d^4x \sqrt{-g} \left[\frac{M_{pl}^2}{2} R - \frac{1}{2} (\partial\varphi)^2 - V(\varphi) \right], \quad (1.1)$$

where R is the Ricci scalar and g is the determinant of the metric.

We can write the equations of motion for the background, which is a Klein-Gordon equation for a time-dependent scalar field in an expanding universe

$$\ddot{\bar{\varphi}} + 3H\dot{\bar{\varphi}} + V_{,\varphi} = 0, \quad (1.2)$$

where $V_{,\varphi} \equiv \partial V / \partial \bar{\varphi}$ and $H = \dot{a}/a$ is the Hubble expansion rate. This equation resembles a damped harmonic oscillator with H as the damping term. In other words, the expansion of the universe acts as a “frictional” force acting against the force created by the potential of the field.

Let us now determine under what conditions (1.2) leads to an inflationary period. There are two conditions that need to be met, first, an accelerated phase of expansion with a slowly varying Hubble parameter that is approximately de Sitter. Note that reaching an exact de Sitter expansion fails to explain observed features of the universe. Second, this period of acceleration must last for sufficient time so that inflation solves the standard cosmological model problems.

To clarify these points, we define two important parameters: ϵ_H and η . The first slow-roll parameter is defined as

$$\epsilon_H \equiv -\frac{\dot{H}}{H^2} = -\frac{d \ln H}{dN} < 1, \quad (1.3)$$

where $dN \equiv d \ln a = H dt$ measures the number of e-folds N in the inflationary expansion, in other words N is the number of Hubble times passed. Consequently, the energy density of the fluid representation of this expansion must have constant energy density and a negative equation of state.

The second important condition for the inflationary period is that to solve the horizon problem we need the inflationary expansion to last long enough, $N \sim 40 - 60$ e-folds. In other words we need ϵ_H to stay small for a long period of time, we have parametrised this quantity in η

$$\eta \equiv \frac{d \ln \epsilon_H}{dN} = \frac{\dot{\epsilon}_H}{H \epsilon_H}. \quad (1.4)$$

Successful inflation means we have $\epsilon_H < 1$ and $|\eta| < 1$.

Let us now go back to the toy model we defined above and see how to impose these conditions for ϵ_H and η in a single scalar field setup.

In scalar single field inflation we have

$$\epsilon_H = \frac{\dot{\varphi}^2}{2M_{pl}^2 H^2}, \quad \eta = 2(\epsilon_H - \delta), \quad (1.5)$$

where $\delta \equiv -\ddot{\varphi}/(H\dot{\varphi})$ is the dimensionless acceleration per Hubble time. Hence, inflation happens and lasts long enough if $\epsilon_H, |\delta| \ll 1$ which leads to $\epsilon_H, |\eta| \ll 1$.

We use a technique called the slow-roll approximation many times in this thesis, so it is best to define it right here. By slow-roll we mean that the kinetic energy is sub-dominant to the potential energy, in other words $1/2\dot{\varphi}^2 \ll V(\varphi)$ where we have dropped the second time derivatives. So $|\delta| \ll 1$ will lead to a simplification of the Klein-Gordon equation to $3H\dot{\varphi} \approx -V_{,\varphi}$.

In order to make sure that we can get inflation with a given potential $V(\varphi)$ in the single scalar field model, we have to make sure that $\epsilon_\varphi, |\eta_\varphi| \ll 1$ is satisfied, where

$$\epsilon_\varphi \equiv \frac{M_{pl}^2}{2} \left(\frac{V_{,\varphi}}{V} \right)^2, \quad |\eta_\varphi| \equiv M_{pl}^2 \frac{|V_{,\varphi\varphi}|}{V}. \quad (1.6)$$

1.1.1 Cosmological Perturbations

In this section we take a brief detour on how scalar and tensor fluctuations behave in an accelerated universe following [11, 12, 13, 14, 15].

1.1.1.1 Perturbations in General Relativity

We begin by perturbing the metric and the energy momentum tensors about their backgrounds

$$g_{\mu\nu}(x^\alpha) = \bar{g}_{\mu\nu}(t) + \delta g_{\mu\nu}(x^\alpha), \quad T_{\mu\nu}(x^\alpha) = \bar{T}_{\mu\nu}(t) + \delta T_{\mu\nu}(x^\alpha), \quad (1.7)$$

where $\bar{g}_{\mu\nu}(t)$ is the Friedmann-Lemaître-Robertson-Walker (FLRW) metric. The non-zero components of $\bar{T}_{\mu\nu}(t)$ are $\bar{T}^{00}(t) = \bar{\rho}(t)$ and $\bar{T}^{ij}(t) = -\bar{p}(t)\delta^{ij}a^{-2}(t)$ for a perfect fluid in the absence of anisotropic stress at the linear order.

It is more convenient to rewrite the energy-momentum tensor in the covariant perfect fluid form

$$\bar{T}_{\mu\nu}(t) = (\bar{\rho} + \bar{p})\bar{u}_\mu\bar{u}_\nu - \bar{g}_{\mu\nu}\bar{p}, \quad (1.8)$$

where $\bar{u}^\mu(t) = (1, 0, 0, 0)^T$ is the normalized 4-velocity vector of a comoving observer. In the perturbed spacetime, the energy momentum can be written in a more general form

$$T_{\mu\nu}(x^\alpha) = [\rho(x^\alpha) + p(x^\alpha)]u_\mu(x^\alpha)u_\nu(x^\alpha) - g_{\mu\nu}(x^\alpha)p(x^\alpha) + \Pi_{\mu\nu}(x^\alpha), \quad (1.9)$$

where in addition to the perfect fluid terms, we have the anisotropic stress tensor, $\Pi_{\mu\nu}$, for which [16]

$$\begin{aligned} \Pi_{0\mu} &= 0, & \Pi_{ij} &= a^2 [\partial_i \partial_j \pi^S + \partial_i \pi_j^V + \partial_j \pi_i^V + \pi_{ij}^T], \\ \delta_{ij} \partial_i \pi_j^V &= 0, & \delta_{ij} \partial_i \pi_{jk}^T &= 0, & \delta_{ij} \pi_{ij}^T &= 0. \end{aligned} \quad (1.10)$$

The quantities π^S , π_i^V and π_{ij}^T are the scalar, divergence-free vector and transverse-traceless tensor anisotropic inertia terms, respectively, characterising (small) departures from the perfect fluid form of the energy-momentum tensor.

We now write out the perturbations $\delta g_{\mu\nu}(x^\alpha)$ and $\delta T_{\mu\nu}(x^\alpha)$. The perturbed metric can be written in conformal time, $d\tau \equiv dt/a(t)$ as

$$\begin{aligned} ds^2 &= (\bar{g}_{\mu\nu} + \delta g_{\mu\nu}) dx^\mu dx^\nu \\ &= -(1 - 2\phi) a^2(\tau) d\tau^2 + 2(\partial_i B + B_i) a^2(\tau) dx^i d\tau \\ &\quad + [(1 + 2\psi) \delta_{ij} - 2\partial_i \partial_j E - \partial_j E_i - \partial_i E_j - \tilde{h}_{ij}] a^2(\tau) dx^i dx^j. \end{aligned} \quad (1.11)$$

where $\phi(x^\sigma)$, $B(x^\sigma)$, $\psi(x^\sigma)$, $E(x^\sigma)$ are the scalar metric perturbations, $B_i(x^\sigma)$, $E_i(x^\sigma)$ are the divergence-free 3-vector metric perturbations, and $\tilde{h}_{ij}(x^\sigma)$ is the traceless transverse 3-tensor metric perturbation (i.e., the one describing the gravitational waves).

As mentioned we can decompose the above perturbations into a irreducible set of modes: the scalar, vector and tensor modes which is known as the SVT decomposition. The SVT decomposition is useful since at linear level, the Einstein equation for each mode is decoupled from the others and we can treat their evolution separately.

We then perturb the energy density, pressure and 4-velocity fields

$$\rho(x^\alpha) = \bar{\rho}(\tau) + \delta\rho(x^\alpha), \quad p(x^\alpha) = \bar{p}(\tau) + \delta p(x^\alpha), \quad u_\mu(x^\alpha) = \bar{u}_\mu(\tau) + \delta u_\mu(x^\alpha), \quad (1.12)$$

where

$$\bar{u}_\mu = (a, 0, 0, 0)^T, \quad \delta u_\mu \equiv (\delta u_0, \partial_i \delta u^\parallel + \delta u_i^\perp)^T, \quad (1.13)$$

and $\partial_i u_i^\perp = 0$. Since the 4-velocity vector is normalized,

$$\bar{g}_{\mu\nu} \bar{u}^\mu \bar{u}^\nu = 1, \quad g_{\mu\nu} u^\mu u^\nu = 1, \quad (1.14)$$

we can show that to linear order in perturbations $\delta u_0 = a\phi$. We also find $u^\mu = a^{-1}(1 - \phi, -a^{-1}\partial_i \delta u^\parallel - a^{-1}\delta u_i^\perp - \partial_i B - B_i)^T$, to leading order in the perturbations. The perturbed energy momentum tensor then takes the following form

$$\begin{aligned} \delta T^\mu{}_\nu &= (\delta\rho + \delta p) \bar{u}^\mu \bar{u}_\nu - \delta p \delta_\nu^\mu + (\bar{\rho} + \bar{p}) \bar{u}^\mu \delta u_\nu + (\bar{\rho} + \bar{p}) \delta u^\mu \bar{u}_\nu + \bar{g}^{\mu\gamma} \Pi_{\gamma\nu}, \\ \delta T^0{}_0 &= \delta\rho, \quad \delta T^0{}_i = (\bar{\rho} + \bar{p}) a^{-1} (\partial_i \delta u^\parallel + \delta u_i^\perp), \\ \delta T^i{}_0 &= -(\bar{\rho} + \bar{p}) a^{-1} (a^{-1} \partial_i \delta u^\parallel + a^{-1} \delta u_i^\perp + \partial_i B + B_i), \\ \delta T^i{}_j &= -\delta p \delta_{ij} - \partial_i \partial_j \pi^S - \partial_i \pi_j^V - \partial_j \pi_i^V - \pi_{ij}^T. \end{aligned} \quad (1.15)$$

After decomposing the perturbations into scalars, divergence-free vectors and traceless transverse tensors, we can now review their transformations under infinitesimal diffeomorphisms

$$x^\mu \rightarrow x'^\mu = x^\mu + \xi^\mu(x^\alpha), \quad (1.16)$$

where $\xi^\mu = (\xi^0, \partial_i \xi^\parallel + \xi_i^\perp)^T$. Since under the diffeomorphisms the metric transforms as

$$g'_{\mu\nu}(x'^\alpha) = \frac{\partial x^\beta}{\partial x'^\mu} \frac{\partial x^\gamma}{\partial x'^\nu} g_{\beta\gamma}(x^\alpha), \quad (1.17)$$

then to leading order the metric perturbations (at x^α) change by

$$\begin{aligned}\Delta\delta g_{\mu\nu}(x^\alpha) &\equiv \delta g'_{\mu\nu}(x^\alpha) - \delta g_{\mu\nu}(x^\alpha) = g'_{\mu\nu}(x^\alpha) - g_{\mu\nu}(x^\alpha) \\ &\approx g'_{\mu\nu}(x'^\alpha) - \frac{\partial g_{\mu\nu}}{\partial x^\beta} \xi^\beta - g_{\mu\nu}(x^\alpha) \\ &\approx -\bar{g}_{\beta\nu}(x^\alpha) \frac{\partial \xi^\beta}{\partial x^\mu} - \bar{g}_{\mu\beta}(x^\alpha) \frac{\partial \xi^\beta}{\partial x^\nu} - \frac{\partial \bar{g}_{\mu\nu}(x^\alpha)}{\partial x^\beta} \xi^\beta.\end{aligned}\quad (1.18)$$

and

$$\Delta\delta T^\mu{}_\nu(x^\alpha) \approx \bar{T}^\beta{}_\nu(x^\alpha) \frac{\partial \xi^\mu}{\partial x^\beta} - \bar{T}^\mu{}_\beta(x^\alpha) \frac{\partial \xi^\beta}{\partial x^\nu} - \frac{\partial \bar{T}^\mu{}_\nu(x^\alpha)}{\partial x^\beta} \xi^\beta. \quad (1.19)$$

The gravitational waves, \tilde{h}_{ij} , are diff-invariant, but the scalar and vector modes exhibit a gauge ambiguity that have no physical importance. To avoid this gauge redundancy, it is important to adopt a gauge invariant description where we construct gauge invariant quantities independent of ξ^μ , the Bardeen variables

$$\begin{aligned}\Phi &= \phi - \frac{1}{a} \partial_\tau [a(B - \partial_\tau E)], \\ \Psi &= \psi + \mathcal{H}(B - \partial_\tau E),\end{aligned}\quad (1.20)$$

where $\mathcal{H} \equiv a'/a$ is the comoving Hubble parameter. Another gauge invariant quantity that will be used frequently is the so-called comoving curvature perturbation

$$\mathcal{R} \equiv \psi + \frac{\mathcal{H}}{a} \delta u^\parallel. \quad (1.21)$$

This quantity is conserved for long wavelength perturbations, bigger than the Hubble radius.

We can also solve the gauge redundancy problem by fixing a gauge. This amounts to imposing conditions to fix the number of variables that are redundant. The most used gauges in cosmology are the Newtonian, synchronous and spatially flat gauge:

- *Newtonian or longitudinal gauge:*

$$B = 0, \quad E = 0, \quad (1.22)$$

where in terms of Bardeen variables this translates to

$$\Phi = \phi, \quad \Psi = \psi. \quad (1.23)$$

- *Synchronous gauge:*

$$\phi = 0, \quad B = 0. \quad (1.24)$$

- *Spatially flat gauge:*

$$\Phi = B = 0. \quad (1.25)$$

1.1.1.2 Quantum Fluctuations

As discussed above, during inflation, quantum fluctuations are generated. These fluctuations consist of scalar, vector and tensor perturbations and understanding the features of these perturbations can allow us to constrain our models using observational data. To achieve this, we need to treat inflation from a semiclassical point of view. In this part we study the scalar and tensor fluctuations first, then, the next step is to study their key features. To track the features of the primordial fluctuations, we use the following important tools: (i) the scalar and tensor power spectra, $\mathcal{P}_{\mathcal{R}}$ and \mathcal{P}_h respectively, (ii) the scalar and tensor spectral indices n_s and n_t , (iii) the tensor-to-scalar ratio r , and (iv) non-Gaussianity of scalar or tensor perturbations.

Scalar Fluctuations

Now we consider the metric perturbations in the so-called ADM formalism [17]

$$ds^2 = -N^2 dt^2 + h_{ij}(N^i dt + dx^i)(N^j dt + dx^j), \quad (1.26)$$

where $N \equiv N(t, x)$ is the lapse function, $N^i \equiv N^i(t, x)$ is the shift function and h_{ij} is the induced metric on three-dimensional hypersurfaces of constant time t . The spatial slices are characterized by the intrinsic curvature $R_{ij}^{(3)}$ and the extrinsic curvature

$$K_{ij} \equiv \frac{1}{2N}(h'_{ij} - \nabla_i N_j - \nabla_j N_i). \quad (1.27)$$

After writing the inflaton action given in (1.1) using the formalism above we fix the gauge to the spatially flat gauge and continue our calculations. This gauge is very convenient since it simplifies the computation of the curvature perturbations, that are linked to the density perturbations that seeded the structures of our universe. In the spatially flat gauge, the diff-invariant comoving curvature perturbation is given by

$$\mathcal{R} \equiv \frac{\mathcal{H}}{\phi'} \delta\varphi. \quad (1.28)$$

Expanding the (1.1) in second order and after some integration by parts, we find

$$S_2 = \int \frac{1}{2} d\tau d^3x a^3 \left[(\delta\varphi')^2 - \frac{1}{a^2} (\partial\delta\varphi)^2 - \left[V'' - 2(3\epsilon - \epsilon^2 + \epsilon\eta)H^2 \right] \delta\varphi^2 \right]. \quad (1.29)$$

Therefore, the equations of motion for the Fourier components of the canonically normalized field $\nu \equiv a\delta\varphi$ is

$$\ddot{\nu}_k + \left[k^2 + a^2(V'' - 6\epsilon H^2) - \frac{\ddot{a}}{a} \right] \nu_k = 0, \quad (1.30)$$

where we have dropped terms in the effective mass that are higher order in slow-roll parameters.

With the quadratic action in hand, we can proceed to the canonical quantization of this system

$$\hat{\nu}(\tau, \mathbf{x}) = \int \frac{d^3k}{(2\pi)^{3/2}} \left[u_k(\tau) \hat{a}_{\mathbf{k}} e^{i\mathbf{k}\cdot\mathbf{x}} + u_k^*(\tau) \hat{a}_{-\mathbf{k}}^\dagger e^{-i\mathbf{k}\cdot\mathbf{x}} \right], \quad (1.31)$$

where the u_k are the mode functions and $\hat{a}_{\mathbf{k}}$ and $\hat{a}_{-\mathbf{k}}^\dagger$ are the annihilation and creation operators satisfying the commutation relations

$$[\hat{a}_{\mathbf{k}}, \hat{a}_{\mathbf{q}}^\dagger] = \delta^{(3)}(\mathbf{k} - \mathbf{q}), \quad [\hat{a}_{\mathbf{k}}, \hat{a}_{\mathbf{q}}] = 0, \quad (1.32)$$

considering the normalisation of the mode functions $u_k u_k' - u_k' u_k^* \equiv i$. We can write the momentum conjugate to the canonically normalized field ν as

$$\pi \equiv \frac{\partial \mathcal{L}}{\partial \dot{\nu}} \quad (1.33)$$

and promote the field $\pi(\tau, \mathbf{x})$ to a quantum operator as well $\hat{\pi}(\tau, \mathbf{x})$. The operators we defined satisfy the equal time commutation relation

$$[\hat{\nu}(\tau, \mathbf{x}), \hat{\pi}(\tau, \mathbf{x}')] = i\delta(\mathbf{x} - \mathbf{x}'). \quad (1.34)$$

We can set the initial conditions for our solutions by choosing the lowest energy state of the fluctuations. The quantum states in the Hilbert space are constructed by defining the vacuum state $|0\rangle$

$$\hat{a}_k |0\rangle = 0. \quad (1.35)$$

Power Spectrum

To compare the perturbations produced during inflation with the observations we need to evaluate the power spectrum which is essentially the two point correlation function of the canonical variables. The power spectrum of \mathcal{R} is given by

$$\mathcal{P}_{\mathcal{R}}(k) = \left(\frac{\mathcal{H}}{\phi'} \right)^2 \left(\frac{H}{2\pi} \right)^2, \quad (1.36)$$

evaluated at horizon crossing $k = aH$.

Given the weak scale dependence of the power spectrum, we can parametrize it as the following power law form

$$\mathcal{P}_{\mathcal{R}}(k) = A_s \left(\frac{k}{k_*} \right)^{n_s - 1}, \quad (1.37)$$

where the amplitude and the spectral index are

$$A_s \equiv \frac{1}{8\pi^2} \frac{1}{\epsilon_*} \frac{H_*^2}{M_{pl}^2}, \quad (1.38)$$

$$n_s \equiv 1 - 2\epsilon_* - \eta_*, \quad (1.39)$$

where k_* is a reference scale that exits the horizon at $\tau_* = -1/k_*$, $H_* \equiv H(\tau_*)$ and $\epsilon_* \equiv \epsilon(\tau_*)$. There is a very tight observational constraint on the spectral index: the latest Planck data [18] indicates a slightly red tilted spectral index $n_s = 0.9649 \pm 0.0042$. The measured scalar amplitude is $A_s = (2.101 \pm 0.031) \times 10^{-9}$ (at $k_* = 0.05 \text{Mpc}^{-1}$).

Non-Gaussianity

According to the CMB observations the scalar power spectrum is highly Gaussian [19]. If a given statistical distribution is Gaussian the power spectrum or in other words the two-point correlation function contain all the information about the fluctuations. More complicated models of inflation compared to the single scalar field model such as multi field inflation or considering non-standard kinetic terms induce small deviations from Gaussianity. This small deviation can be probed using higher order correlation functions, such as the bispectrum, which is the three-point correlation function

$$(2\pi)^3 \delta(\mathbf{k}_1 + \mathbf{k}_2 + \mathbf{k}_3) B_{\delta\varphi}(k_1, k_2, k_3) = \left\langle \delta\varphi(\tau, \mathbf{k}_1) \delta\varphi(\tau, \mathbf{k}_2) \delta\varphi(\tau, \mathbf{k}_3) \right\rangle. \quad (1.40)$$

Tensor Fluctuations

Finally, we briefly discuss the last and most exciting prediction of inflation, i.e. the existence of a stochastic background of gravitational waves needed to determine the remaining tools for describing the features of the primordial fluctuations. We consider the tensor metric perturbations as

$$ds^2 = a^2(\tau) \left[-d\tau^2 + (\delta_{ij} + \tilde{h}_{ij}) dy^i dy^j \right], \quad (1.41)$$

where \tilde{h}_{ij} is a transverse and traceless tensor, i.e. $\partial^i \tilde{h}_{ij} = \tilde{h}_i^i = 0$. We define the Fourier transformed right and left-handed circular polarization states as

$$\tilde{h}_{ij}(\tau, y) = \int \sum_{A=L,R} \frac{d^3k}{(2\pi)^{3/2}} e_{ij}^A(k) \tilde{h}_A(\tau, k) e^{ik \cdot y}, \quad (1.42)$$

where e_{ij}^A is the polarization state tensor for the right ($A = R$) and left-handed ($A = L$) circular polarization states and satisfies the following relations

$$ik_a \epsilon^{ab} e_{db}^R = k e_{cd}^R, \quad ik_a \epsilon^{ab} e_{db}^L = -k e_{cd}^L, \quad e_{ab}^L(-k) = e_{ab}^{*L}(k) = e_{ab}^R(k), \quad (1.43)$$

where ϵ^{ab}_c is the three dimensional anti-symmetric symbol and the tensors are normalized such that $e_{ab}^L(k) e_{ab}^L(-k) = e_{ab}^R(k) e_{ab}^R(-k) = 1$. For simplicity, we assume that the gravitational waves are propagating along the z spatial direction as shown in Fig. 1.1

$$ds^2 = a^2(\tau) \left[-d\tau^2 + (1 + \tilde{h}_+(\tau, z)) dx^2 + (1 - \tilde{h}_+(\tau, z)) dy^2 + 2\tilde{h}_\times(\tau, z) dx dy + dz^2 \right]. \quad (1.44)$$

For convenience, we work with the canonically normalised tensor perturbations

$$h_{ij} \equiv a \frac{M_{pl}}{\sqrt{2}} \tilde{h}_{ij}. \quad (1.45)$$

We define the left and the right helicities as

$$h_{L,R} \equiv \frac{1}{\sqrt{2}} (h_+ \pm i h_\times). \quad (1.46)$$

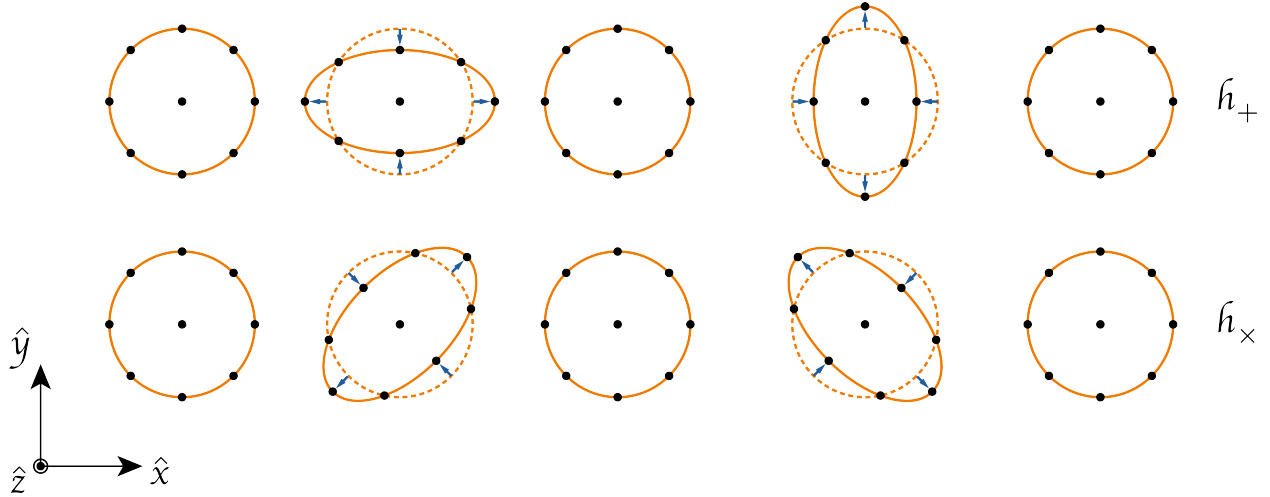


Figure 1.1: Two polarization of gravitational waves \tilde{h}_+ and \tilde{h}_\times .

The equation of motion for each polarization of the gravitational waves $A = L, R$ is

$$h''_A + \left(k^2 - \frac{a''}{a}\right)h_A = 0. \quad (1.47)$$

Power Spectrum

Finally, we can derive the tensor power spectrum

$$\mathcal{P}_h(k) = A_t \left(\frac{k}{k_*}\right)^{n_t}, \quad (1.48)$$

where the amplitude and the spectral index are

$$A_t \equiv \frac{2}{\pi^2} \frac{H_*^2}{M_{pl}^2}, \quad (1.49)$$

$$n_t \equiv -2\epsilon_{H_*}. \quad (1.50)$$

Tensor-to-scalar Ratio

At last, we can write the tensor-to-scalar ratio r , i.e. the ratio of the tensor and scalar power spectra

$$r \equiv \frac{A_t}{A_s} = 16\epsilon_{H_*}. \quad (1.51)$$

We can also relate r to the total inflaton field excursion during inflation $\Delta\varphi$, i.e. the total field excursion between the time when CMB fluctuations exited the horizon and the end of inflation through the so-called Lyth's bound [20]

$$\frac{\Delta\varphi}{M_{pl}} = \mathcal{O}(1) \times \left(\frac{r}{0.01}\right)^{1/2}. \quad (1.52)$$

Hence, large values of the tensor-to-scalar ratio, $r > 0.01$, correlate with super-Planckian field excursions, $\Delta\varphi > M_{pl}$. This only holds for the single scalar field models of inflation.

In Fig. 1.2 we can see the current constraints on n_s and r from CMB measurements. Currently no detection of r exists and there are only upper limits available. The best limits come from CMB experiments, $r < 0.06$ at 95% CL, from the combination of the B-mode polarization data of the BICEP2/Keck [21] and Planck 2018 data [18].

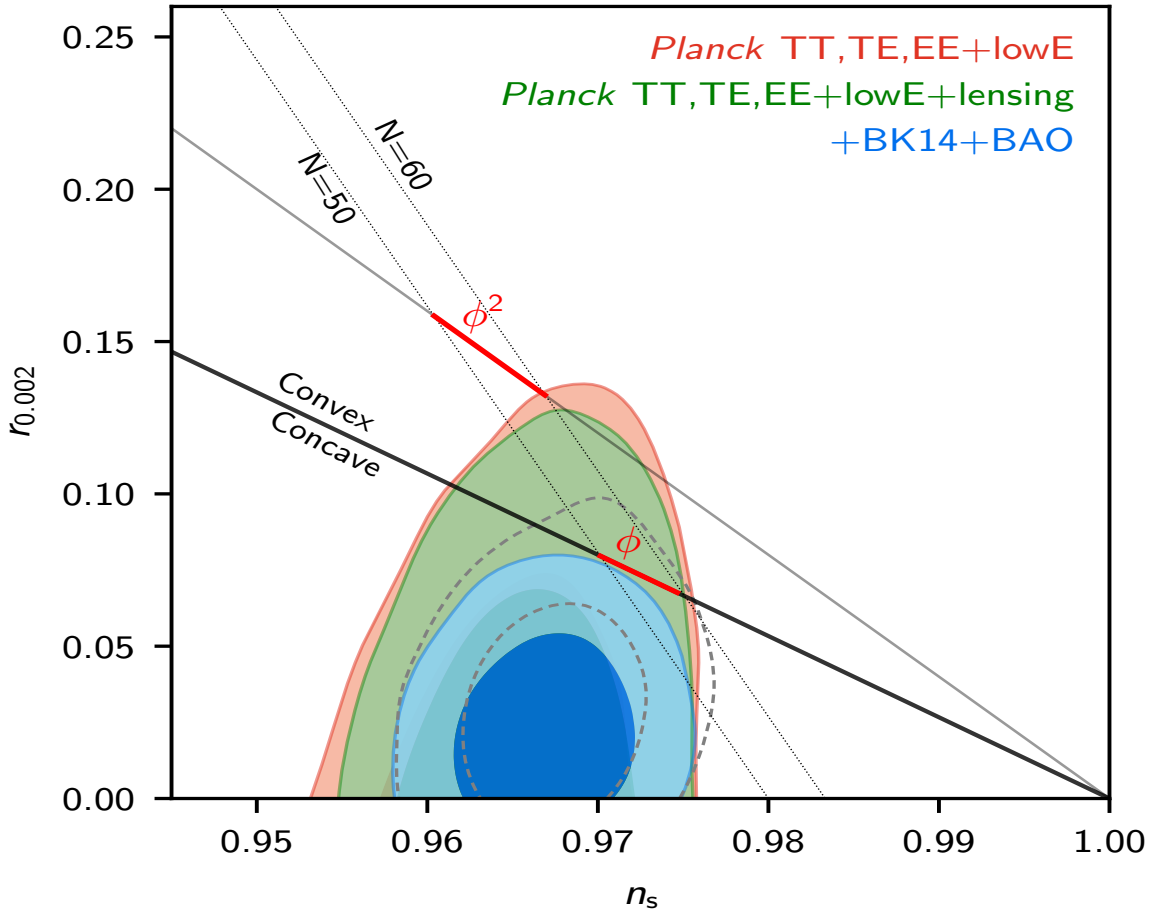


Figure 1.2: Current constraints on n_s and r from CMB measurements of Planck 2018, using Planck TT,TE,EE+lowE and Planck TT,TE,EE+lowE+lensing (red and green respectively), and joint constraint with BAO and 2014 BICEP2/Keck (blue). This plot is taken from [18].

1.2 Alternatives to Single Scalar Field Inflation

In the single scalar field model of inflation, a detection of the primordial tensor fluctuations and hence the tensor-to-scalar ratio r , can give us two very important pieces of information about inflation, namely, the energy scale of inflation and the inflaton field displacement during inflation. Therefore, the interpretation of the data coming from the next generation of experiments is arguably one of the most important tasks in the future of cosmology. However, a correct understanding of these measurements is only possible if we are certain about the sources of the gravitational wave signal that has been detected. In the context of inflationary models, vacuum tensor fluctuations are not the only known mechanism to generate gravitational waves. Gravitational waves can be produced from scalar sources [22, 23, 24, 25] and through particle production during inflation [26, 27], to give two examples of external sources for gravitational waves. In none of these cases the one to one correspondence between the energy scale of inflation and r holds.

Another possibility to produce sourced gravitational waves, which are the focus of this thesis, is the so-called axion-SU(2) gauge field spectator model of inflation. Coupled axion and SU(2) gauge fields during inflation [28, 29, 30, 31] provide a rich phenomenology that is not shared by canonical single scalar field inflation models (see [32] for a review). E.g., one feature that distinguishes this approach from vacuum gravitational waves, is the generations of a stochastic background of *chiral* gravitational waves [33, 32, 34, 35] which are non-Gaussian [36, 37, 38, 39]. It has also been shown [40, 41, 42, 43, 44, 45, 46, 47] that generation of chiral gravitational waves leads to a non-zero parity-violating gravitational anomaly, $R\tilde{R}$, which, in turn, violates the lepton number conservation and generates the baryon asymmetry of the universe.

The upcoming LiteBIRD [48, 49] and CMB Stage-4 experiments [50] will provide further constraints on the gravitational waves, which could constrain the axion-gauge field models of inflation [51, 52, 53]. However, before the predictions of these models are taken seriously, it is important to check if these models are viable both phenomenologically and theoretically.

From the phenomenological point of view, it is important to see if the couplings of SU(2) gauge fields to other fields lead to particle production and their backreaction on the axion-gauge field backgrounds do not spoil the model setup. In [54], a charged scalar field is coupled to the SU(2) gauge field, and production and backreaction of pairs of charged particles is studied in de Sitter spacetime. In [55], the backreaction of the extra spin-2 field in this setup is analytically studied for all the inflationary models involving the SU(2) gauge field. In [56, 57] a pair of massive Dirac fermions are coupled to the SU(2) gauge field. The coupling to a massless fermion is studied in [58]. In all these cases there exists a parameter space in which the backreaction of the particles on the SU(2) background is negligible. The nonlinear impact on the scalar perturbations of the chromo-natural inflation and the spectator sector during inflation has been studied in [59, 60]. Anisotropic initial conditions are discussed in [61].

From the theoretical point of view, it is important to consider all different classes of parity-violating terms that arise from the same physics. For example, if coupling to a

massive degree of freedom, such as axially coupled heavy fermions, is considered, then radiative fermion loops generate not only $F\tilde{F}$, but also $R\tilde{R}$ [62]. String theory predicts the existence of axions that couple to both terms simultaneously [63, 64, 65]. Hence, these two parity-violating terms arise at the same time and should be effectively considered on the same level in the theory. Moreover, given that $R\tilde{R}$ can introduce a ghost instability, it is important to check the stability of these models up to their cut-off scales.

Organization of this thesis This thesis is organized as follows. In Chapter 2, we introduce the axion-SU(2) gauge field models of inflation that are the central theme of this thesis starting from chromo-natural inflation (CNI), we discuss the inflationary background and the cosmological perturbations in this setup and show that CNI is ruled out observationally by its predicted values for n_s and the tensor-to-scalar ratio r . We then explore the axion-SU(2) spectator sector proposed by Dimastrogiovanni, Fasiello and Fujita [66], containing a scalar inflaton, a pseudoscalar axion and SU(2) gauge fields. We show that a large amplitude of helical, tensor modes can be generated by spectator SU(2) gauge fields during inflation, at linear order. We briefly discuss gravitational leptogenesis in these models to generate the baryon asymmetry of the universe and at the end, we shortly discuss the bispectrum in this model. The bispectrum is generated at tree-level as the gauge fields contain a tensor degree of freedom, and its production is dominated by self-coupling of the gauge fields.

In Chapter 3, we study the effect of the gravitational Chern-Simons term coupled to the axion field on the production and propagation of gravitational waves during inflation with the spectator axion-SU(2) sector [66]. Both parity-violating terms $R\tilde{R}$ and $F\tilde{F}$ exist simultaneously. We find that the effect of the $R\tilde{R}$ term on chiral gravitational waves can be as large as a fifty percent amplification for the left-handed helicity mode functions compared to the case without the $R\tilde{R}$ term. Using the existing bounds on the free parameters from the spectator axion-SU(2) gauge field sector, and requiring that the cut-off scale of the theory, Λ , is in the conservative case $\Lambda = M_{pl}$ and in a more radical case $\Lambda = 20H$, we put constraints on the new free parameter in our model to remain in the ghost-free regime, and we conclude that the inflation models with the spectator axion-SU(2) sector remain phenomenologically viable in the presence of the gravitational Chern-Simons term.

In Chapter 4, we focus on studying the evolution of a Dirac field doublet which is covariantly coupled to an axion and an isotropic SU(2) gauge field background in de Sitter spacetime. We assumed the fermion field to have a Dirac mass term. We discovered that the SU(2) background, in combination with the Dirac mass term, leads to non-trivial couplings between fermion components of different flavors and chirality. Next, we compute the expectation values of the induced currents, to estimate for what model parameters backreaction effects become important. More specifically, we consider the isotropic part of the SU(2) matter current, as well as the 4-divergence of the axial current, which can be used to estimate the fermionic backreaction on the gauge field and axion backgrounds, respectively. To find the vacuum expectation values of bilinearies in fermionic fields, such as the currents, we have to deal with UV-divergent integrals. We extend the idea of an

existing instantaneous vacuum subtraction scheme [67], which involves the subtraction of the contribution of zero-point fluctuations to the currents. We extensively discuss this extension to fermionic models with most generic Hamiltonians which permit only a numerical treatment. Finally, we show that the $SU(2)$ -background experiences strong backreaction due to fermions only for model parameters which are already excluded on observational and/or theoretical grounds and that the background dynamics of an axion- $SU(2)$ gauge field spectator sector remains unaffected by the production of fermions.

Finally, in Chapter 5, we summarize the main findings of this thesis and discuss the prospects of these models regarding the possibility of their detection in the near future.

Chapter 2

Axion-SU(2) Gauge Fields Models of Inflation

2.1 Historical Development

As discussed in Chapter 1, it is phenomenologically easy to write a potential that satisfies (1.6). In other words, these requirements translate to having a proper potential that inflates long enough to solve the flatness and horizon problem. The scalar field must roll very slowly, which is to say that the potential must be flat compared to its height, i.e. the potential must be shallow or the curvature of the potential must be very small. The question we have to answer before we proceed at this point is whether these fine-tuned potentials are protected against the quantum corrections or not, from which a number of problems arise. The most significant among these is the so-called η -problem of inflation which any model of inflation has to address one way or the other. The problem is so-called because the letter η is used to represent the curvature of the potential.

Scalar field theories generally lack symmetries that can protect their potential against higher order quantum corrections. These corrections can be large and they can spoil the flatness of the potential. Many solutions have been proposed to evade this problem and, among these solutions, the most relevant one to the subject of this thesis is natural inflation first proposed in [68]. In this setup, a pseudo Nambu-Goldstone boson, an axion field, is identified as the inflaton field, and the flat potential emerges as a result of a softly broken shift symmetry, i.e. symmetry under a constant shift of $\varphi \rightarrow \varphi + c$. The shallowness of the potential is protected from quantum corrections by this shift symmetry. Note that the potential is only totally protected from quantum corrections under a full shift symmetry. In the case discussed, given that the symmetry is only softly broken, the potential is protected against most quantum corrections but not all. In [69], it was shown that to match the observations from CMB experiments, the model must have a Planck scale axion decay constant. This requirement makes it challenging to embed this theory in a higher energy UV-complete setup such as string theory [70] and makes this model disfavoured by many theorists. Possible solutions to this problem have been proposed using axion

monodromy [71, 72], through coupling the axion to a 4-form [73] and modifying the axion evolution [74, 75, 76].

Another possible solution is to make the axion interact with a gauge field to achieve an effectively flat potential for a long enough inflationary period while the inflaton potential is steep enough to protect and evade the η -problem. This was first proposed in [77] in the context of Abelian gauge fields and later on using non-Abelian gauge fields called the chromo-natural inflation (CNI) [30, 31] and gauge-flation [28, 29] which does not involve axions or any other scalar field. In [78, 79], it was shown that CNI reduces to gauge-flation once the axion is integrated out. Detailed perturbations analysis of CNI have been made in [34, 31] and a thorough analysis of perturbations of gauge-flation can be found in [32, 80].

In the rest of this chapter, we provide a detailed description of CNI and its perturbations following [34, 31, 80].

2.2 Chromo-Natural Inflation

The CNI action, S_{CNI} , contains an axion χ with a sub-Planckian decay constant $f \ll M_{pl}$, a potential $U(\chi)$ and a collection of non-Abelian SU(2) gauge fields. However, this proposal does not rely on a specific gauge group and any SU(N) can be used. Thus, the action has the following form

$$S_{CNI} = \int d^4x \sqrt{-g} \left[\frac{M_{pl}^2}{2} R - \frac{1}{2} (\partial\chi)^2 - U(\chi) - \frac{1}{4} F_{\mu\nu}^a F^{a\mu\nu} + \frac{\lambda\chi}{4f} F_{\mu\nu}^a \tilde{F}^{a\mu\nu} \right], \quad (2.1)$$

where

$$U(\chi) = \mu^4 \left(1 + \cos\left(\frac{\chi}{f}\right) \right), \quad (2.2)$$

with μ being the energy scale of the axion with decay constant f . Later on, we will show that the existence of inflationary solutions does not depend on this potential at all.

The field strength tensor of the SU(2) gauge field is

$$F_{\mu\nu}^a = \partial_\mu A_\nu^a - \partial_\nu A_\mu^a - g_A \epsilon^{abc} A_\mu^b A_\nu^c, \quad (2.3)$$

with g_A being the self-coupling constant and ϵ^{abc} the three dimensional anti-symmetric symbol.

The SU(2) gauge fields are

$$A_\mu = A_\mu^a \frac{\sigma^a}{2}, \quad (2.4)$$

with $\{\sigma^1, \sigma^2, \sigma^3\}$ being the three Pauli matrices

$$\sigma^1 = \begin{pmatrix} 0 & 1 \\ 1 & 0 \end{pmatrix}, \quad \sigma^2 = \begin{pmatrix} 0 & -i \\ i & 0 \end{pmatrix}, \quad \sigma^3 = \begin{pmatrix} 1 & 0 \\ 0 & -1 \end{pmatrix}. \quad (2.5)$$

Here we are following convention in [81].

The last term in S_{CNI} (2.1) is the Chern-Simons interaction, where λ/f parametrizes its coupling strength and $\tilde{F}^{\alpha\mu\nu} \equiv \varepsilon^{\mu\nu\alpha\beta} F_{\alpha\beta}^a/2$ is the dual of $F_{\mu\nu}^a$. The $\varepsilon^{\mu\nu\alpha\beta}$ symbol is defined as $\varepsilon^{\mu\nu\alpha\beta} \equiv \epsilon^{\mu\nu\alpha\beta}/\sqrt{-g}$, where $\epsilon^{\mu\nu\alpha\beta}$ is the totally anti-symmetric symbol with $\epsilon^{0123} = 1$. The S_{CNI} is invariant under the local SU(2) transformation

$$A_\mu \rightarrow UA_\mu U^{-1} - \frac{i}{g_A} (\nabla_\mu U) U^{-1}, \quad (2.6)$$

where

$$U = e^{(-ig_A \beta^a x^a)}, \quad \beta = \beta^a \sigma^a / 2. \quad (2.7)$$

The term $F\tilde{F}$ is a total derivative and for $\chi = \text{const.}$ it reduces to a surface term. Hence, we can write $F\tilde{F}$ as

$$F\tilde{F} = \nabla_\mu C^\mu, \quad (2.8)$$

with

$$C^\mu = 2\varepsilon^{\mu\nu\alpha\beta} \left(A_\nu^a \partial_\alpha A_\beta^a - \frac{1}{3} \varepsilon^{abc} A_\nu^a A_\alpha^b A_\beta^c \right). \quad (2.9)$$

Now that we constructed the model, we study the requirements for this model to describe an inflationary solution in the next part.

2.2.1 Inflationary Dynamics

In this setup to get an inflationary background using non-Abelian gauge fields and axions, we need a rotationally invariant, homogeneous background. Mathematically, what happens is the following. Using vector fields in the background violates its rotational invariance but this can be compensated with a global gauge transformation and a rotationally invariant solution can be achieved. The existence of rotationally invariant solutions to the Einstein-Yang Mills equations was first realized in [82, 83, 84, 85, 86].

The vacuum expectation value (VEV) of the gauge field is given by a classical vacuum expectation value by [87, 88, 28, 29]

$$A_0^a = 0, \quad A_i^a = \delta_i^a a(t) Q(t). \quad (2.10)$$

This means that the SU(2) gauge field has a solution that respects the homogeneity and isotropy of space-time, and makes SU(2) a decent candidate for inflationary scenarios since it is compatible with the FLRW metric. It has been shown that this configuration is stable and has an attractor configuration [89, 90, 61].

Given the background field configuration in (2.10) the field strength components are

$$F_{0i}^a = \partial_i (a(t) Q(t)) \delta_i^a, \quad F_{ij}^a = -g_A (a(t) Q(t))^2 \epsilon_{ij}^a. \quad (2.11)$$

The Einstein equations are

$$3M_{\text{pl}}^2 H^2 = \frac{\dot{\chi}^2}{2} + U(\chi) + \frac{3}{2} (\dot{Q} + HQ)^2 + \frac{3}{2} g_A^2 Q^4, \quad (2.12)$$

$$-2M_{pl}^2\dot{H} = \dot{\chi}^2 + 2(\dot{Q} + HQ)^2 + 2g_A^2Q^4. \quad (2.13)$$

The equations of motion for the inflaton and gauge fields are given by [30, 66]

$$\ddot{\chi} + 3H\dot{\chi} - \frac{\mu^4}{f} \sin\left(\frac{\chi}{f}\right) = -3\frac{g_A\lambda}{f}Q^2(\dot{Q} + HQ), \quad (2.14)$$

$$\ddot{Q} + 3H\dot{Q} + (\dot{H} + 2H^2)Q + 2g_A^2Q^3 = \frac{g_A\lambda}{f}\dot{\chi}Q^2, \quad (2.15)$$

where dots show derivatives with respect to the cosmic time t and $H \equiv \dot{a}/a$ is the Hubble expansion rate. The key ingredient in this model is the new interaction term on the right hand side of (2.14). This term makes slow roll inflation possible away from the hilltop, even for sub-Planckian axion decay constant.

Recalling the definitions of energy density and isotropic pressure of a perfect fluid,

$$\bar{\rho} \equiv 3M_{pl}^2H^2, \quad \bar{\rho} + 3\bar{p} \equiv -6M_{pl}^2(\dot{H} + H^2) \quad (2.16)$$

we find

$$\bar{\rho}_{\text{CNI}} = \frac{\dot{\chi}^2}{2} + U(\chi) + \frac{3}{2}(\dot{Q} + HQ)^2 + \frac{3}{2}g_A^2Q^4, \quad (2.17)$$

$$\bar{p}_{\text{CNI}} = \frac{\dot{\chi}^2}{2} - U(\chi) + \frac{1}{2}(\dot{Q} + HQ)^2 + \frac{1}{2}g_A^2Q^4. \quad (2.18)$$

From (2.17) and (2.18) it is visible that the gauge sector has the equation of state of radiation $p_A = \rho_A/3$, hence the gauge field alone cannot source inflation. The interaction term between the gauge sector and the axion does not contribute to either energy density nor pressure.

For the slow-roll parameters defined in Chapter 1, $\epsilon_H \equiv -\dot{H}/H^2$ we can write [66]

$$\epsilon_H = \epsilon_\chi + \epsilon_B + \epsilon_E, \quad (2.19)$$

where

$$\epsilon_\chi \equiv \frac{\dot{\chi}^2}{2H^2M_{pl}^2}, \quad \epsilon_B \equiv \frac{g_A^2Q^4}{H^2M_{pl}^2}, \quad \epsilon_E \equiv \frac{(\dot{Q} + HQ)^2}{H^2M_{pl}^2}, \quad (2.20)$$

are all much smaller than unity.

Also we define the following dimensionless parameters

$$m_Q \equiv \frac{g_A Q}{H}, \quad \xi \equiv \frac{\lambda \dot{\chi}}{2fH}. \quad (2.21)$$

The fourth term in the left hand side of (2.15) becomes $2m_Q^2H^2Q$; thus m_Q can be regarded as the mass of Q (divided by H).

Next, let us look for a slowly rolling inflationary solution in this set-up. Neglecting $\ddot{\chi}$, \ddot{Q} , and \dot{H} will make our coupled system of equations decoupled and we can solve for $\dot{\chi}$ and \dot{Q} [30, 34]

$$\dot{\chi} \simeq \frac{g_A\lambda f Q^2 H \left(\frac{2g_A^2 Q^3}{H} - HQ - \frac{fU_{,\chi}}{g_A\lambda Q^2} \right)}{3f^2H^2 + g_A^2\lambda^2Q^4}, \quad (2.22)$$

and

$$\dot{Q} \simeq -\frac{HQ(2f^2H^2 + 2g_A^2f^2Q^2 + g_A^2\lambda^2Q^4) + g_A\lambda Q^2 fU_{,x}}{3f^2H^2 + g_A^2\lambda^2Q^4}. \quad (2.23)$$

We choose the parameters such that the following assumptions hold

$$3f^2H^2 \ll g_A^2\lambda^2Q^4, \quad \lambda^2Q^2 \gg 2f^2. \quad (2.24)$$

Rewriting the equations for $\dot{\chi}$ and \dot{Q} using the assumption above we obtain [34]

$$\dot{\chi} \simeq \frac{fH}{g_A\lambda Q^2} \left(\frac{2g_A^2Q^3}{H} - HQ - \frac{fU_{,x}}{g_A\lambda Q^2} \right), \quad (2.25)$$

and

$$\dot{Q} \simeq -HQ - \frac{fU_{,x}}{3g_A\lambda Q^2}. \quad (2.26)$$

Notice that we can rewrite the equation (2.26) by considering the right-hand side as the slope of an effective potential for the gauge field

$$H\dot{Q} + \frac{\partial V_{\text{eff}}(Q)}{\partial Q} = 0, \quad V_{\text{eff}} \equiv \frac{H^2Q^2}{2} - \frac{fHU_{,x}}{3g_A\lambda Q}, \quad (2.27)$$

where this effective potential has a minimum at

$$Q_{\min} = \left(\frac{\mu^4 \sin(\chi/f)}{3g_A\lambda H} \right)^{1/3}. \quad (2.28)$$

This leads to

$$\xi \simeq m_Q + \frac{1}{m_Q}. \quad (2.29)$$

When the gauge field takes this value (i.e. when $\dot{Q} \simeq 0$) the right-hand side of (2.14) is basically equal to the gradient of the axions potential, which means that the axion, or in other words the inflaton, rolls very slowly as its motion is dominated by classical energy that is transferred into the gauge sector.

Let us re-write the equation (2.25) by plugging in $Q = Q_{\min}$. This provides us with an effective equation governing the evolution of the axion in terms of the axion alone [34]

$$\dot{\chi} \simeq \frac{2f^{4/3}}{3^{2/3}\lambda^{4/3}} \frac{3\lambda^{2/3}f^{-2/3}H^{8/3} + 3^{1/3}g_A^{4/3}(-U_{,x})^{2/3}}{g_A^{2/3}H^{1/3}(-U_{,x})^{1/3}}. \quad (2.30)$$

This shows us that the axion dynamics is no longer controlled by the gradient of its potential and the Hubble damping, but the axion is evolving slowly on a flat effective potential provided by the interaction between the axion and VEV of the gauge field.

Now we have to calculate the so-called inflation parameters ϵ_H and η which are given by [34]

$$\epsilon_H \simeq \frac{Q^2}{M_{pl}^2} + \frac{g_A^2 Q^4}{H^2 M_{pl}^2}, \quad (2.31)$$

and

$$\eta = \frac{\dot{\epsilon}_H}{H\epsilon_H} = \frac{2g_A^2 Q^4}{H^2 M_{pl}^2} + \frac{\dot{Q}}{HM_{pl}^2 \epsilon_H} \left(2Q + \frac{4g_A^2 Q^3}{H^2} \right). \quad (2.32)$$

From (2.30), we can compute the number of e-folds $N = \int H dt$

$$N \simeq \frac{3y^{1/2}\lambda}{2} \int \frac{dx}{2y + x - xy^3}, \quad (2.33)$$

where

$$x \equiv \left(1 - \cos\left(\frac{\chi}{f}\right) \right)^{1/3}, \quad y \equiv \left(\frac{\lambda\mu^4}{3g_A^2 M_{pl}^4} \right)^{2/3}. \quad (2.34)$$

By putting proper bounds on x and y we can set an upper limit on N to evaluate how big λ is supposed to be in order to get $N \sim 40 - 60$ e-folds necessary to solve the horizon and flatness problems. If all the assumptions and the slow-roll approximation we have made so far hold for all χ , we can put a bound on x

$$0 \leq x \leq 2^{1/3}, \quad (2.35)$$

the maximum value for $y \simeq 1$, hence, the upper bound on N is

$$N \leq 0.6\lambda. \quad (2.36)$$

For enough number of e-folds we need to have $\lambda \gg 1$, this makes a low value for $f \ll M_{pl}$ possible for all parameters in this models. The equations (2.31) and (2.32) show that for satisfying the slow-roll conditions $\epsilon_H, |\eta| \ll 1$, we need to have

$$Q^2 \ll \frac{H}{\sqrt{2}g_A}, \quad |Q| \ll \frac{\mu}{\sqrt{g_A}}, \quad (2.37)$$

which places a strong condition on Q .

To summarize, when the gauge field is in its VEV, as described above, the equation of motion of the inflaton, which is given by the axion in this model, gets a new term on the right-hand side. This term is the key ingredient in this model that leads to a slow-rolling axion even when the potential of the axion is not shallow as expected in natural inflation. Slow-roll is achieved through the efficient transfer of axionic energy into classical gauge field instead of the dissipation via Hubble friction. The steps that we took were the following. First, we decoupled the system of coupled differential equations, using proper slow-roll assumptions. After getting two decoupled equations, we got an effective potential for the gauge field $V_{\text{eff}}(Q)$, this potential has a minimum at Q_{min} . When $Q \simeq Q_{min}$, the gauge field can be integrated out during slow-roll since the fluctuations on the gauge field

VEV are large $m_Q^2 = 3H^2$, so we can safely assume $\dot{Q} \simeq 0$. At this stage, we derived an equation for $\dot{\chi}$ in terms of χ which is precisely what we wanted and we can look for the parameter spaces that make inflation happen.

The system of equations mentioned above can be easily solved numerically. For the Figures 2.1 and 2.2, we have numerically solved the equations for the following set of parameters

$$\mu = 3.16 \times 10^{-4}, \quad f = 0.01 M_{pl}, \quad g_A = 2 \times 10^{-6}, \quad \lambda = 200. \quad (2.38)$$

In Figure 2.1, we show the region of field space over which the axion ranges during the inflationary period. The left panel shows the potential and the right panel shows the position of the axion as a function of time before inflation ends. In the left panel of Figure 2.2, we show the evolution of the gauge field as a function of the number of e-foldings $N_e \equiv N$ before inflation ends. In the right panel of Figure 2.2 we can see how the total number of e-foldings N depends on the value of λ .

A proper perturbation analysis is required in order to test the stability of the solutions above, in the next section we will focus on the stability analysis of CNI.

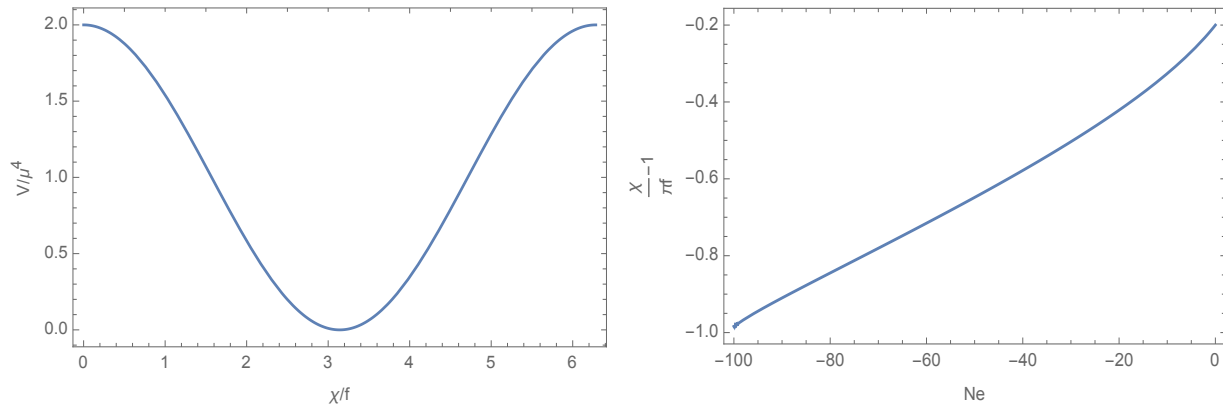


Figure 2.1: **(Left panel)** The bare axion potential is shown for the choice of parameters $\{\mu, f, g_A, \lambda\} = \{3.16 \times 10^{-4}, 0.01, 2.0 \times 10^{-6}, 200\}$. **(Right panel)** The full range of values that axion takes during inflation as a function of the e-folding number is shown for the same choice of parameters.

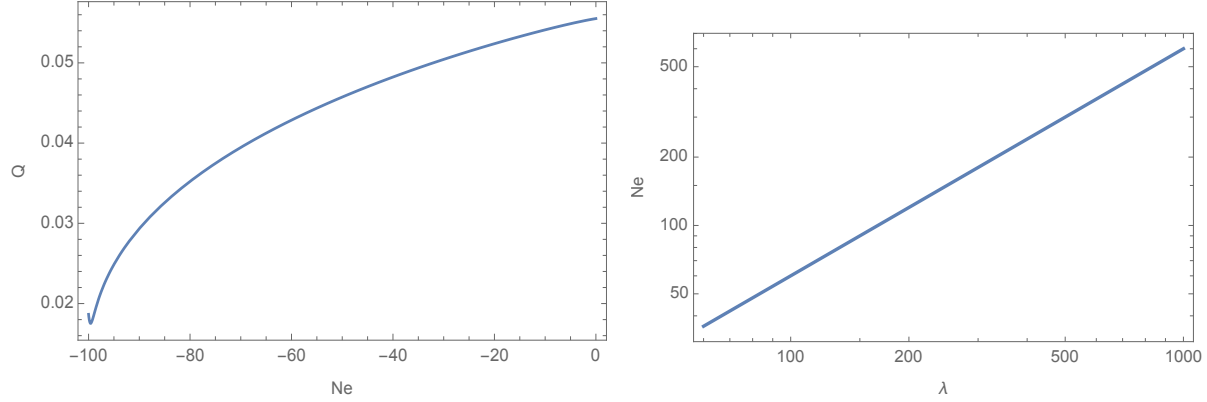


Figure 2.2: **(Left panel)** The behaviour of the gauge field as inflation proceeds for the same set of parameters as 2.1 is shown. **(Right panel)** The number of e-foldings of inflation produced as λ is varied, while the other parameters are kept fixed.

2.3 Perturbations of CNI

After finding homogeneous and isotropic inflationary solutions, to test the stability of these solutions we need to study the model in small departures from the FLRW approximation. We will focus on the fields and their perturbations in our setup following [34, 31].

2.3.1 Degrees of Freedom of CNI

The energy momentum tensor of CNI is

$$\begin{aligned}
 T_{\mu\nu} &= \frac{2}{\sqrt{-g}} \frac{\delta S}{\delta g^{\mu\nu}} \\
 &= 2Tr(F_{\mu\alpha}F_{\nu}^{\alpha}) - \frac{g_{\mu\nu}}{2}Tr(F_{\alpha\beta}F^{\alpha\beta}) + \partial_{\mu}\chi\partial_{\nu}\chi - g_{\mu\nu}\left[\frac{1}{2}g^{\rho\sigma}\partial_{\rho}\chi\partial_{\sigma}\chi + U(\chi)\right].
 \end{aligned}
 \tag{2.39}$$

Lets us now focus on the fields and their perturbations. This system has 23 degrees of freedom, 12 coming from the SU(2) gauge field, 10 from the metric and 1 from the axion which is playing the role of the inflaton here

$$\begin{aligned}
 \chi &= \bar{\chi} + \delta\chi, \\
 A_0^a &= \delta A_0^a = a(Y_a + \partial_a Y), \\
 A_i^a &= \bar{A}_i^a + \delta A_i^a = a\left[(Q + \delta Q)\delta_i^a + \partial_i(M_a + \partial_a M) + g_A Q\epsilon_{aic}(U_c + \partial_c U) + \tilde{t}_{ia}\right].
 \end{aligned}
 \tag{2.40}$$

Under infinitesimal diffeomorphisms, see Eqs. (1.16) and (1.19), the gauge fields transform as

$$\Delta\delta A_{\mu}^a(x^{\alpha}) \approx -\bar{A}_{\beta}^a(x^{\alpha})\frac{\partial\xi^{\beta}}{\partial x^{\mu}} - \frac{\partial\bar{A}_{\mu}^a(x^{\alpha})}{\partial x^{\beta}}\xi^{\beta},
 \tag{2.41}$$

whereas under infinitesimal SU(2) transformations, see Eq. (2.6),

$$\delta A_{\mu}^a \rightarrow \delta A_{\mu}^a - \partial_{\mu}\beta^a + g_A\epsilon^{abc}\beta^b\bar{A}_{\mu}^c,
 \tag{2.42}$$

where $\beta^a = \partial_a \beta^{\parallel} + \beta_a^{\perp}$.

Next, we decompose these degrees of freedom into scalar, vector and tensor based on how they behave under spatial rotations. Considering metric perturbations given in (1.11)

- Tensor degrees of freedom: 4 degrees of freedom \tilde{t}_{ai} and \tilde{h}_{ij} . Assuming $\partial_i \tilde{h}_{ij} = \partial_i \tilde{t}_{ai} = \tilde{h}_{ii} = \tilde{t}_{ii} = 0$.
- Vector degrees of freedom: 10 degrees of freedom Y_a, M_a, U_c, B_i and E_i . Assuming $\partial_i Y_i = \dots = \partial_i E_i = 0$.
- Scalar degrees of freedom: 9 degrees of freedom $\delta\chi, Y, \delta Q, M, U, \phi, B, \psi$ and E .

Now we proceed with fixing the gauge. We can remove the redundancy associated to general coordinate and SU(2) transformations. Using (1.16), with parameter $\xi^\mu = [\xi^0, \partial_i \xi^{\parallel} + \xi_i^{\perp}]^T$, the metric degrees of freedom transform as

$$\begin{aligned}\psi &\rightarrow \psi - \mathcal{H}\xi^0, \\ E &\rightarrow E - \xi, \\ E_i &\rightarrow E_i - \xi_i^{\perp},\end{aligned}\tag{2.43}$$

and we fix the spacetime slicing at linear order in perturbations by setting

$$\psi = 0, \quad E = 0, \quad E_i = 0.\tag{2.44}$$

We can fix the freedom associated to the SU(2) transformations by $U = U_i = 0$ considering an SU(2) transformation with an infinitesimal parameter. We are left with 16 degrees of freedom that take the following form, although not all of them correspond to dynamical degrees of freedom, in other words, not all of these degrees of freedom appear with their time derivative in the quadratic action [34]

$$\chi = \chi + \delta\chi,\tag{2.45}$$

$$A_\mu^a = a \begin{pmatrix} Y_1 & Q + \delta Q + \tilde{t}_+ & \tilde{t}_\times & \partial_z M_1 \\ Y_2 & \tilde{t}_\times & Q + \delta Q - \tilde{t}_+ & \partial_z M_2 \\ \partial_z Y & 0 & 0 & Q + \delta Q + \partial_z \partial_z M \end{pmatrix},\tag{2.46}$$

$$g_{\mu\nu} = a^2 \begin{pmatrix} -1 + 2\phi & B_1 & B_2 & \partial_z B \\ & 1 + \tilde{h}_+ & \tilde{h}_\times & 0 \\ & & 1 - \tilde{h}_+ & 0 \\ & & & 1 \end{pmatrix},\tag{2.47}$$

where $\tilde{h}_+, \tilde{h}_\times, \tilde{t}_+$ and \tilde{t}_\times are the + and \times polarization of tensor perturbations defined in (1.44).

Therefore, the perturbations are decoupled from each other at the linear order and the quadratic action for the perturbations splits into three decoupled parts

$$S_{\text{quadratic}} = S_{\text{scalar}} + S_{\text{vector}} + S_{\text{tensor}},\tag{2.48}$$

where all are Hermitian. The tensor action contains only dynamical modes, while the vector and the scalar actions contain both dynamical and non-dynamical modes.

2.3.2 Quantization and Power Spectrum

In this subsection we study the quadratic action for the perturbations in a general setting, quantize the perturbations and give an expression for the power spectrum. Let us call the vector formed by perturbations in one of these three systems X_i . We can make a transformation [34]

$$X_i = W_{ij}\Delta_j, \quad (2.49)$$

to have the following action for each one of these perturbations [34, 80]

$$S = \frac{1}{2} \int d\tau d^3k \left[\Delta'^{\dagger} \Delta' + \Delta'^{\dagger} A \Delta - \Delta^{\dagger} A \Delta' - \Delta^{\dagger} B \Delta \right], \quad (2.50)$$

where A is an anti-Hermitian and B is a Hermitian matrix, given that the action is Hermitian. Next we quantize (2.50) and write down the commutation relations between the variables and their conjugate momenta, and obtain the initial conditions.

We can quantize each field Δ_i and its conjugate momentum Π_i

$$\Pi_i \equiv \frac{\partial \mathcal{L}}{\partial \Delta'_i} = \Delta'^{\dagger} - \Delta^{\dagger} A \quad (2.51)$$

and impose equal time commutation relations as:

$$\Delta_i \equiv \mathcal{D}_{ij} a_j + \mathcal{D}_{ij}^* a_j^{\dagger}, \quad [a_i(k), a_j^{\dagger}(k')] = \delta^3(k - k') \delta_{ij}, \quad (2.52)$$

$$[\Delta_i(t, x), \Pi_j(t, y)] = i \delta_{ij} \delta^3(x - y). \quad (2.53)$$

Now we decompose Π in terms of the same annihilation and creation operators as in (2.52)

$$\Pi_i = \pi_{ij} a_j + \pi_{ij}^* a_j^{\dagger}. \quad (2.54)$$

The product of $\pi \pi^{\dagger}$ and $\mathcal{D} \mathcal{D}^{\dagger}$ must be real, hence

$$\pi \pi^{\dagger} - \pi^* \pi^T = \mathcal{D} \mathcal{D}^{\dagger} - \mathcal{D}^* \mathcal{D}^T = 0, \quad (2.55)$$

should be satisfied for the initial conditions that are chosen according to the positive frequency initial adiabatic vacuum. Starting from these initial condition, we can get the equations of motion for the mode functions following (2.50)

$$\mathcal{D}'' + 2A\mathcal{D}' + (B + A')\mathcal{D} = 0. \quad (2.56)$$

Let δ_i be the original field in real space corresponding to X_i in (2.49)

$$\delta_i = \int \frac{d^3k}{(2\pi)^{3/2}} e^{ik \cdot x} X_i. \quad (2.57)$$

Hence we can define the two point correlator assuming statistical isotropy as

$$\frac{1}{2} \langle \delta_i(\tau, x) \delta_j(\tau, y) + \delta_j(\tau, y) \delta_i(\tau, x) \rangle = \int \frac{dk}{k} \frac{\sin(kr)}{kr} \mathcal{P}_{ij}(k), \quad (2.58)$$

where $r = |x - y|$ and

$$\mathcal{P}_{ij}(k) = \frac{k^3}{2\pi^2} \Re \left[(X X^{\dagger})_{ij} \right], \quad (2.59)$$

is the power spectrum.

2.3.3 Scalar Fluctuations

In this subsection, we provide the explicit form of the quadratic action for the scalar perturbations in the form of (2.50).

The scalar degrees of freedom we are left with after gauge fixing include the axion as the inflaton $\delta\chi$, three degrees of freedom coming from the SU(2) gauge field, Y , δQ and M and the last two coming from the metric perturbations ϕ and B . Out of these six degrees of freedom, only three of them are dynamical. Y , ϕ and B appear without their time derivative in the quadratic action, therefore they are non-dynamical degrees of freedom and can be integrated out. To make the analysis of scalar perturbations easier we neglect the metric perturbations and integrate out the non-dynamical degree of freedom coming from the gauge field. For a detailed analysis considering the scalar metric perturbations, the reader may refer to the Appendix in [34].

After integrating out Y and setting $\phi = B = 0$, we define the remaining scalar perturbations in terms of $\Delta = (\Delta_1, \Delta_2, \Delta_3)^T$, where

$$\begin{aligned}\delta\chi &\equiv \frac{\Delta_1}{a}, \\ \delta Q &\equiv \frac{\Delta_2}{\sqrt{2}a}, \\ \delta M &\equiv \frac{g_A a Q \Delta_2 + \sqrt{k^2 + 2g_A^2 a^2 Q^2} \Delta_3}{\sqrt{2}g_A k^2 a^2 Q}.\end{aligned}\tag{2.60}$$

The action is given by [34]

$$\begin{aligned}A_{s,12} &= a \frac{g_A \lambda Q^2}{\sqrt{2}f}, \\ A_{s,13} &= a \frac{-g_A^2 \lambda Q^3}{\sqrt{2}f \sqrt{k_{phy}^2 + 2g_A^2 Q^2}}, \\ A_{s,23} &= 0,\end{aligned}\tag{2.61}$$

and

$$\begin{aligned}
B_{s,11} &= a^2 \left[k_{phy} + \frac{g_A^2 \lambda^2 k_{phy}^2 Q^4}{f^2 (k_{phy}^2 + 2g_A^2 Q^2)} + \frac{g_A^2 Q^4}{M_{pl}^2} + U_{,xx} - 2H^2 + \frac{\dot{\chi}}{2M_{pl}^2} + \frac{(\dot{Q} + HQ)^2}{M_{pl}^2} \right], \\
B_{s,12} &= a^2 \left[\frac{3g_A \lambda H Q^2}{\sqrt{2}f} + \frac{\sqrt{2}g_A \lambda Q \dot{Q}}{f} \right], \\
B_{s,13} &= a^2 \left[-\frac{\sqrt{2}\lambda}{f} \left(\frac{g_A^2 H Q^3}{2\sqrt{k_{phy}^2 + 2g_A^2 Q^2}} + \frac{2k_{phy}^4 + 3g_A^2 k_{phy}^2 Q^2 + 4g_A^4 Q^4}{2(k_{phy}^2 + 2g_A^2 Q^2)^{3/2}} (\dot{Q} + HQ) \right) \right], \\
B_{s,22} &= a^2 \left[k_{phy}^2 + 4g_A^2 Q^2 - \frac{g\lambda Q \dot{\chi}}{f} \right], \\
B_{s,23} &= a^2 \left[-\sqrt{k_{phy}^2 + 2g_A^2 Q^2} (2g_A Q - \frac{\lambda}{f} \dot{X}) \right], \\
B_{s,33} &= a^2 \left[k_{phy}^2 + \frac{4g_A^2 Q^2 (k_{phy}^2 + g_A^2 Q^2)}{k_{phy}^2 + 2g_A^2 Q^2} - \frac{g_A \lambda k_{phy}^2 Q \dot{\chi}}{f (k_{phy}^2 + 2g_A^2 Q^2)} + \frac{6g_A^2 k_{phy}^2 (\dot{Q} + HQ)^2}{(k_{phy}^2 + 2g_A^2 Q^2)^2} \right].
\end{aligned} \tag{2.62}$$

The matrices $A_{s,s}$ and $B_{s,s}$ are 3×3 matrices. The index s represents scalar perturbations and $k_{phy} \equiv k/a$.

Following the instruction as outlined in 2.3.2, we can now write the equations of motion, quantize each field Δ_i and provide their initial conditions. Hence, following (2.56), each Δ_i , ($i = 1, 2, 3$) defined as the field on the left hand side of (2.60), behaves like a free oscillator. Since we have three quantum fields here, we need to evolve each coupled equation under three different sets of initial conditions.

Finally, let us determine the curvature power spectrum, where the curvature perturbations are defined as

$$\mathcal{R} \simeq -\frac{H}{\dot{\chi}} \delta\chi, \tag{2.63}$$

the curvature power spectrum is

$$\mathcal{P}_{\mathcal{R}} = \frac{H^2}{\dot{\chi}^2} \mathcal{P}_{ij}, \tag{2.64}$$

where \mathcal{P}_{ij} is defined in (2.59).

A very detailed discussion of the instability analysis of the scalar modes can be found in [34, 31]. To summarize their finding we can say that the scalar fluctuations suffer from an instability on sub-horizon scales if $m_Q < \sqrt{2}$. In other words the inflationary solution is stable if and only if the gauge field is sufficiently heavy, since m_Q can be regarded as the mass of Q (divided by H). In Section 2.3.5 we will show that it is impossible to satisfy current observational bounds with this model.

2.3.4 Tensor Fluctuations

In this subsection we consider the tensor sector of CNI. It is easier to work with the left-handed and right-handed helicity mode functions, since the quadratic action for the tensor perturbations splits in two decoupled parts for each helicity doublet defined below

$$S_{tensor} = S_L + S_R. \quad (2.65)$$

The two polarizations are defined as (1.46) using (1.42) in Chapter 1

$$h_{L,R} \equiv \frac{1}{\sqrt{2}}(h_+ \pm ih_\times), \quad t_{L,R} \equiv \frac{1}{\sqrt{2}}(t_+ \pm it_\times). \quad (2.66)$$

For our convenience we work with the canonically normalised tensor perturbations

$$h_{ij} \equiv a \frac{M_{pl}}{\sqrt{2}} \tilde{h}_{ij}, \quad t_i^a \equiv \sqrt{2} a \tilde{t}_i^a. \quad (2.67)$$

Let us now define the respective Δ to have the quadratic action of the form (2.50)

$$\Delta_{L,R} = \begin{pmatrix} h_{L,R} \\ t_{L,R} \end{pmatrix}. \quad (2.68)$$

Here we only consider the quadratic action for the right-handed helicity doublet while the action for the left-handed helicity doublet is related to the right one by $k \rightarrow -k$.

The action is given by [34]

$$\begin{aligned} A_{t,12} &= \frac{1}{M_{pl}}(Q' + \mathcal{H}Q), \\ B_{t,11} &= k^2 - 2\mathcal{H}^2 + \frac{\chi'^2}{2M_{pl}^2} - \frac{(Q' + \mathcal{H}Q)^2}{M_{pl}^2} + \frac{3g_A^2 a^2 Q^4}{M_{pl}^2}, \\ B_{t,12} &= ak \frac{2g_A Q^2}{M_{pl}} + \frac{\mathcal{H}}{M_{pl}}(Q' + \mathcal{H}Q) - \frac{g_A \lambda a Q^2 \chi'}{f M_{pl}}, \\ B_{t,22} &= k^2 - ak \left(2g_A Q + \frac{\lambda a \chi'}{f} \right) + \frac{g_A \lambda a Q \chi'}{f}, \end{aligned} \quad (2.69)$$

where the index t represents tensor perturbations. It is clear from (2.69) that the effective frequency squared $B_{t,22}$ goes negative for the right-handed helicity mode function of the gauge tensor t_R close to the horizon crossing which translates to a tachyonic instability and growth of this mode. Since the gauge tensor modes are linearly coupled to the metric tensor perturbations, as the result of this instability, h_R grows signalling a violation of parity invariance in the tensor sector in this setup and hence the production of chiral gravitational waves. The same growth does not happen in the left-handed helicity mode function since the linear term in k has the opposite sign. The difference between the right- and left-handed helicity mode functions is shown in Figure 2.3.

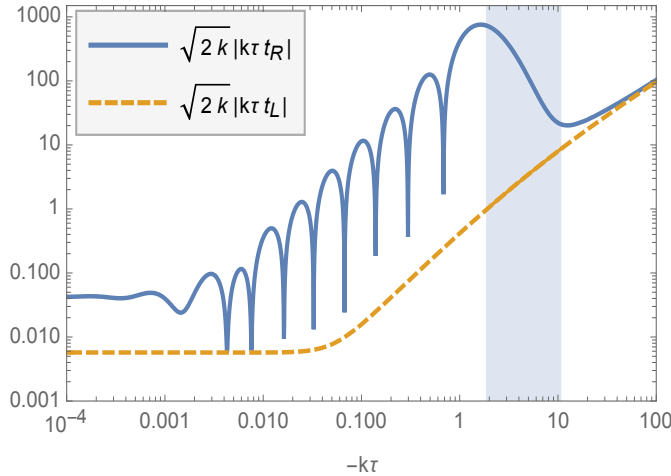


Figure 2.3: The right-handed helicity gauge tensor mode function $\sqrt{2k}|k\tau t_R|$ (solid blue) along side the left-handed helicity gauge tensor mode function $\sqrt{2k}|k\tau t_L|$ (dashed orange) is shown for the choice of parameters $\{m_Q, \epsilon_B, \epsilon_E\} = \{3, 3 \times 10^{-4}, 3 \times 10^{-5}\}$. The right-handed helicity gauge tensor grows around the horizon crossing. The shaded blue area shows the tachyonic instability region.

The time length of the tachyonic region can be calculated from the equations of motion [31] and is given by

$$2m_Q + \frac{1}{m_Q} - \sqrt{2m_Q^2 + 2 + \frac{1}{m_Q^2}} < x < 2m_Q + \frac{1}{m_Q} + \sqrt{2m_Q^2 + 2 + \frac{1}{m_Q^2}}. \quad (2.70)$$

This means that as m_Q increases the length of the tachyonic region increases as well. In other words, the instability persists for a longer period for larger m_Q . Since the scalar fluctuations are unstable when $m_Q < \sqrt{2}$ as shown in the previous section, we only focus on the regions for which $m_Q > \sqrt{2}$.

More discussion on the tensor perturbations and numerical solutions will be given in Section 2.8.1.

2.3.5 Observational Constraints

In [31] a thorough parameter search for the four free parameters g_A , μ , f and λ in this model is accomplished. The authors used numerical solutions of the full set of equations of motion for the scalar perturbations to compute the tensor-to-scalar ratio r as a function of the model parameters. The result of their parameter exploration is summarized in Figure 2.4. This figure shows that it is impossible to simultaneously satisfy the observational constraints on r , n_s , and the power spectrum amplitude using this model. When m_Q is large enough to produce an acceptable n_s , the enhanced gravitational wave spectrum is too

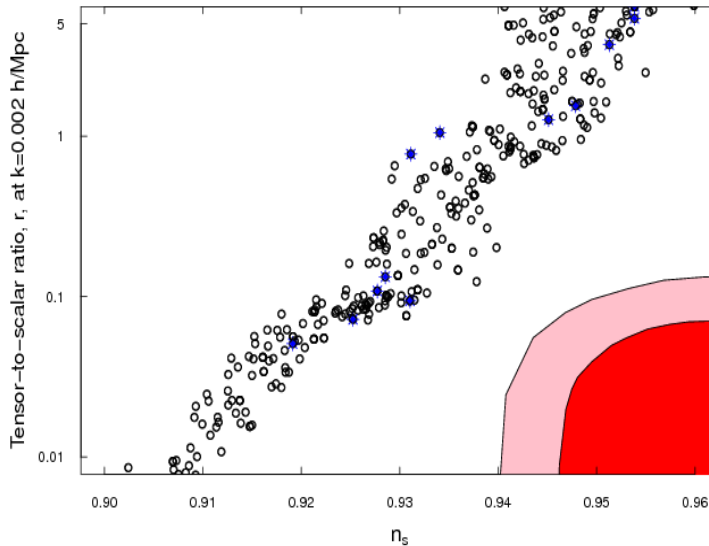


Figure 2.4: Comparison of the tensor-to-scalar ratio, r and the spectral index, n_s (evaluated at $k = 0.05 \text{ Mpc}^{-1}$). The value for r presented here includes the contributions from both gravitational wave helicities and is computed numerically using the gravitational wave mode functions. The open black circles represent parameter combinations whose scalar power spectrum amplitudes are outside of the Planck error bars; blue stars represent models with acceptable power spectrum amplitudes. The Planck one and two sigma contours are plotted in red and pink, respectively. This plot is taken from [33, 31].

large. Hence CNI model of inflation is ruled out observationally. Nonetheless, theoretically speaking, the most important feature of the CNI mechanism is that it evades the simple version of the so-called Lyth's bound [20] explained in Chapter 1 in (1.52).

Different models have been suggested to rescue this model from being totally ruled out. In the rest of this thesis, we will focus on the model proposed by the authors in [66]. This model suggests putting the axion-SU(2) in a spectator sector and considers an inflaton sector that takes care of inflation independent of the axion and the gauge field. Other models in the literature such as [91, 92], suggest that CNI can be made consistent with observational data if the SU(2) gauge symmetry is spontaneously broken. Another extension that saves the model and makes it consistent with observations is considered in [93].

2.4 Relation to Gauge-flation

It was shown that CNI reduces to a class of models of inflation where the axion has been integrated out, known as gauge-flation ([29, 28]), [78, 79]. Gauge-flation is described by the following Lagrangian

$$\mathcal{L}_{GF} = \sqrt{-g} \left[\frac{M_{pl}^2}{2} R - \frac{1}{4} F_{\mu\nu}^a F^{a\mu\nu} + \frac{\kappa}{384} (F_{\mu\nu}^a \tilde{F}^{a\mu\nu})^2 \right]. \quad (2.71)$$

The last term replaces the axion terms and the interaction between the axion and the gauge fields. In [79] it was shown that the gauge-flation model corresponds to CNI model once the axion is close to the bottom of its potential which translates to $\chi \simeq \pi f$. Reviving back the axion and fixing κ to be

$$\kappa \equiv 3 \frac{\lambda^2}{\mu^4}, \quad (2.72)$$

we can get back the action for CNI.

It has also been shown that gauge-flation is a special case of CNI by comparing the trajectories of gauge-flation to CNI since CNI has a much larger model space. This happens because CNI had two additional parameters compared to gauge-flation which translate to more freedom in the model.

As shown in right hand panel of Figure 2.5 taken from [78], both trajectories overlap while CNI has much larger trajectories.

2.5 The case with U(1)

So far the effort has been to build an inflation model with the SU(2) gauge fields, where a sizeable r can be generated from sources, without violating stringent observational constraints on the scalar perturbation. From a historical point of view these efforts did not start originally from considering SU(2) gauge fields, but started from considering U(1) as the gauge field [77, 94, 95, 96, 97, 98]. Although U(1) violates the isotropy of the space-time it was still used for inflationary models.

Following the mentioned references, let us consider the following action with the difference that now A_μ is an Abelian vector field as in U(1):

$$S_{U(1)} = \int d^4x \sqrt{-g} \left(\frac{M_{pl}^2}{2} R - \frac{1}{2} (\partial\chi)^2 - U(\chi) - \frac{1}{4} F_{\mu\nu} F^{\mu\nu} + \frac{\lambda_1 \chi}{4f} F_{\mu\nu} \tilde{F}^{\mu\nu} \right), \quad (2.73)$$

where

$$U(\chi) = \mu^4 \left(1 + \cos\left(\frac{\chi}{f}\right) \right), \quad (2.74)$$

with μ being the energy scale of the axion with decay constant f . Note that the existence of inflationary solutions does not depend on this potential at all.

The field strength tensor of the U(1) gauge field is

$$F_{\mu\nu} = \partial_\mu A_\nu - \partial_\nu A_\mu, \quad (2.75)$$

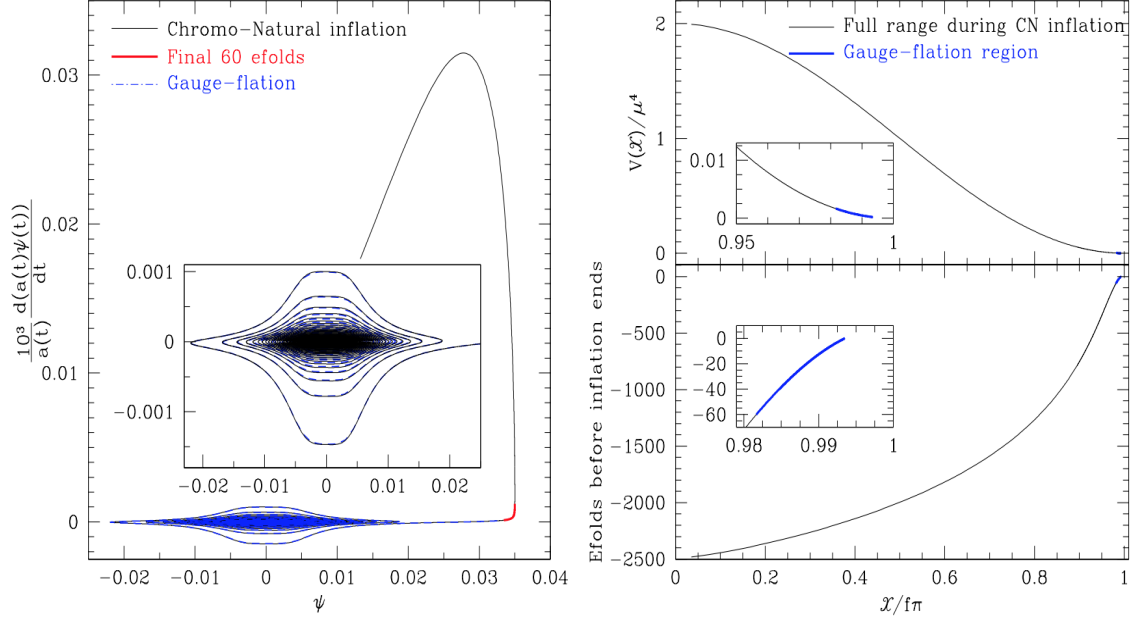


Figure 2.5: **(Left panel)** A phase portrait of the gauge field. The solid black curve corresponds to the period of exponential expansion, inflation. The red curve shows the final ~ 60 e-foldings of inflation and CNI ends at the end of the red curve. The dashed blue line shows the result of evolving the equations that follow from the action after the axion has been integrated i.e. gauge-flation. **(Right panel)** The full range of the axion. The region that corresponds to the gauge-flation regime is shown in blue. This figure is taken from [78].

and can be written in terms of the electric and the magnetic fields as:

$$F_{\mu\nu} = a^2 \begin{pmatrix} 0 & -E_x & -E_y & -E_z \\ E_x & 0 & B_z & -B_y \\ E_y & -B_z & 0 & B_x \\ E_z & B_y & -B_x & 0 \end{pmatrix}. \quad (2.76)$$

Hence

$$-\frac{1}{4}F_{\mu\nu}F^{\mu\nu} = \frac{1}{2}(\vec{E} \cdot \vec{E} - \vec{B} \cdot \vec{B}), \quad (2.77)$$

is a parity even term, whereas

$$\frac{1}{4}F_{\mu\nu}\tilde{F}^{\mu\nu} = -\vec{B} \cdot \vec{E}, \quad (2.78)$$

is a parity odd term.

The background equations of motion in this case are

$$\chi'' + 2a\mathcal{H}\chi' - \nabla^2\chi - a^2U_{,\chi} = \frac{\lambda}{f}a^2\vec{E} \cdot \vec{B}, \quad (2.79)$$

$$\vec{E}' + 2a\mathcal{H}\vec{E} - \nabla \times \vec{B} = -\frac{\lambda}{f}\chi'\vec{B} - \frac{\lambda}{f}\vec{\nabla}\chi \times \vec{E}, \quad (2.80)$$

$$\vec{\nabla} \cdot \vec{E} = -\frac{\lambda}{f}(\vec{\nabla}\chi) \cdot \vec{B}, \quad (2.81)$$

considering the vector potential $\vec{A}(\tau, x)$ with

$$a^2\vec{B} = \vec{\nabla} \times A, \quad a^2\vec{E} = -\vec{A}'. \quad (2.82)$$

The equation of motion for $\vec{A}(\tau, x)$ reads

$$\left[\frac{\partial^2}{\partial\tau^2} - \nabla^2 - \frac{\lambda\chi'}{f}\vec{\nabla} \times \right] \vec{A} = 0, \quad \vec{\nabla} \cdot \vec{A} = 0. \quad (2.83)$$

Following the steps as the previous sections we can write the vector field $\vec{A}(\tau, x)$ into circular polarized modes in the Coloumb gauge that obey the following equations of motion

$$\left[\frac{\partial^2}{\partial\tau^2} + k^2 \pm \frac{2k\xi}{\tau} \right] A_{\pm}(\tau, k) = 0, \quad (2.84)$$

where again $\xi \equiv (\lambda\dot{\chi})/(2fH)$.

In this scenario one can get inflation with a flat potential and a reasonable axion decay constant which is the same as in CNI model. But the question that now remains is what feature of this model made it so unsatisfactory as compared to non-Abelian vector fields?

The issue with U(1) lies in the perturbations. If we do the standard perturbation theory for this case to see the agreement with data coming from observations, we see that U(1) produces too much non-Gaussian scalar perturbations that is above the allowed bounds coming from observations. The reason behind that lies in the important difference between this model and CNI, which is in the case of U(1) the tensor modes are produced at the non-linear level by the vector fields produced by the rolling inflaton. These vector modes cannot source the tensor modes linearly and to get a sizeable contribution to the gravitational waves the same non-linear source generates too much non-Gaussian scalar perturbations that are at odds with data coming from CMB experiments. In Table 2.1 the differences between the properties of perturbations and background in both cases can be seen.

U(1) gauge fields	SU(2) gauge fields
preferred direction	isotropic
chiral tensor perturbations	chiral tensor perturbations
non-Gaussian scalar perturbations	Gaussian scalar perturbations
non-Gaussian tensor perturbations	non-Gaussian tensor perturbations

Table 2.1: U(1) gauge field versus SU(2) gauge field properties

2.6 Mimetic Chern-Simons SU(2)

In order to make the CNI consistent with observational data, we considered an extension of the model using mimetic construction proposed in [99] (see [100] for a review). For more details on the mimetic construction see [101, 102, 103, 104, 105]. Similar extensions of the mimetic construction using axions and Abelian and non-Abelian gauge fields have been considered in [106, 107, 108]. Unfortunately, the same problems as in CNI raises in this setup. Here, we adequately present a possible slow-roll solution that provides us with sufficient inflation in this setup. We will not discuss the perturbations of this model in this thesis.

We consider the following action

$$S = \int d^4x \sqrt{-g} \left[\frac{M_{\text{Pl}}^2}{2} R - \frac{1}{2} \text{Tr}(\mathbf{F}_{\mu\nu} \mathbf{F}^{\mu\nu}) - \lambda \left(\frac{1}{2} \text{Tr}(\mathbf{F}_{\mu\nu} \tilde{\mathbf{F}}^{\mu\nu}) - \Lambda_4 \right) \right], \quad (2.85)$$

where the terms are all defined as in the previous sections, minus the last term which is the mimetic Chern-Simons constraint, with $\bar{\lambda}$ being a dimensionless Lagrange multiplier defined as $\lambda = \bar{\lambda} + \delta\lambda$, where $\delta\lambda$ is its perturbation. The term Λ_4 is a constant with mass dimension four.

We can get the equations of motion

$$\partial_\beta [\sqrt{-g} F^{\beta\alpha a}] + \sqrt{-g} g_A^b A_\beta^a F^{\beta\alpha c} \epsilon^{abc} + \partial_\beta [\sqrt{-g} \lambda \tilde{F}^{\beta\alpha a}] + \sqrt{-g} \lambda g_A^b A_\beta^a \tilde{F}^{\beta\alpha c} \epsilon^{abc} = 0, \quad (2.86)$$

where the right-hand side of equation for gauge field background is now modified,

$$\ddot{Q} + 3H\dot{Q} + (\dot{H} + 2H^2)Q + 2g_A^2 Q^3 = g_A \dot{\lambda} Q^2. \quad (2.87)$$

Varying S with respect to λ yields the mimetic constraint

$$\frac{1}{4} F_{\mu\nu a} \tilde{F}^{\mu\nu a} = \Lambda_4, \quad (2.88)$$

which, at the background level reduces to

$$3g_A Q^2 (QH + \dot{Q}) = \Lambda_4. \quad (2.89)$$

The Friedmann equations are

$$3M_{\text{Pl}}^2 H^2 = -\bar{\lambda} \Lambda_4 + \frac{3}{2} (\dot{Q} + HQ)^2 + \frac{3}{2} g_A^2 Q^4, \quad (2.90)$$

$$M_{\text{Pl}}^2 \dot{H} = -(\dot{Q} + HQ)^2 - g_A^2 Q^4. \quad (2.91)$$

We can derive the energy density and pressure as in the previous sections

$$\begin{aligned} \bar{\rho} &= -\bar{\lambda} \Lambda_4 + \frac{3}{2} \left[(\dot{Q} + HQ)^2 + g_A^2 Q^4 \right], \\ \bar{p} &= \bar{\lambda} \Lambda_4 + \frac{1}{2} \left[(\dot{Q} + HQ)^2 + g_A^2 Q^4 \right]. \end{aligned} \quad (2.92)$$

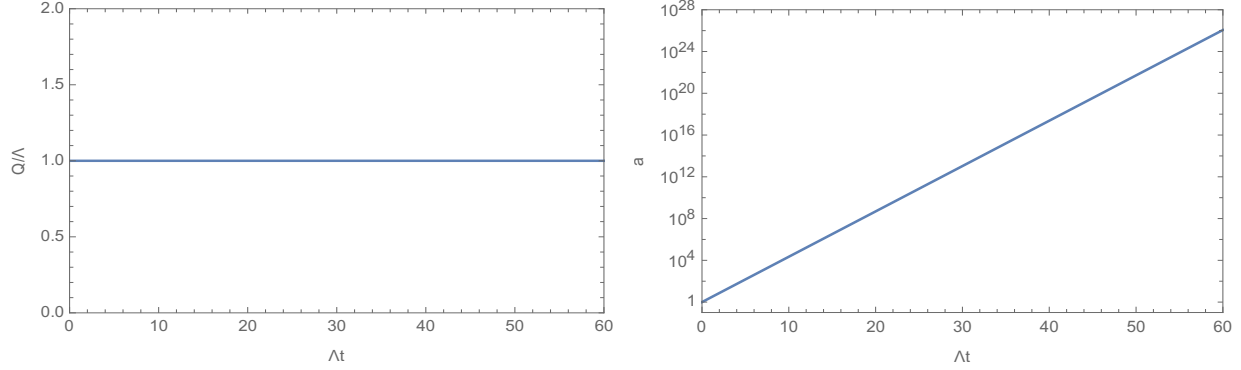


Figure 2.6: Realisation of slow-roll inflation for over 60 e -folds for the parameter choice in Eq. (2.101). Here $\Lambda \equiv \Lambda_4^{1/4}$.

The second terms in each line represent the radiation contribution due to the gauge field, with energy density

$$\rho_A \equiv \frac{3}{2} \left[\left(\dot{Q} + HQ \right)^2 + g_A^2 Q^4 \right], \quad (2.93)$$

and equation of state 1/3. The Lagrange multiplier terms play the role of a cosmological constant, with energy density

$$\rho_\Lambda \equiv -\bar{\lambda}\Lambda_4, \quad (2.94)$$

and equation of state -1 . If it dominates it can give rise to an inflationary stage of expansion. We now find the inflationary field configuration.

From Eqs. (2.89) and (2.90) one can express the Lagrange multiplier only in terms of Q and \dot{Q} ,

$$\bar{\lambda} = \frac{1}{\Lambda_4} \left[\frac{3}{2} \left(\frac{\Lambda_4}{Q^2} \right)^2 + \frac{3}{2} g_A^2 Q^4 - 3M_{\text{Pl}}^2 \left(\frac{\Lambda_4}{3g_A Q^3} - \frac{\dot{Q}}{Q} \right)^2 \right]. \quad (2.95)$$

One can also express H and \dot{H} only in terms of Q from Eqs. (2.89) and (2.91). We can then substitute for H , \dot{H} and $\bar{\lambda}$ in Eq. (4.96) to find the effective equation of motion of Q

$$\begin{aligned} \ddot{Q} + 3 \left(\frac{\Lambda_4 \dot{Q}}{3g_A Q^3} - \frac{\dot{Q}^2}{Q} \right) + \left\{ 2 \left[\frac{\Lambda_4}{3g_A Q^3} - \frac{\dot{Q}}{Q} \right]^2 - \left[\left(\frac{\Lambda_4}{M_{\text{Pl}} Q^2} \right)^2 + \frac{g_A^2 Q^4}{M_{\text{Pl}}^2} \right] \right\} Q + 2g_A^2 Q^3 \\ = \frac{6g_A Q^2}{\Lambda_4} \left[\left(g_A^2 Q^3 - \frac{\Lambda_4^2}{Q^5} \right) \dot{Q} + M_{\text{Pl}}^2 \left(\frac{\Lambda_4}{3g_A Q^3} - \frac{\dot{Q}}{Q} \right) \left(\frac{\Lambda_4 \dot{Q}}{g_A Q^4} + \frac{\ddot{Q}}{Q} - \frac{\dot{Q}^2}{Q^2} \right) \right]. \end{aligned} \quad (2.96)$$

To find a slow-roll solution for Q we start by applying the slow-roll approximation, which entails neglecting \ddot{Q} . We also assume

$$\frac{\Lambda_4}{3g_A Q^2} \gg |\dot{Q}|, \quad (2.97)$$

which implies $H \approx \Lambda_4/(3g_A Q^3)$.

Then for

$$M_{\text{Pl}} \gg Q \sim \Lambda_4^{1/4}, \quad g_A \ll 1, \quad (2.98)$$

to leading order in \dot{Q} , Eq. (2.96) reduces to

$$\dot{Q} \approx \frac{\Lambda_4}{9g_A M_{\text{Pl}}^2}, \quad (2.99)$$

which is consistent with Eqs. (2.97) and (2.98). Note that this gives us a slow-roll solution, since

$$\frac{\dot{Q}}{HQ} \approx \frac{Q^2}{3M_{\text{Pl}}^2} \ll 1. \quad (2.100)$$

For the parameters choice

$$Q = \Lambda_4^{1/4} = 10^{-8} M_{\text{Pl}}, \quad g_A = 10^{-2}, \quad (2.101)$$

one gets readily slow-roll inflation at 10^{15} GeV of at least 60 e -folds, as shown in Figure 2.6. In Figure 2.6 we plot the solution of the full equation of motion given in Eq. (2.96), with initial conditions for $Q(t)$ given by Eqs. (2.99) and (2.101).

It is interesting to note that, in its original version, mimetic gravity can provide an energy density that mimics the role of dark matter in the cosmological background. Taken into account with a SU(2) Einstein-Yang-Mills system, it was shown in [107] that the model can provide energy density that behaves as radiation evolving as $\propto a^{-4}$ and evolving as $\propto a^{-2}$. Moreover, if taken with the Chern-Simons term, it can play the role of a cosmological constant as it was shown here and in [108] in the context of a Weyl-invariant and generally-covariant theory for the cosmological constant.

2.7 Axion-SU(2) Gauge Field Spectator Sector

As it was shown in the previous section, the scalar perturbations in the CNI model present tension with the observational data. It is impossible to simultaneously satisfy the bounds on r and on the scalar spectral index, n_s , as shown in 2.4. Therefore, the simple models of CNI are ruled out by observations. In order to relax these tensions and revive the model, the authors in [66] proposed putting the axion-SU(2) in a spectator sector and consider an inflaton sector that takes care of inflation independently. As a result the motivation for solving the η problem in inflation is lost, but we can still benefit from the unique signatures and phenomenological power of these models. We will briefly discuss the axion-SU(2) gauge field spectator model of inflation here, since this is the model considered in the rest of this dissertation.

In the axion-SU(2) gauge field spectator model, the action of CNI given in (2.1) is modified to

$$S = \int d^4x \sqrt{-g} \left(\frac{M_{\text{pl}}^2}{2} R - \frac{1}{2} (\partial\varphi)^2 - V(\varphi) - \frac{1}{2} (\partial\chi)^2 - U(\chi) - \frac{1}{4} F_{\mu\nu}^a F^{a\mu\nu} + \frac{\lambda_1 \chi}{4f} F_{\mu\nu}^a \tilde{F}^{a\mu\nu} \right), \quad (2.102)$$

where φ is a single-field inflaton sector with a generic potential $V(\varphi)$.

We will now redo the steps in the previous section for this model to examine the validity of this model. Let us start with determining the background equations.

The background equations for χ and Q are as before, described in (2.14) and (2.15) respectively. The Einstein equations are now modified since an independent sector that takes care of inflating the universe is added:

$$\bar{\rho} \equiv 3M_{pl}^2 H^2, \quad \bar{\rho} + 3\bar{p} \equiv -6M_{pl}^2(\dot{H} + H^2) = \frac{\ddot{a}}{a}, \quad (2.103)$$

where

$$\begin{aligned} \bar{\rho} &= \rho_\varphi + \rho_\chi + \rho_A = \frac{\dot{\varphi}^2}{2} + V(\varphi) + \frac{\dot{\chi}^2}{2} + U(\chi) + \frac{3}{2}(\dot{Q} + HQ)^2 + \frac{3}{2}g_A^2 Q^4, \\ \bar{p} &= p_\varphi + p_\chi + p_A = \frac{\dot{\varphi}^2}{2} - V(\varphi) + \frac{\dot{\chi}^2}{2} - U(\chi) + \frac{1}{2}(\dot{Q} + HQ)^2 + \frac{1}{2}g_A^2 Q^4. \end{aligned} \quad (2.104)$$

We can define the dimension-less slow-roll parameters as done before, where we have added an extra slow-roll parameter for the inflaton ϵ_φ :

$$\epsilon_\varphi \equiv \frac{\dot{\varphi}^2}{2H^2 M_{pl}^2}, \quad \epsilon_\chi \equiv \frac{\dot{\chi}^2}{2H^2 M_{pl}^2}, \quad \epsilon_B \equiv \frac{g_A^2 Q^4}{H^2 M_{pl}^2}, \quad \epsilon_E \equiv \frac{(\dot{Q} + HQ)^2}{H^2 M_{pl}^2}, \quad (2.105)$$

where

$$\epsilon_H \equiv -\frac{\dot{H}}{H^2} = \epsilon_\varphi + \epsilon_\chi + \epsilon_B + \epsilon_E. \quad (2.106)$$

In the above paragraph the parameters m_Q and ξ are the same as before and the slow-roll solutions in (2.28) and (2.29) are still applicable.

By putting the axion and the gauge field in the spectator sector we are making the inflaton the most dominant field during inflation. Let us focus on the inflaton sector a bit. We need to specify the essential slow-roll parameters meanwhile keeping the sector as general as possible so we do not have to specify which model of inflation we are considering. We need to keep track of ϵ_φ while keeping η_φ constant and $\epsilon_\varphi \simeq \epsilon_H$. One can show that

$$\dot{\epsilon}_\varphi = (4\epsilon_\varphi - 6\epsilon_\varphi^* + 1 - n_s^*)H\epsilon_\varphi, \quad (2.107)$$

where $n_s = -6\epsilon_\varphi + 2\eta_\varphi + 1 \approx 0.9649$ is the spectral index.

In Figure 2.7, the authors in [66] have plotted the dimensionless parameters defined above as inflation proceeds as a function of N , the number of e-folds during inflation. One can see that ϵ_φ remains much bigger than the others, which is consistent with putting the axion-SU(2) gauge fields in the spectator sector.

2.7.1 Perturbations of Axion-SU(2) Spectator Sector

In this subsection we summarize the result of [66] for the scalar perturbations. A numerical study of the tensor perturbations is given in 2.8.1.

Let us again consider Δ_i as defined in (2.60) and study their effect on the curvature perturbations \mathcal{R} . The equations of motion are the same as (2.56)

$$\partial_x^2 \Delta_i - 2A_{ij} \partial_x \Delta_j + (B_{ij} - \partial_x A_{ij}) \Delta_j = 0, \quad (2.108)$$

where $x \equiv -k\tau$.

The entries of matrices A and B are the same as (2.61) and (2.62) with a minor difference due to the spectator sector. We will give the entries of these two 3×3 matrices here in terms of the dimensionless parameters defined above [66]

$$\begin{aligned} A_{s,12} &= \frac{\Lambda m_Q}{\sqrt{2x}}, \\ A_{s,13} &= -\frac{\Lambda m_Q^2}{\sqrt{2x} \sqrt{x^2 + 2m_Q^2}}, \end{aligned} \quad (2.109)$$

and

$$\begin{aligned} B_{s,11} &= 1 - \frac{2 + \epsilon_\chi + \epsilon_B + \epsilon_E + \epsilon_\varphi}{x^2} + \frac{U_{,\chi\chi}}{H^2 x^2} + \frac{m_Q^2 \Lambda^2}{x^2 + 2m_Q^2}, \\ B_{s,12} &= \frac{3\Lambda m_Q}{\sqrt{2x^2}} \left[1 + \frac{2}{3} \epsilon_Q \right], \\ B_{s,13} &= -\frac{\Lambda m_Q^2}{\sqrt{2x^2} \sqrt{x^2 + 2m_Q^2}} - \Lambda(1 + \epsilon_Q) \frac{2x^4 + 3x^2 m_Q^2 + 4m_Q^4}{2x^2 (x^2 + 2m_Q^2)^{3/2}}, \\ B_{s,22} &= 1 + \frac{4m_Q^2 - 2\xi m_Q}{x^2}, \\ B_{s,23} &= -2 \frac{m_Q - \xi}{x^2} \sqrt{x^2 + 2m_Q^2}, \\ B_{s,33} &= 1 + \frac{4m_Q^2 (x^2 + m_Q^2)}{x^2 (x^2 + 2m_Q^2)} - \frac{2\xi m_Q}{x^2 + 2m_Q^2} + \frac{6m_Q^2 (1 + \epsilon_Q)^2}{(x^2 + 2m_Q^2)^2}, \end{aligned} \quad (2.110)$$

where $\Lambda \equiv \lambda Q/f$ and $\epsilon_Q \equiv \dot{Q}/QH$. The numerical solutions of Δ_i are shown in Figure 2.7.

From Figure 2.7 it is clear that the axion perturbation Δ_1 freezes after horizon crossing, while the gauge field scalar perturbations, Δ_2 and Δ_3 , evolve on super-horizon scales and eventually decay. Note that in this case $m_Q \simeq 3$ so there is no instability.

We can now study the effect of Δ_i on the curvature perturbations \mathcal{R} . In the flat gauge \mathcal{R} is given by [109]

$$\mathcal{R} = \frac{\sum_i \delta \rho_i}{3 \sum_i (\rho_i + p_i)}, \quad (2.111)$$

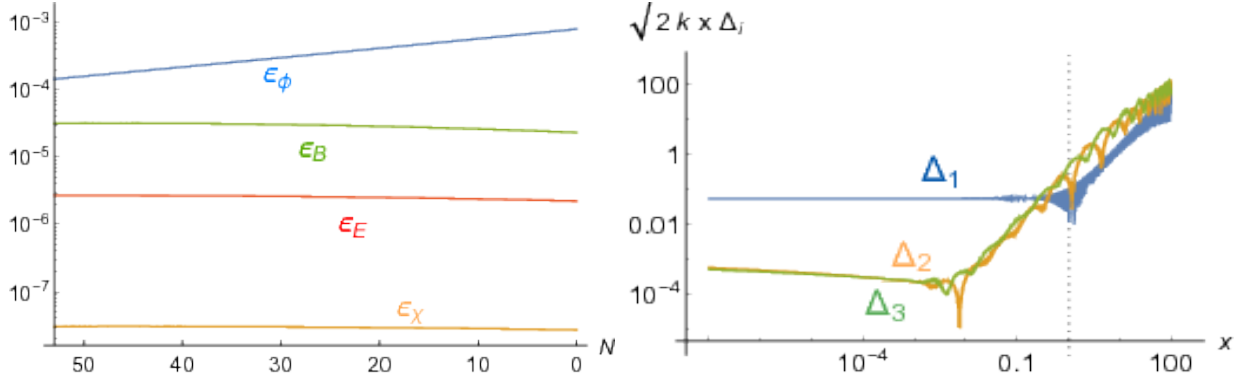


Figure 2.7: **(Left panel)** The various components of (2.106) is shown. As expected ϵ_H is dominated by ϵ_φ labelled as ϵ_ϕ in the figure. **(Right panel)** Numerically integrated scalar perturbations in the axion-SU(2) gauge field spectator sector. This figure is taken from [66].

where $i = \{\varphi, \chi, A\}$. The expression for ρ_i and p_i are given in 2.104, and $\delta\rho_i$ is the energy density perturbation of each component. We can define the energy density fraction Ω_i as

$$\Omega_i = \frac{\rho_i}{3H^2 M_{pl}^2}, \quad (2.112)$$

hence,

$$\mathcal{R} \approx \frac{\Omega_\varphi \delta\rho_\varphi / \rho_\varphi + \Omega_\chi \delta\rho_\chi / \rho_\chi + \Omega_A \delta\rho_A / \rho_A}{2\epsilon_\varphi}. \quad (2.113)$$

Notice that in the expression above we have neglected the contributions from ϵ_χ , ϵ_B and ϵ_E in the denominator for reasons discussed below. The observational constraints on the scalar curvature power spectrum can be satisfied if one shows that the contribution from the last two terms in the numerator above are negligible.

Let us first consider the gauge field, namely the last term in the numerator of 2.113. As soon as the axion χ reaches the minimum of the potential and stops generating the gauge field, this term is negligible. Furthermore, the gauge field produces axion perturbations that can contribute to \mathcal{R} in different ways. One way is through the second term in the numerator, which is negligible after inflation as $\Omega_\chi \rightarrow 0$. The second way is through the first term, that can make a sizeable contribution for large values of m_Q . Nonetheless for the chosen values of $m_Q \sim 3$, it is smaller than vacuum contribution by large and can be neglected. Therefore, the main contribution to the curvature perturbations is coming from the inflaton sector, hence we can satisfy the strict bounds on $\mathcal{P}_{\mathcal{R}}$ and save these models from being totally ruled out.

2.8 Signatures and Bonuses

Although the current valid version of these models prevents us from solving the η -problem, it provides a very rich phenomenology to explain other open problems in cosmology and

the standard model of particle physics such as the matter asymmetry in the universe.

The question that we should answer now is: how can we differentiate between B-modes generated from vacuum fluctuations of the metric and those from sources, once the primordial gravitational waves are observed?

The short answer to this question is: through the features and signatures of the primordial gravitational waves. The vacuum gravitational waves are almost all the time scale invariant with a slight red tilt [110]. On the other hand, depending on the model the sourced gravitational waves can have a red or blue tilt or have a completely non-power-law spectrum. The other feature of the vacuum fluctuations is that they produce parity-even B-modes. As seen in the previous sections, one of the unique signatures of axion-SU(2) models is the production of chiral gravitational waves with a larger amplitude since the gauge tensor modes are linearly coupled to gravitons producing parity-odd B-modes. This feature can be seen as a non-vanishing TB/EB correlation in the CMB [111, 112, 51, 62, 113, 114, 53]. The last feature of the axion-SU(2) gauge field sourced gravitational waves is that they are highly non-Gaussian [36, 37, 38, 39], which is different from the tensor modes induced by the vacuum fluctuations of the metric [115, 116].

In Table 2.2, we summarize the differences between the axion-SU(2) sourced gravitational waves, versus the vacuum ones.

Vacuum	Axion-SU(2) gauge fields
scale invariant	non-scale invariant
non-chiral	chiral
Gaussian	non-Gaussian

Table 2.2: Gravitational waves from vacuum versus axion-SU(2) gauge field

We discuss the three strengths of these models briefly below, starting with the chiral gravitational waves, moving on to the gravitational leptogenesis and explaining the non-Gaussianity at the end.

2.8.1 Chiral Gravitational Waves

In this section we look at the equations of motion for the metric and the gauge tensor perturbations, and obtain numerical solutions. As it was shown in the previous sections, we have four tensor degrees of freedom: two metric tensor degrees of freedom that represent the gravitational waves and two additional tensor degrees of freedom associated with the SU(2) gauge field. We consider a perturbed FLRW metric as follows

$$ds^2 = a^2(\tau) \left[-d\tau^2 + (\delta_{ij} + \tilde{h}_{ij}) dy^i dy^j \right], \quad (2.114)$$

where \tilde{h}_{ij} is a transverse and traceless tensor, i.e. $\partial^i \tilde{h}_{ij} = \tilde{h}_i^i = 0$. We define the Fourier transformed right and left-handed circular polarization states as seen in Chapter 1 and we write the tensor perturbations of the gauge field as $\delta A_i^a = a \tilde{t}_i^a$, where \tilde{t}_i^a is chosen to be transverse and traceless, i.e. $\partial_i \tilde{t}_i^a = \tilde{t}_i^{ai} = 0$. We write the gauge tensor perturbations

as $\delta A_i^1 = a(\tilde{t}_+, \tilde{t}_\times, 0)$ and $\delta A_i^2 = a(\tilde{t}_\times, -\tilde{t}_+, 0)$. For our convenience we work with the canonically normalised tensor perturbations

$$h_{ij} \equiv a \frac{M_{pl}}{\sqrt{2}} \tilde{h}_{ij}, \quad t_i^a \equiv \sqrt{2} a \tilde{t}_i^a. \quad (2.115)$$

We define the left and the right helicities

$$h_{L,R} \equiv \frac{1}{\sqrt{2}}(h_+ \pm i h_\times), \quad t_{L,R} \equiv \frac{1}{\sqrt{2}}(t_+ \pm i t_\times). \quad (2.116)$$

The equations of motion for the tensor modes up to leading order in slow-roll parameters are

$$\partial_x^2 t_A + \left[1 + \frac{2}{x^2}(m_Q \xi_1 - s x(m_Q + \xi_1))\right] t_A = -\frac{2\sqrt{\epsilon_E}}{x} \partial_x h_A + \frac{2}{x^2} \left[(m_Q - s x)\sqrt{\epsilon_B} + \sqrt{\epsilon_E}\right] h_A, \quad (2.117)$$

$$\left[\partial_x^2 h_A + \left(1 - \frac{2}{x^2}\right) h_A\right] = \frac{2\sqrt{\epsilon_E}}{x} \partial_x t_A + \frac{2}{x^2} \left[(m_Q - s x)\sqrt{\epsilon_B}\right] t_A, \quad (2.118)$$

where $x \equiv -k\tau$, $A = L, R$ and $s = -1, +1$ for L, R respectively.

Before solving the above system of coupled equations numerically, we need to specify the initial conditions. Since the tensor-like perturbations in the gauge fields and the tensor metric perturbations are linearly coupled, we expand both in terms of the same pair of creation and annihilation operators [16]

$$\begin{aligned} h_A(\tau, k) &= \sum_{n=h,t} \left[a_{n,k}^A h_{A,n} + a_{n,-k}^{A\dagger} h_{A,n}^* \right], \\ t_A(\tau, k) &= \sum_{n=h,t} \left[a_{n,k}^A t_{A,n} + a_{n,-k}^{A\dagger} t_{A,n}^* \right], \end{aligned} \quad (2.119)$$

where we have the standard commutators

$$[a_{n,k}^A, a_{m,q}^{B\dagger}] = \delta_{n,m} \delta_{A,B} \delta^{(3)}(k - q). \quad (2.120)$$

We have to specify the vacuum for the gravitational and gauge fields separately. We divide the vacuum into two subspaces corresponding to each field as [34, 80, 43]:

$$\begin{aligned} h_{A,n}(\tau, k) &= \frac{1}{\sqrt{2k}} \delta_{n,h} e^{-ik\tau}, & h'_{A,n}(\tau, k) &= -\frac{1}{\sqrt{2k}} ik \delta_{n,h} e^{-ik\tau}, \\ t_{A,n}(\tau, k) &= \frac{1}{\sqrt{2k}} \delta_{n,t} e^{-ik\tau}, & t'_{A,n}(\tau, k) &= -\frac{1}{\sqrt{2k}} ik \delta_{n,t} e^{-ik\tau}. \end{aligned} \quad (2.121)$$

The solution $h_{A,n=h}$ can be interpreted as the vacuum gravitational wave, whereas $h_{A,n=t}$ as the sourced one (by the vacuum gauge field, $t_{A,n=t}$).

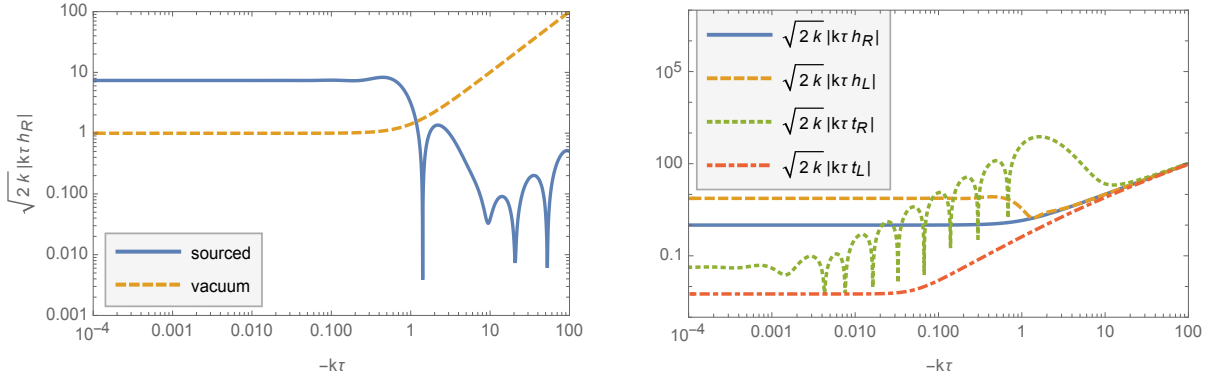


Figure 2.8: **(Left panel)** The sourced right-handed linear gravitational wave $\sqrt{2k}|k\tau h_{R,n=t}|$ (solid blue) and the vacuum gravitational waves $\sqrt{2k}|k\tau h_{R,n=h}|$ (dashed orange) are shown. **(Right panel)** The sourced linear gravitational wave $\sqrt{2k}|k\tau h_R|$ (solid blue), the left-handed gravitational waves $\sqrt{2k}|k\tau h_L|$ (dashed orange) and the linear right- and left-handed gauge tensor mode functions $\sqrt{2k}|k\tau t_R|$ (dotted green) and $\sqrt{2k}|k\tau t_L|$ (dot-dashed red) are shown. The right-handed helicity gravitational wave grows around the horizon crossing and stays constant afterwards.

In the right panel of Figure 2.8 we show the amplification of $|t_R| = \sqrt{\langle t_R^\dagger t_R \rangle}$ (green line) around horizon crossing ($|k\tau| \sim 1$), assuming m_Q , ξ_1 , ξ_2 , H , ϵ_B and ϵ_E are constant. In all the plots in this section and the next we use the following parameters

$$m_Q = 3, \quad \epsilon_B = 3 \times 10^{-4}, \quad \epsilon_E = 3 \times 10^{-5}, \quad H = 10^{13} \text{ GeV}. \quad (2.122)$$

In the left panel of Figure 2.8 we plot the sourced right-handed helicity mode function of gravitational waves $h_{R,n=t}$ (by the vacuum gauge field, $t_{R,n=t}$) (solid blue) and the right-handed helicity mode function of the vacuum gravitational wave $h_{A,n=h}$ (dashed orange).

The current observational upper bound on r coming from the most recent CMB experiments [21] is

$$r \equiv \frac{\mathcal{P}_h(k_{\text{CMB}})}{\mathcal{P}_{\mathcal{R}}(k_{\text{CMB}})} < 0.06, \quad (2.123)$$

where $\mathcal{P}_{\mathcal{R}}$ is the power spectrum of curvature perturbations defined in Chapter 1 and $k_{\text{CMB}} = 0.05 \text{ Mpc}^{-1}$.

As we saw in this model, two types of gravitational waves contribute to \mathcal{P}_h . First the vacuum fluctuation coming from the metric perturbations h^{vac} and the sourced gravitational waves coming from the axion-SU(2) spectator sector h^{sourced} . We consider the right-handed helicity mode function for the tensor modes since they are the ones with more sizeable contribution. By calculating the tensor fluctuations numerically we can conclude that the power spectrum for the sourced gravitational waves in the super-horizon

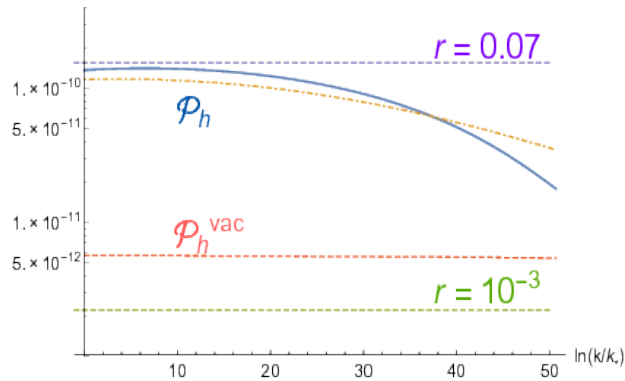


Figure 2.9: The $\mathcal{P}_h^{\text{sourced}}$ (solid blue), the vacuum gravitational wave power spectra $\mathcal{P}_h^{\text{vac}}$ (dashed red) is shown. The green and purple dashed lines show $r = 0.07$ and $r = 10^{-3}$ respectively. This figure is taken from [66].

limit is

$$\mathcal{P}_h^{\text{sourced}} = \frac{H^2}{\pi^2 M_{pl}^2} \left| \sqrt{2kx} \lim_{x \rightarrow 0} h_R^{\text{sourced}} \right|^2 = \frac{H^2}{\pi^2 M_{pl}^2} \left| \sqrt{2kx} \lim_{x \rightarrow 0} h_{R,n=t} \right|^2. \quad (2.124)$$

Let us call the ratio between the sourced gravitational waves and the gravitational waves from vacuum R_{GW} [66], considering the definition of ϵ_B and m_Q , then the tensor-to-scalar-ratio r is given

$$r = \frac{\mathcal{P}_h^{\text{sourced}} + \mathcal{P}_h^{\text{vac}}}{\mathcal{P}_{\mathcal{R}}} = \frac{2g_A^2 \epsilon_B}{\pi^2 m_Q^4 \mathcal{P}_{\mathcal{R}}} (1 + R_{\text{GW}}), \quad (2.125)$$

where $H^2/M_{pl}^2 = g_A^2 \epsilon_B/m_Q^4$.

We are interested in the parameter region that $R_{\text{GW}} > 1$, i.e. where the sourced gravitational waves are larger than the vacuum gravitational waves. We also need r to satisfy the observational upper bound given in (2.123). Since the upcoming CMB observation missions aim at achieving a sensitivity $r \approx 10^{-3}$, the parameter region predicting $r \geq 10^{-3}$ is very interesting.

In Figure 2.9, the authors of [66], show the gravitational waves power spectra. It is visible that $\mathcal{P}_h^{\text{sourced}}$ shown in (solid blue) is larger than $\mathcal{P}_h^{\text{vac}}$ (dashed red), while still not exceeding the upper bound on $r = 0.07$ they are considering.

In [53], the authors have examined the detectability of the axion-SU(2) sourced gravitational waves for the future CMB B-mode polarization, space interferometers and ground-based interferometers.

2.8.2 Gravitational Leptogenesis

Another interesting feature of axion-SU(2) gauge field models of inflation is the possibility of a mechanism to explain the baryon asymmetry of the universe through gravitational leptogenesis. Leptogenesis in gauge field inflation models that use this process has been

previously considered in [40, 41, 42, 43, 44, 45, 46, 47]. In this section we briefly discuss this subject.

A successful baryogenesis requires the following conditions to be satisfied

- Violation of baryon number
- CP violation
- Out of equilibrium state

these conditions are known as the Sakharov conditions [117].

The above conditions are satisfied in these models through gravitational leptogenesis. The chiral asymmetry of the gravitational waves background generated in this setup leads to a non-zero parity-violating gravitational anomaly, $R\tilde{R}$, which, in turn, violates the lepton number conservation and generates the baryon asymmetry of the universe. The configurations of the axion field χ and the gauge field A_μ^α break the CP symmetry and the inflationary solutions for the VEV of the fields are out of equilibrium.

The gravitational anomaly and the lepton current are related through

$$\nabla_\mu J^\mu = \frac{N_{R-L}}{24(16\pi^2)} R_{\mu\nu\alpha\beta} \tilde{R}^{\mu\nu\alpha\beta}, \quad (2.126)$$

where N_{R-L} is the number of right-handed minus left-handed Weyl fermions [118]. What goes on physically is that the asymmetric gravitational wave spectrum acts as a background for the evolution of the Dirac equation and pairs of fermions are created asymmetrically. Lets first define the number density of chiral fermions

$$n_\ell = \frac{N_{R-L}}{24(16\pi^2)a^3} \int d\tau a^4 R\tilde{R}. \quad (2.127)$$

In order to determine the magnitude of the asymmetry, we have to evaluate the number density of chiral fermions generated

$$\langle n_\ell \rangle = \frac{N_{R-L}}{24(8\pi^2)a^3} \int d\tau \int \frac{d^3k}{(2\pi)^{3/2}} \frac{d^3k'}{(2\pi)^{3/2}} e^{i(k-k')\cdot x} (2\pi)^3 \delta(k-k') (F_R(k) - F_L(k)), \quad (2.128)$$

where

$$F_A = \frac{d}{d\tau} \left[k^3 (|h_{A,h}|^2 + |h_{A,t}|^2) - k (|h'_{A,h}|^2 + |h'_{A,t}|^2) \right]. \quad (2.129)$$

Assuming the difference between the right- and left-handed circularly polarized gravitational waves vanishes in the super-horizon limit, we can re-write the above integral as

$$\langle n_\ell \rangle = \frac{N_{R-L}}{24(8\pi^2)a^3} \int d \ln k \left[k^3 (\Delta_R^2 - \Delta_L^2) - k (\Delta_R'^2 - \Delta_L'^2) \right], \quad (2.130)$$

where

$$\Delta_A^2 = \frac{k^3}{\pi^2} (|h_{A,h}|^2 + |h_{A,t}|^2), \quad \Delta_A'^2 = \frac{k^3}{\pi^2} (|h'_{A,h}|^2 + |h'_{A,t}|^2). \quad (2.131)$$

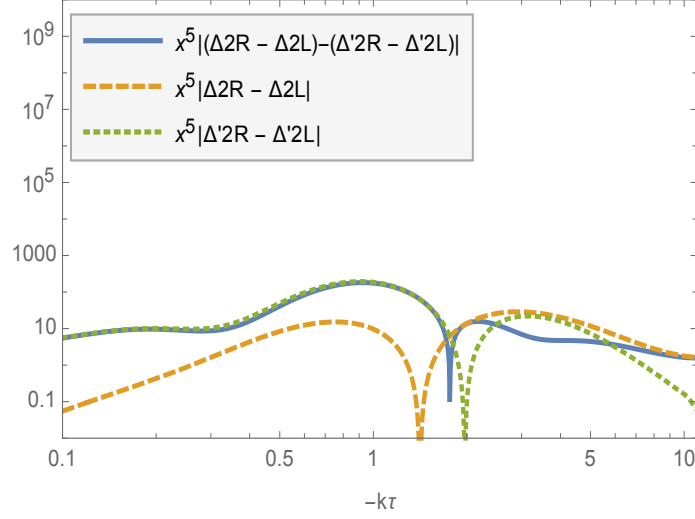


Figure 2.10: The integrand of (2.132) is illustrated (solid blue) as a function of $x = -k\tau$. Separate contributions from $(\Delta_R^2 - \Delta_L^2)$ (dashed orange) and $(\Delta_R'^2 - \Delta_L'^2)$ (dotted green) are shown separately.

In the literature the asymmetry is expressed in terms of a ratio between the lepton asymmetry density $\langle n_\ell \rangle$ and the entropy density s

$$\frac{\langle n_\ell \rangle}{s} = \frac{N_{R-L}}{24(8\pi^2)a_{end}^3} \frac{\int d \ln k \left[k^3(\Delta_R^2 - \Delta_L^2) - k(\Delta_R'^2 - \Delta_L'^2) \right]}{C g_*^{1/4} (H_{end} M_{pl})^{3/2}}, \quad (2.132)$$

where the subscript “end” indicates the value of the parameters at the end of inflation. The parameter g_* is the number of entropy degrees of freedom and $C \simeq 2.3$.

To evaluate the above ratio we need to evaluate the integral and then convert the net lepton number into the net baryon number to compare the results with the observed value for $n_B/n_\gamma = 6.1(\pm 0.04) \times 10^{-10}$. The integrand of (2.132) is shown in Figure 2.10. For deep sub-horizon modes, there is no chiral asymmetry as shown in Figure 2.10, as we approach the horizon the chirality becomes visible. The $n_B/n_\gamma = (-28/79 \langle n_\ell \rangle / s) / 0.14 = 6.1 \times 10^{-10}$ is calculated in [43] that matches the observed value of baryon to photon ratio.

2.8.3 Tensor non-Gaussianity

Another important signature of the gravitational waves produced from the axion-SU(2) gauge fields during inflation is their large non-Gaussianity [36, 37, 38, 39]. In order to evaluate the amplitude of non-Gaussianity of the tensor modes, one has to evaluate the ratio B_h/P_h^2 , where B_h is the bispectrum of the gravitational waves. In these studies it was shown that the amplitude of non-Gaussianity is inversely proportional to the energy density fraction of the gauge field.

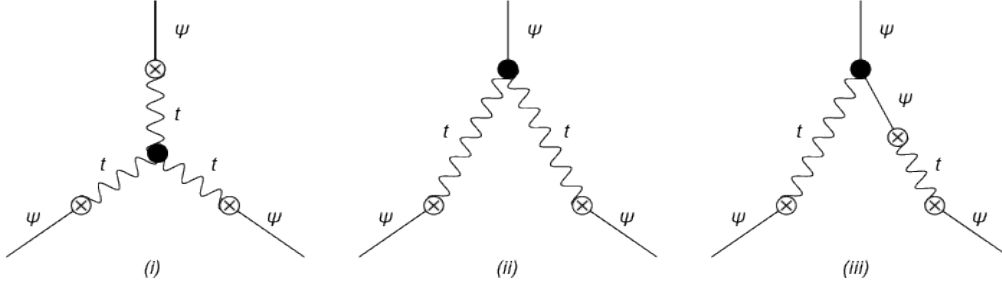


Figure 2.11: Feynman diagrams illustrating the tree-level contributions from the cubic interactions to the bispectrum of gravitational waves. The straight lines show $h_{ij} \equiv \psi_{ij}$ in this plot and the curly lines show t_{ij} . This plot is taken from [36, 37, 109].

Physically, what happens is that the self-interaction of the SU(2) gauge field gives a bispectrum on the tree-level hence this signature is unique to non-Abelian models. Perturbative expansion of the Lagrangian in terms of t_{ij} provides us with a cubic term that represents the three-point vertices (black dots) in the Feynman diagram as shown in Figure 2.11.

Considering (2.114), we can write the bispectrum of the right-handed gravitational waves (we are ignoring the left-handed mode for now since only the right-handed mode function is amplified) in the super-horizon limit as

$$(2\pi)^3 \delta(\mathbf{k}_1 + \mathbf{k}_2 + \mathbf{k}_3) B_h^R(k_1, k_2, k_3) = \lim_{\tau \rightarrow 0} \left(\frac{2}{aM_{pl}} \right)^3 \left\langle \tilde{h}_R(\tau, \mathbf{k}_1) \tilde{h}_R(\tau, \mathbf{k}_2) \tilde{h}_R(\tau, \mathbf{k}_3) \right\rangle. \quad (2.133)$$

For the equilateral shape, the bispectrum is given by $B_h^{R, \text{sourced}}(k, k, k) / |P_h^{R, \text{sourced}}(k)|^2 \simeq 1.816 \exp(0.841m_Q) / \epsilon_B \simeq 0.908 \exp(0.841m_Q) / \Omega_A$ where ϵ_B is given in (2.20) is much smaller than unity and $\Omega_A \equiv (\epsilon_B + \epsilon_E) / 2 \simeq (1 + m_Q^{-2}) \epsilon_B / 2$ is the energy density fraction of the gauge field [37]. This value holds for $3 \lesssim m_Q \lesssim 5$ and is much larger than the contribution from the vacuum, hence the bispectrum is a great tool to distinguish the gravitational waves sourced by axion-SU(2) gauge fields from the gravitational waves coming from the

vacuum.

Chapter 3

Effects of Gravitational Chern-Simons during Axion-SU(2) Inflation

Much of the content of this chapter has been published in [119].

3.1 Introduction

In this chapter we consider the axion-SU(2) gauge field spectator sector [66] together with the gravitational Chern-Simons term coupled to the axion field. In this setup we have the parity-violating terms on both sides of the equation of motion for the tensor metric perturbations; the left-hand side due to the gravitational Chern-Simons term and the right-hand side due to the axion-SU(2) sector. There are many studies focused on the cosmological signatures of the gravitational Chern-Simons term [62, 120, 121, 122, 111, 123, 124, 125, 126, 127, 128, 129, 130]. In this study, we extend these studies to the axion-SU(2) models. In [131, 132, 133, 134], the authors have considered both $F\tilde{F}$ and $R\tilde{R}$ originating from string theory. The non-Abelian gauge field in their consideration does not share the same vacuum expectation value as in our case, hence it does not source gravitational waves linearly.

This chapter, is organized as follows. In section 3.2 we present the model and analyze the background evolution. In section 3.3 we present the second-order Lagrangian for tensor perturbations and compare the gravitational waves with and without the gravitational Chern-Simons term. We discuss the stability and the cut-off scale of the model in section 3.4. We conclude in section 3.5.

3.2 Model Setup and Introduction

3.2.1 Action

We consider the following action. This action minus the last term is equivalent to the action considered in 2.102 in Chapter 2

$$S = S_{EH} + S_\varphi + S_{SPEC} + S_{GCS}, \quad (3.1)$$

where S_{EH} is the Einstein-Hilbert action and S_φ is the inflaton sector action given by

$$S_{EH} = \int d^4x \sqrt{-g} \frac{M_{pl}^2}{2} R, \quad (3.2)$$

$$S_\varphi = \int d^4x \sqrt{-g} \left(-\frac{1}{2} (\partial\varphi)^2 - V(\varphi) \right). \quad (3.3)$$

The spectator sector action S_{SPEC} contains axion and SU(2) gauge fields, where χ is an axion field with potential $U(\chi)$ and a decay constant f :

$$S_{SPEC} = \int d^4x \sqrt{-g} \left(-\frac{1}{2} (\partial\chi)^2 - U(\chi) - \frac{1}{4} F_{\mu\nu}^a F^{a\mu\nu} + \frac{\lambda_1 \chi}{4f} F_{\mu\nu}^a \tilde{F}^{a\mu\nu} \right), \quad (3.4)$$

where

$$F_{\mu\nu}^a = \partial_\mu A_\nu^a - \partial_\nu A_\mu^a - g_A \epsilon^{abc} A_\mu^b A_\nu^c, \quad (3.5)$$

is the field strength tensor of the SU(2) gauge fields, with g_A being the self-coupling constant and ϵ^{abc} the three dimensional anti-symmetric symbol.

The last term in S_{SPEC} is the Chern-Simons interaction, where λ_1/f parametrizes its coupling strength and $\tilde{F}^{a\mu\nu} \equiv \epsilon^{\mu\nu\alpha\beta} F_{\alpha\beta}^a/2$ is the dual of $F_{\mu\nu}^a$. $\epsilon^{\mu\nu\alpha\beta}$ is defined as $\epsilon^{\mu\nu\alpha\beta} \equiv \epsilon^{\mu\nu\alpha\beta}/\sqrt{-g}$, where $\epsilon^{\mu\nu\alpha\beta}$ is the totally anti-symmetric symbol with $\epsilon^{0123} = 1$. The S_{SPEC} is invariant under the local SU(2) transformation. $F\tilde{F}$ is a total derivative and for $\chi = const$, it reduces to a surface term. Hence, we can write $F\tilde{F}$ as

$$F\tilde{F} = \nabla_\mu C^\mu, \quad (3.6)$$

with

$$C^\mu = 2\epsilon^{\mu\nu\alpha\beta} \left(A_\nu^a \partial_\alpha A_\beta^a - \frac{1}{3} \epsilon^{abc} A_\nu^a A_\alpha^b A_\beta^c \right). \quad (3.7)$$

The last term in (3.1) is the gravitational Chern-Simons term coupled to the axion, with coupling strength of λ_2/f :

$$S_{GCS} = \int d^4x \sqrt{-g} \frac{\lambda_2 \chi}{4f} R\tilde{R}, \quad (3.8)$$

where

$$R\tilde{R} = R^\beta{}_\alpha{}^{\gamma\delta} \tilde{R}^\alpha{}_{\beta\gamma\delta}, \quad (3.9)$$

$R^\beta{}_\alpha{}^{\gamma\delta}$ is the Riemann tensor and the dual of the Riemann tensor is

$$\tilde{R}^\alpha{}_{\beta\gamma\delta} = (1/2)\varepsilon_{\sigma\tau\gamma\delta}R^\alpha{}_\beta{}^{\sigma\tau}. \quad (3.10)$$

We can also write $R\tilde{R}$ as

$$R\tilde{R} = 2\nabla_\mu K^\mu, \quad (3.11)$$

with

$$K_\mu = 2\varepsilon^{\mu\alpha\beta\gamma}\left(\frac{1}{2}\Gamma_{\alpha\tau}^\sigma\partial_\beta\Gamma_{\gamma\sigma}^\tau + \frac{1}{3}\Gamma_{\alpha\tau}^\sigma\Gamma_{\beta\eta}^\tau\Gamma_{\gamma\sigma}^\eta\right). \quad (3.12)$$

The gravitational Chern-Simons term is also a total derivative. For $\chi = \text{const}$, it reduces to a surface term.

3.2.2 Background Evolution

In this section, we describe the evolution of the background. As $R\tilde{R}$ vanishes in a Friedmann-Lemaître-Robertson-Walker (FLRW) background, there is no contribution to the background.

The vacuum expectation value of the gauge field is given by [28, 29]

$$A_0^a = 0, \quad A_i^a = \delta_i^a a(t)Q(t). \quad (3.13)$$

The 00-component of the Einstein equations is [66]

$$3M_{pl}^2 H^2 = \frac{\dot{\varphi}^2}{2} + V(\varphi) + \frac{\dot{\chi}^2}{2} + U(\chi) + \frac{3}{2}(\dot{Q} + HQ)^2 + \frac{3}{2}g_A^2 Q^4. \quad (3.14)$$

The equations of motion for the axion and gauge fields are given by [30, 66]

$$\ddot{\chi} + 3H\dot{\chi} + \partial_\chi U = -3\frac{g_A\lambda_1}{f}Q^2(\dot{Q} + HQ), \quad (3.15)$$

$$\ddot{Q} + 3H\dot{Q} + (\dot{H} + 2H^2)Q + 2g_A^2 Q^3 = \frac{g_A\lambda_1}{f}\dot{\chi}Q^2, \quad (3.16)$$

where dots show derivatives with respect to the cosmic time t and $H \equiv \dot{a}/a$ is the Hubble expansion rate. It is useful to define the slow-roll parameters $\epsilon_H \equiv -\dot{H}/H^2$ and write [66]

$$\epsilon_H = \epsilon_\varphi + \epsilon_\chi + \epsilon_B + \epsilon_E, \quad (3.17)$$

where

$$\epsilon_\varphi \equiv \frac{\dot{\varphi}^2}{2H^2M_{pl}^2}, \quad \epsilon_\chi \equiv \frac{\dot{\chi}^2}{2H^2M_{pl}^2}, \quad \epsilon_B \equiv \frac{g_A^2 Q^4}{H^2M_{pl}^2}, \quad \epsilon_E \equiv \frac{(\dot{Q} + HQ)^2}{H^2M_{pl}^2}, \quad (3.18)$$

are all much smaller than unity.

Also we define the following dimensionless parameters

$$m_Q \equiv \frac{g_A Q}{H}, \quad \xi_1 \equiv \frac{\lambda_1 \dot{\chi}}{2fH}, \quad \xi_2 \equiv \frac{1}{2} \frac{\lambda_2 \dot{\chi}}{2fH} \left(\frac{H}{M_{pl}} \right)^2. \quad (3.19)$$

The fourth term in the left hand side of (3.16) becomes $2m_Q^2 H^2 Q$; thus m_Q can be regarded as the mass of Q (divided by H).

In the slow-roll approximation, the following relation holds between m_Q and ξ_1 [66]

$$\xi_1 \simeq m_Q + \frac{1}{m_Q}. \quad (3.20)$$

To prevent instabilities of the scalar perturbations (lower bound) and strong backreaction on the gauge background (upper bound), we consider $\sqrt{2} < m_Q \lesssim 4$ [34, 37, 66, 55]. This implies

$$\xi_2 \simeq \frac{\lambda_2}{2\lambda_1} \left(\frac{H}{M_{pl}} \right)^2 \left(m_Q + \frac{1}{m_Q} \right) \lesssim 10^{-9} \left(\frac{\lambda_2}{\lambda_1} \right), \quad (3.21)$$

where we have used $(H/M_{pl})^2 \lesssim 10^{-9}$. Thus, a sizeable ξ_2 , e.g., $\xi_2 \simeq 10^{-2}$, requires large λ_2/λ_1 , e.g., $(\lambda_2/\lambda_1) = 10^7$. A large hierarchy between λ_2 and λ_1 i.e., $(\lambda_2/\lambda_1) \gg 1$, is in principle allowed, since all the degrees of freedom are coupled to the gravitational Chern-Simons term, but only the charged ones are coupled to the SU(2) Chern-Simons term. Specifically, $\lambda_2 \propto (f/\Lambda)N$ where N is the number of integrated out degrees of freedom and Λ is the cut-off scale of the effective field theory, e.g., the mass of fermions in the loops. Note that this holds assuming that we are integrating out the massive fermions as an example at the same energy scale to get $F\tilde{F}$ and $R\tilde{R}$ simultaneously.

3.3 Tensor Perturbations

Now, we consider tensor perturbations during inflation at linear level. The tensor perturbations are amplified due to the tachyonic instability, whereas the scalar and vector perturbations are not amplified for $m_Q > \sqrt{2}$ [66, 32, 31, 34] in the spectator axion-SU(2) sector.

We have four tensor degrees of freedom: two metric tensor degrees of freedom that represent the gravitational waves and two additional tensor degrees of freedom associated with the SU(2) gauge field. We consider a perturbed FLRW metric as follows

$$ds^2 = a^2(\tau)(-d\tau^2 + (\delta_{ij} + \tilde{h}_{ij})dy^i dy^j), \quad (3.22)$$

where $\tau \simeq -1/aH$ is the conformal time and \tilde{h}_{ij} is a transverse and traceless tensor, i.e. $\partial^i \tilde{h}_{ij} = \tilde{h}_i^i = 0$. We define the Fourier transformed right and left-handed circular polarization states as

$$\tilde{h}_{ij}(\tau, y) = \int \sum_{A=L,R} \frac{d^3k}{(2\pi)^{3/2}} e_{ij}^A(k) \tilde{h}_A(\tau, k) e^{ik \cdot y}, \quad (3.23)$$

where e_{ij}^A is the polarization state tensor for the right ($A = R$) and left-handed ($A = L$) circular polarization states and satisfies the relation

$$ik_a \epsilon^{ab} e_{cb}^R = ke_{cd}^R, \quad ik_a \epsilon^{ab} e_{cb}^L = -ke_{cd}^L, \quad (3.24)$$

where ϵ^{ab}_c is the three dimensional anti-symmetric symbol. For simplicity, we assume that the gravitational waves are propagating along the z spatial direction

$$ds^2 = a^2(\tau) \left[-d\tau^2 + (1 + \tilde{h}_+(\tau, z))dx^2 + (1 - \tilde{h}_+(\tau, z))dy^2 + 2\tilde{h}_\times(\tau, z)dxdy + dz^2 \right]. \quad (3.25)$$

We write the tensor perturbations of the gauge field as $\delta A_i^a = a\tilde{t}_i^a$, where \tilde{t}_i^a is chosen to be transverse and traceless, i.e. $\partial_i \tilde{t}_i^a = \tilde{t}_i^{ai} = 0$. We write the gauge tensor perturbations as $\delta A_i^1 = a(\tilde{t}_+, \tilde{t}_\times, 0)$ and $\delta A_i^2 = a(\tilde{t}_\times, -\tilde{t}_+, 0)$. For our convenience we work with the canonically normalised tensor perturbations

$$h_{ij} \equiv a \frac{M_{pl}}{\sqrt{2}} \tilde{h}_{ij}, \quad t_i^a = \sqrt{2} a \tilde{t}_i^a. \quad (3.26)$$

We define the left and the right helicities as [66]

$$h_{L,R} \equiv \frac{1}{\sqrt{2}}(h_+ \pm ih_\times), \quad t_{L,R} \equiv \frac{1}{\sqrt{2}}(t_+ \pm it_\times). \quad (3.27)$$

Now we write the second order action for the tensor perturbations.

$$\begin{aligned} S = \frac{1}{2} \sum_{A=L,R} \int d\tau d^3k \left\{ \left(1 - \frac{s\lambda_2 \chi'}{4faM_{pl}^2 a} \right) \left[h_A^\dagger h'_A + (-k^2 + 2\mathcal{H}^2) h_A^\dagger h_A - 2\mathcal{H}\Re(h_A^\dagger h_A) \right] \right. \\ \left. + t_A^\dagger t_A \left[sak \left(2g_A Q + \frac{\lambda_1}{f} a\chi' \right) - k^2 - \frac{g_A a Q \lambda_1}{f} \chi' \right] + 2\Re \left[h_A^\dagger t_A - h_A^\dagger t'_A \right] \left(\frac{Q' + \mathcal{H}Q}{M_{pl}} \right) \right. \\ \left. + t_A^\dagger t'_A + 2\Re(h_A t_A^\dagger) \left[-sak \frac{2g_A Q^2}{M_{pl}} - \frac{\mathcal{H}(Q' + \mathcal{H}Q)}{M_{pl}} + \frac{g_A \lambda_1 Q^2 a}{f M_{pl}} \chi' \right] \right\}, \quad (3.28) \end{aligned}$$

where $s = -1, 1$ for the left- and right-handed helicities respectively. A prime denotes the derivative with respect to the conformal time τ , and $\mathcal{H} \equiv a'/a$.

Using the parameters defined in (3.19) in the action, we find

$$\begin{aligned} S = \frac{1}{2} \sum_{A=L,R} \int d\tau d^3k \left\{ \left(1 - s \frac{\xi_2}{\mathcal{H}} k \right) \left[h_A^\dagger h'_A + h_A^\dagger h_A (-k^2 + 2\mathcal{H}^2) - 2\mathcal{H}\Re(h_A^\dagger h_A) \right] \right. \\ \left. + \left(2\Re(h_A^\dagger t_A) - 2\Re(h_A^\dagger t'_A) \right) \mathcal{H}\sqrt{\epsilon_E} + t_A^\dagger t_A \left[2s\mathcal{H}m_Q k + 2s\mathcal{H}\xi_1 k - 2\mathcal{H}^2 m_Q \xi_1 - k^2 \right] \right. \\ \left. + t_A^\dagger t'_A + 2\Re(h_A t_A^\dagger) \left(-2s\mathcal{H}\sqrt{\epsilon_B} k + 2\mathcal{H}^2 \sqrt{\epsilon_B} \xi_1 - \mathcal{H}^2 \sqrt{\epsilon_E} \right) \right\}. \quad (3.29) \end{aligned}$$

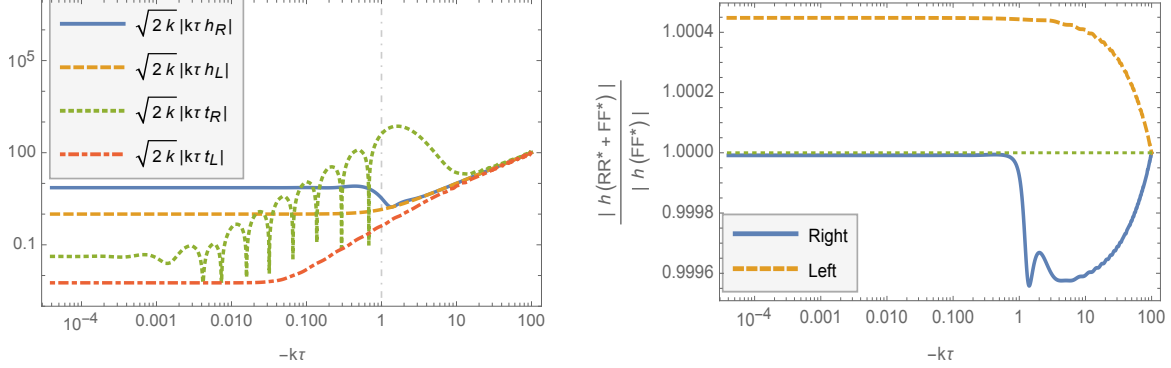


Figure 3.1: **(Left panel)** The sourced linear gravitational wave $\sqrt{2k}|k\tau h_R|$ (solid blue), the left-handed gravitational waves $\sqrt{2k}|k\tau h_L|$ (dashed orange) and the linear right- and left-handed gauge tensor mode functions $\sqrt{2k}|k\tau t_R|$ (dotted green) and $\sqrt{2k}|k\tau t_L|$ (dot-dashed red) are shown. The right-handed helicity gravitational wave grows around the horizon crossing and stays constant afterwards. **(Right panel)** The ratios of the right- (solid blue) and left-handed (dashed orange) helicity mode functions for $\xi_2 = 4.5 \times 10^{-6}$ with respect to those for $\xi_2 = 0$. The horizontal dotted line shows unity.

The equations of motion for the tensor modes up to leading order in slow-roll parameters are

$$\partial_x^2 t_A + \left[1 + \frac{2}{x^2}(m_Q \xi_1 - sx(m_Q + \xi_1))\right] t_A = -\frac{2\sqrt{\epsilon_E}}{x} \partial_x h_A + \frac{2}{x^2} \left[(m_Q - sx)\sqrt{\epsilon_B} + \sqrt{\epsilon_E}\right] h_A, \quad (3.30)$$

$$\left(1 - s\xi_2 x\right) \left[\partial_x^2 h_A + \left(1 - \frac{2}{x^2}\right) h_A\right] - 2s\xi_2 \partial_x h_A = \frac{2\sqrt{\epsilon_E}}{x} \partial_x t_A + \frac{2}{x^2} \left[(m_Q - sx)\sqrt{\epsilon_B}\right] t_A, \quad (3.31)$$

where $x \equiv -k\tau$.

Next we calculate the four tensor modes numerically.

The initial conditions are set as in Chapter 2. Since the tensor-like perturbations in the gauge fields and the tensor metric perturbations are linearly coupled, we expand both in terms of the same pair of creation and annihilation operators [16]

$$h_A(\tau, k) = \sum_{n=h,t} \left[a_{n,k}^A h_{A,n} + a_{n,-k}^{A\dagger} h_{A,n}^* \right], \quad (3.32)$$

$$t_A(\tau, k) = \sum_{n=h,t} \left[a_{n,k}^A t_{A,n} + a_{n,-k}^{A\dagger} t_{A,n}^* \right],$$

where we have the standard commutators

$$[a_{n,k}^A, a_{m,q}^{B\dagger}] = \delta_{n,m} \delta_{A,B} \delta^{(3)}(k - q). \quad (3.33)$$

We have to specify the vacuum (when $-k\tau \gg m_Q$ and $-k\tau\xi_2 < 1$) for the gravitational and gauge fields separately. We divide the vacuum space to two subspaces corresponding

to each field as [34, 80, 43]:

$$\begin{aligned} h_{A,n}(\tau, k) &= \frac{1}{\sqrt{2k}} \delta_{n,h} e^{-ik\tau}, & h'_{A,n}(\tau, k) &= -\frac{1}{\sqrt{2k}} ik \delta_{n,h} e^{-ik\tau}, \\ t_{A,n}(\tau, k) &= \frac{1}{\sqrt{2k}} \delta_{n,t} e^{-ik\tau}, & t'_{A,n}(\tau, k) &= -\frac{1}{\sqrt{2k}} ik \delta_{n,t} e^{-ik\tau}. \end{aligned} \quad (3.34)$$

The solution $h_{A,n=h}$ can be interpreted as the vacuum gravitational wave, whereas $h_{A,n=t}$ as the sourced one (by the vacuum gauge field, $t_{A,n=t}$).

Only the right-handed helicity mode of the tensor perturbations of the SU(2) gauge field t_R is amplified unlike the gravitational waves. In the left panel of Figure 3.1 we show the amplification of $|t_R| = \sqrt{\langle t_R^\dagger t_R \rangle}$ (green line) around the horizon crossing ($|k\tau| \sim 1$), assuming m_Q , ξ_1 , ξ_2 , H , ϵ_B and ϵ_E are constant. In all the plots in this section we use the following parameters

$$m_Q = 3, \quad \epsilon_B = 3 \times 10^{-4}, \quad \epsilon_E = 3 \times 10^{-5}, \quad H = 10^{13} \text{GeV}. \quad (3.35)$$

3.3.1 Without $F\tilde{F}$

To understand the effect of $R\tilde{R}$, we first consider the case where $\xi_1 = 0$ and $m_Q = 0$ in (3.31). The last term on the left hand side of (3.31) acts as a *friction* term for h_L which prevents it from decaying, whereas it acts as an *anti-friction* term for h_R , which makes h_R decay faster. We plot the metric tensor mode functions for different values of ξ_2 in Figure 3.2. The difference between the right- and left-handed helicity modes are negligible for a small value of ξ_2 , as shown in the top-left panel of Figure 3.2. As ξ_2 becomes larger, the difference between the two helicity modes becomes more visible (middle- and bottom-left panels).

In the right panels of Figure 3.2, we show the ratios of the right- and left-handed helicity mode functions with respect to those for $\xi_1 = 0$, $m_Q = 0$ and no gravitational Chern-Simons term, labelled as $h_{\xi_2=\xi_1=0}$. Contrary to the case where gauge fields are present, the left-handed helicity of the metric tensor perturbations is amplified. This difference depends on the relative sign between the coefficients of the parity-violating terms $F\tilde{F}$ and $R\tilde{R}$, i.e., λ_1 in (3.4) and λ_2 in (3.8). The effect of $R\tilde{R}$ on the enhancement/suppression is nearly symmetric as shown in the right panels of Figure 3.2. This enhancement/suppression occurs already deep inside the horizon. On the other hand, amplification of the right-handed helicity of the gauge field occurs near horizon crossing (see the green dotted line in the left panel of Figure 3.1). This difference becomes important in section 3.3.2.

3.3.2 With $F\tilde{F}$

We turn on the $F\tilde{F}$ term with $\xi_1 = 3.3$ ($m_Q = 3$). To capture the effect of $R\tilde{R}$ in axion-SU(2) gauge field models, we plot the ratio of metric tensor mode functions for different values of ξ_2 with respect to those without the gravitational Chern-Simons term, i.e. $\xi_2 = 0$

in Figure 3.1 and 3.3. In the right panel of Figure 3.1 for $\xi_2 = 4.5 \times 10^{-6}$, the contribution of the gravitational Chern-Simons term is small given such a small value of ξ_2 . In Figure 3.3 we have plotted the same as Figure 3.1 for larger values of ξ_2 . After considering different configurations, we conclude that the contribution from the gravitational Chern-Simons term on the left-handed helicity modes is about fifty percent amplification for $\xi_2 = 4.5 \times 10^{-2}$ as shown in Figure 3.3 while the right-handed helicity modes are largely unaffected. This value of ξ_2 requires a large hierarchy between λ_2 and λ_1 , as noted at the end of section 3.2.

For completeness, the right- and left-handed helicity mode functions for four different cases: with $F\tilde{F}$ and $R\tilde{R}$, without $R\tilde{R}$, without $F\tilde{F}$, and without both terms, for different values of ξ_2 are shown in Figure 3.4.

The right-handed helicity modes are unaffected by the gravitational Chern-Simons coupling because they are sourced by the gauge field after horizon crossing, while the gravitational Chern-Simons coupling affects mode functions already deep inside the horizon.

3.4 Stability Analysis

For $k > \mathcal{H}/\xi_2$, the sign of the kinetic term of h_R in the equation (3.29) becomes negative and, consequently, ghost instabilities may, in principle, be introduced into the model [125, 126]. Existence of ghosts does not necessarily translate to catastrophe in a model but translates to the breaking of the effective theory. Let us rewrite the first term in (3.29), $(1 - k\xi_2/\mathcal{H})$ (this is the only problematic term we have to analyse), in physical coordinates. It is given by $(1 - \frac{\xi_2}{H}k_{phy})$, where $k_{phy} \equiv k/a$ is the physical wave number. To show that the gravitational Chern-Simons term in this model is ghost-free, i.e., stable, we have to show that the effective field theory cut-off, Λ , on the physical wave number, k_{phy} , is below H/ξ_2 . Note that we have two new free parameters in this model, the gravitational Chern-Simons coefficient λ_2 in (3.8) and the cut-off Λ . As there are no *a priori* constraints on λ_2 , our strategy is to work our way backwards. Specifically, relying on independently motivated constraints on ξ_1 , we ask what constraint is imposed on λ_2 in order to guarantee that the theory is healthy. Once this question is answered, we will ask how stringent or natural the resulting constraint is.

Let us first take a look at (3.19) and write the relation for λ_2

$$\lambda_2 = 2\xi_2 \frac{\lambda_1}{\xi_1} \left(\frac{M_{pl}}{H} \right)^2. \quad (3.36)$$

To remain in the ghost-free regime we need the cut-off Λ on k_{phy} to be the following:

$$\frac{\xi_2}{H}\Lambda < 1. \quad (3.37)$$

Here we consider two cases, a conservative case where the cut-off Λ does not exceed M_{pl} , and a more radical case where it is around $20H$. We specify the vacuum (when $-k\tau \gg m_Q$ and $-k\tau\xi_2 < 1$), while choosing a cut-off for the gravitational Chern-Simons term we

should note where the tachyonic instability in the gauge sector exists for a given m_Q . Considering $m_Q = 3$ in the equation of motion for the gauge fluctuation, the tachyonic instability takes place around $x \sim 10$. A reasonable cut-off must be chosen far enough to capture the effects of the instability completely. The cut-off $\Lambda = 20H$ is acceptable considering this criteria.

- **Conservative case:** The inequality in (3.37) boils down to $\xi_2 < H/M_{pl}$ [121, 129], given the assumption that Λ does not exceed M_{pl} . Using this in (3.36), we have:

$$\lambda_2 < 2 \left(\frac{\lambda_1}{\xi_1} \right) \left(\frac{M_{pl}}{H} \right). \quad (3.38)$$

- **More radical case:** The inequality in (3.37) boils down to $\xi_2 < 1/20$, given the assumption that Λ is around $20H$. Using this in (3.36), we have:

$$\lambda_2 < \left(\frac{1}{10} \right) \left(\frac{\lambda_1}{\xi_1} \right) \left(\frac{M_{pl}}{H} \right)^2. \quad (3.39)$$

On the right hand side of both inequalities above we have $\xi_1 \sim O(1)$, which guarantees a slow variation of the gauge field, $\lambda_1 \sim O(10)$, and there is an upper bound on the tensor-to-scalar ratio $r \equiv (\mathcal{P}_h/\mathcal{P}_\mathcal{R}) < 0.06$ from not observing tensor modes in the CMB [21] where \mathcal{P}_h and $\mathcal{P}_\mathcal{R}$ are the power spectra of tensor and curvature perturbations, respectively. In our model both the vacuum fluctuations of the metric and the sourced gravitational waves contribute to \mathcal{P}_h . Using the upper bound on r , the measurement of the dimensionless power spectrum of scalar fluctuations, $\Delta_\mathcal{R} \equiv k^3 \mathcal{P}_\mathcal{R}/2\pi^2 \approx 2.2 \times 10^{-9}$, and the expression for the dimensionless power spectrum of tensor fluctuations only from the metric vacuum fluctuations $\Delta_h^{\text{vac}} \equiv k^3 \mathcal{P}_h^{\text{vac}}/2\pi^2 = 2H^2/(\pi^2 M_{pl}^2)$, we get a bound on the last term $(M_{pl}/H)^2 \gtrsim 1.5 \times 10^9$.

Therefore, in both (3.38) and (3.39), the right side is expected to be a very large number. As there is no stringent constraint on the free parameter λ_2 in our model, the model is not disfavoured by fine-tuning arguments.

3.5 Discussion

We have studied the effect of the gravitational Chern-Simons term coupled to the axion field on production and propagation of gravitational waves during inflation with the spectator axion-SU(2) sector [66]. Both parity-violating terms $R\tilde{R}$ and $F\tilde{F}$ exist simultaneously.

We find that the effect of the $R\tilde{R}$ term on chiral gravitational waves can be as large as fifty percent amplification for the left-handed helicity mode functions compared to the case without the $R\tilde{R}$ term for $\xi_2 = 4.5 \times 10^{-2}$. The effect is smaller for smaller values of ξ_2 . The right-handed helicity mode functions are unaffected regardless of the values of ξ_2 . Moreover, using the existing bounds on m_Q and ξ_1 from the spectator axion-SU(2) gauge field sector, and requiring that the cut-off scale of the theory, Λ , is in the conservative

case $\Lambda = M_{pl}$ and in a more radical case $\Lambda = 20H$, we put constraints on the new free parameter λ_2 in our model to remain in the ghost-free regime. Consequently, values of ξ_2 are related to the cut-off scale of the theory, Λ . $\xi_2 = 4.5 \times 10^{-2}$ is allowed when $\Lambda = 20H$ and $\xi_2 = 4.5 \times 10^{-6}$ is allowed when $\Lambda = M_{pl}$.

We conclude that the inflation models with the spectator axion-SU(2) sector remain phenomenologically viable in the presence of the gravitational Chern-Simons term.

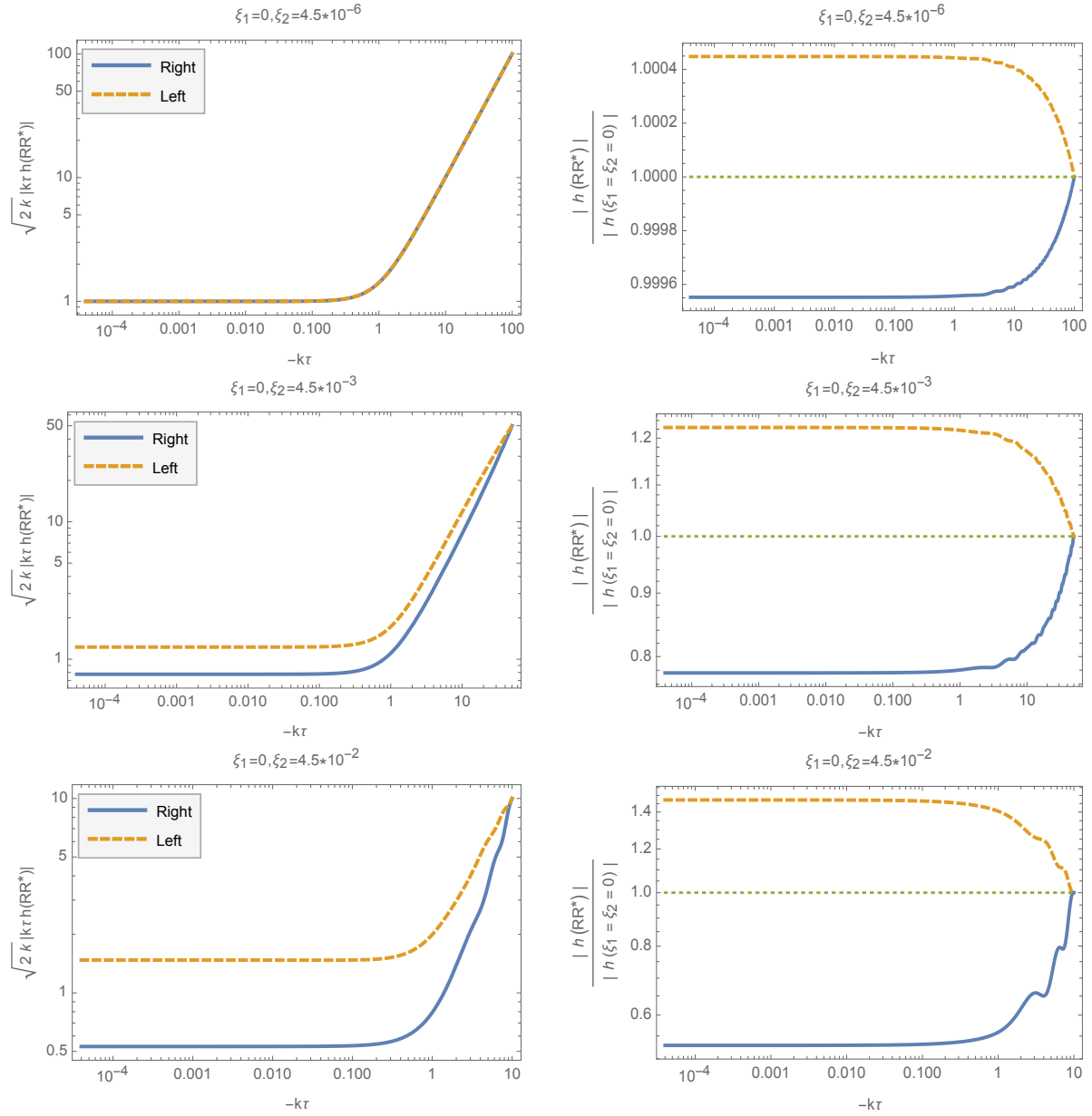


Figure 3.2: **(Left panel)** The right- (solid blue) and left-handed (dashed orange) helicity mode functions of $h_{R,L}$ for different values of ξ_2 and $\xi_1 = 0$. We plot $\sqrt{2k}|k\tau h_{R,L}|$. **(Right panel)** The ratios of the right- (solid blue) and left-handed (dashed orange) helicity mode functions for the same values of ξ_2 as the left panels with respect to those for $\xi_2 = \xi_1 = 0$. The horizontal dotted line shows unity.

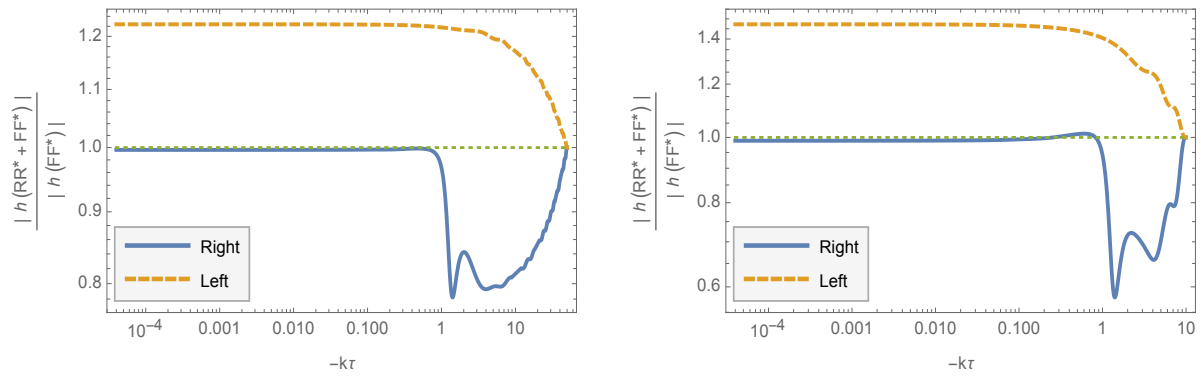


Figure 3.3: Same as the right panel of Figure 3.1, but for $\xi_2 = 4.5 \times 10^{-3}$ (**Left panel**) and $\xi_2 = 4.5 \times 10^{-2}$ (**Right panel**).

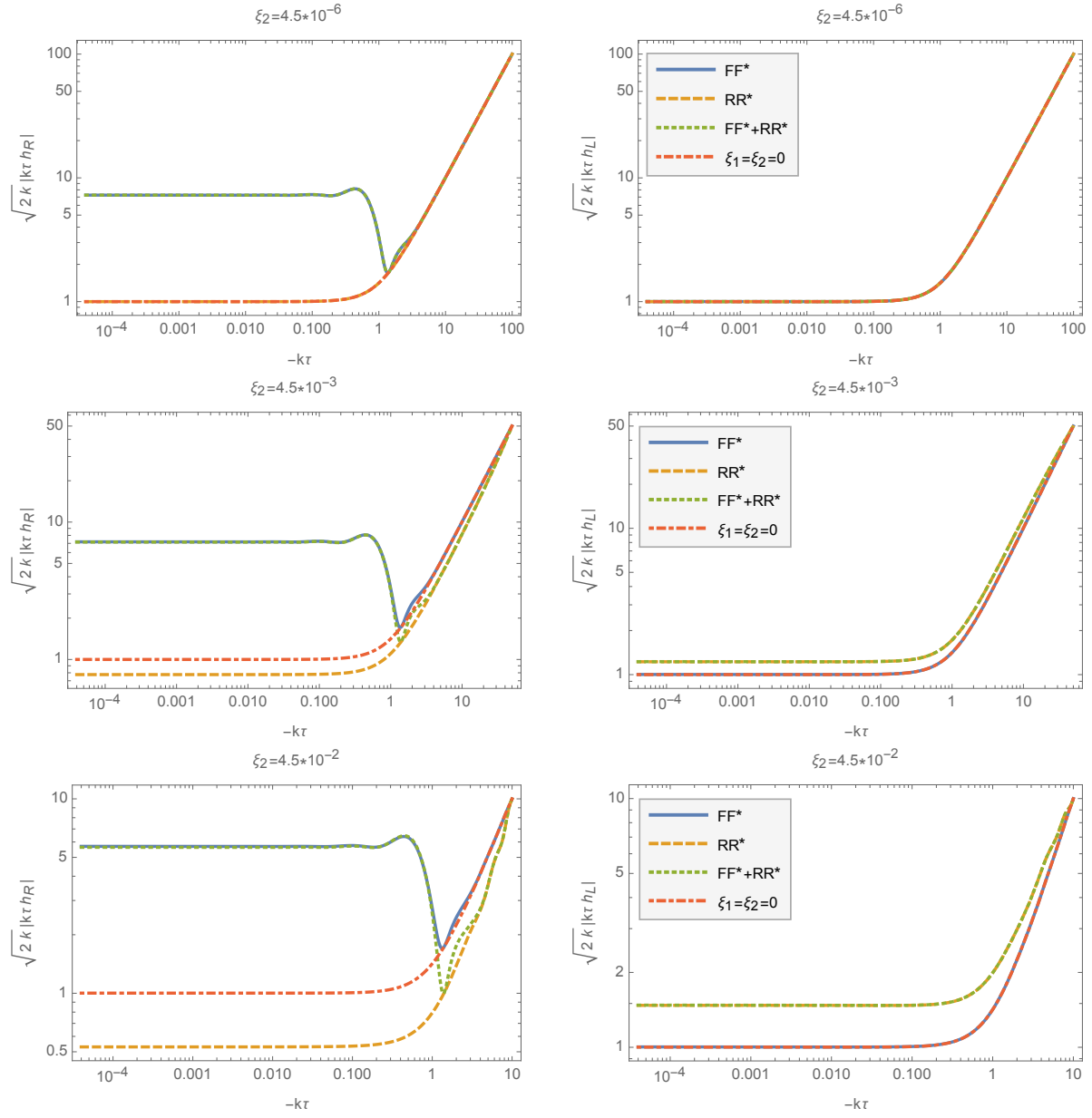


Figure 3.4: **(Left panel)** The right-handed helicity mode functions for four different cases: FF^* and RR^* (dotted green), without RR^* (solid blue), without FF^* (dashed orange), and without both terms (dot-dashed red) for different values of ξ_2 . ξ_1 is always $\xi_1 = 3.3$ ($m_Q = 3$). **(Right panel)** Same as the left panels but for the left-handed modes.

Chapter 4

Fermions Production and Backreaction from Axion-SU(2) Gauge Fields

Much of the content of this chapter has been published in [56].

4.1 Introduction

In this chapter, we continue our investigation of particle production by the axion-SU(2) gauge field during inflation. This time, we study the coupling of the SU(2) gauge field to a pair of massive Dirac fermions, $i\bar{\Psi}\not{D}\Psi$. We also add an interaction between axion and the axial fermionic current, $J^{\mu 5}\partial_{\mu}\varphi/\Lambda$, which is naturally expected in this type of models. We then calculate the backreaction of the fermions on the SU(2) and axion background dynamics during inflation, following the framework we have established in [54, 55].

Fermionic particle production in de Sitter spacetime and its backreaction implications have been studied in the context of U(1) theories. The case of a nontrivial Abelian gauge field background without an axion was studied in [135]; a slowly evolving axion background with no gauge field interactions was studied in [136, 137]; and a combination of the two, assuming a massless fermion, was studied in [138].

As for the SU(2) gauge field background, the simplest fermionic non-Abelian model was studied in the recent work [58], where a massless doublet of Dirac fields is coupled covariantly to the SU(2) gauge field. The main aim of [58] is to describe the fermionic particle production due to the quantum (loop) effects from the Adler-Bell-Jackiw (or chiral) anomaly. Our work not only extends their study to models with massive fermions and coupling to the axion background but also provides the first detailed analysis of the allowed parameter space by cosmological and backreaction constraints.

We find important differences between the Abelian and non-Abelian models. Most notably, the leading order fermionic backreaction on the SU(2) background is significantly smaller than in the fermionic abelian [135] (as well as in the scalar abelian [139, 140, 141,

142, 143]) cases. We find that the tree-level backreaction on the axion field background vanishes, unlike in U(1) theories [136, 137, 138]. We thus conclude that the inflationary scenarios involving an axion-SU(2) gauge field spectator sector remain healthy and unaffected when couplings to gauged fermions are present.

The organization of this chapter is the following. In Section 4.2 we introduce our model. Section 4.3 deals with the evolution and production of fermions in the time-dependent axion-SU(2) background in a de Sitter universe. The results for the induced fermionic backreaction are presented in Section 4.4. Section 4.5 is devoted to discussions and concluding remarks. We have removed some appendices of [56] from the thesis. We refer the reader to the paper if more details are needed.

4.2 Fermions in Axion-SU(2) Gauge Field Inflation

In this work, we study the fermion production by a slowly evolving homogeneous and isotropic SU(2) gauge field during inflation. The class of inflationary models involving such SU(2) VEV has been first introduced in [28, 29]. Since then several different realizations of this class of models have been introduced and studied, e.g. [30, 31]. See section 2 of [55] and the references therein for a recent review on the models so far in the literature.

We assume slow-roll inflation with the background FLRW metric

$$ds^2 = a^2(\tau)(-d\tau^2 + \delta_{ij}dx^i dx^j), \quad (4.1)$$

where τ is the conformal time, and the scale factor, $a(\tau)$, is related to the Hubble parameter, H , as

$$a(\tau) \simeq -\frac{1}{H\tau} \quad \text{and} \quad H \simeq \text{const}, \quad (4.2)$$

Besides, we have a homogeneous and isotropic SU(2) gauge field background generated by one of the possible realizations of this class of models. In the temporal gauge ($\mathbf{A}_0 = 0$), we have in [28, 29]

$$\mathbf{A}_i = A_i^a \mathbf{T}_a = a(\tau)\psi(\tau)\delta_i^a \mathbf{T}_a, \quad (4.3)$$

where $\psi(\tau) \simeq \text{const.}$ during slow-roll inflation and \mathbf{T}_a are the generators of the SU(2) group

$$= i\epsilon^c_{ab} \mathbf{T}_c. \quad (4.4)$$

Therefore, the gauge field has an almost constant energy density during inflation.

To avoid clutter, we suppress the spacetime indices of the Dirac matrices and spinors, unless otherwise stated. For example, γ^0 is a 4×4 matrix, which can act on the four-dimensional column spinor Ψ^1 or can be acted upon by the four-dimensional row spinor $\bar{\Psi}^1 \equiv \Psi^{1\dagger}\gamma^0$. We will have to deal with eight-, four- and two-component spinors which are acted upon by 8×8 , 4×4 and 2×2 matrices, respectively to this end, we adopt the following notation. If the spinor (or the matrix) is eight (or 8×8) dimensional, then it has a tilde(\sim) on top. The notation for the four-dimensional spinor and matrix remains

unaltered, whereas the two-dimensional ones are written in boldface. Finally, \mathbf{I}_n represents the $n \times n$ identity matrix and the gamma matrices are in the Dirac representation unless otherwise stated.

We consider a charged doublet of Dirac fermions,

$$\tilde{\Psi} = \begin{pmatrix} \Psi^1 \\ \Psi^2 \end{pmatrix}, \quad (4.5)$$

with the free theory

$$S_{\text{fermion}} = \int d^4x \sqrt{-g} \left[i \tilde{\Psi} \not{D} \Psi - m \tilde{\Psi} \Psi \right], \quad (4.6)$$

where $\tilde{\Psi} = (\bar{\Psi}_1 \ \bar{\Psi}_2)$, and \not{D} is

$$\not{D} \equiv D_\mu \otimes \gamma^\mu = \mathbf{e}^\mu_\alpha [\mathbf{I}_2 \nabla_\mu - ig_A A_\mu^a \mathbf{T}_a] \otimes \gamma^\alpha, \quad (4.7)$$

in which \otimes is the Kronecker product, $\mathbf{e}^\mu_\alpha = a^{-1}(\tau) \delta^\mu_\alpha$ are the vierbeins given by $g^{\mu\nu} = \mathbf{e}^\mu_\alpha \mathbf{e}^\nu_\beta \eta^{\alpha\beta}$, and γ^α are the flat space Dirac matrices

$$\{\gamma^\alpha, \gamma^\beta\} = 2\eta^{\alpha\beta} \mathbf{I}_4. \quad (4.8)$$

See Appendix A for details. Notice that $\gamma^\mu = \mathbf{e}^\mu_\alpha \gamma^\alpha = a(\tau) \delta^\mu_\alpha \gamma^\alpha$ where α and β represent the local Lorentz indices while μ and ν represent spacetime coordinates.

Since the inflationary setups in this study involves axion fields, the fermionic sector can have the following effective interaction with the axion (see for instance [144])

$$S_{\text{int}} = \int d^4x \sqrt{-g} \left[\beta \frac{\lambda \varphi}{f} \nabla_\mu J_5^\mu \right], \quad (4.9)$$

where φ is the axion field, f is the axion decay constant, λ is the dimensionless coefficient of the Chern-Simons interaction term of the axion, and β is a dimensionless parameter. The quantity β can be of order unity. Here, J_5^μ is the fermionic chiral current given as

$$J_5^\mu \equiv \tilde{\Psi} \mathbf{I}_2 \otimes (\gamma^\mu \gamma^5) \Psi, \quad (4.10)$$

where $\gamma^5 = i\gamma^0\gamma^1\gamma^2\gamma^3$.

In summary, the fermion theory in an SU(2)-axion background given in (4.3) and $\varphi = \varphi(\tau)$ is specified by

$$\begin{aligned} S = \int a^4 d\tau dx^3 \frac{i}{a} \tilde{\Psi} \left[\mathbf{I}_2 (\partial_\tau + \frac{3}{2} \mathcal{H}) \otimes \gamma^0 + \delta_\alpha^i (\mathbf{I}_2 \partial_i - ia g_A \psi \delta_i^a \mathbf{T}_a) \otimes \gamma^\alpha \right. \\ \left. + iam \mathbf{I}_8 + \beta \frac{i\lambda \partial_\tau \varphi}{f} \mathbf{I}_2 \otimes (\gamma^0 \gamma^5) \right] \Psi, \end{aligned} \quad (4.11)$$

where the second term in the right-hand side comes from the spin connection (see (A.2) and (A.7)). As implied by the above action, the canonically normalized field is

$$\tilde{\Psi} \equiv a^{\frac{3}{2}} \tilde{\Psi} /, \quad (4.12)$$

64 4. Fermions Production and Backreaction from Axion-SU(2) Gauge Fields

Using $\mathbf{T}_a = \frac{1}{2}\boldsymbol{\sigma}^i\delta_i^a$ ($\boldsymbol{\sigma}^i$ are the Pauli matrices) in (4.11), we find

$$\mathcal{L} = i\tilde{\Psi}\left[\mathbf{I}_2\partial_\tau \otimes \gamma^0 + \left(\mathbf{I}_2\partial_i - \frac{i}{2}\xi_A\mathcal{H}\boldsymbol{\sigma}^i\right) \otimes \gamma^i + i\mu_m\mathcal{H}\mathbf{I}_8 + 2i\xi_\varphi\mathcal{H}\mathbf{I}_2 \otimes (\gamma^0\gamma^5)\right]\tilde{\Psi}, \quad (4.13)$$

where ξ_A , ξ_φ , and μ_m are dimensionless parameters defined by

$$\xi_A \equiv \frac{g_A\psi}{H}, \quad \xi_\varphi \equiv \beta\frac{\lambda\partial_\tau\varphi}{2afH}, \quad \mu_m \equiv \frac{m}{H}. \quad (4.14)$$

For the sake of completeness, here we define another related dimensionless quantity in the axion inflation backgrounds

$$\xi \equiv \frac{\lambda\partial_\tau\varphi}{2afH}, \quad (4.15)$$

which during slow-roll inflation is related to ξ_A as $\xi \simeq \frac{1+\xi_A^2}{\xi_A}$ in the massless SU(2) models. In our setup, ξ and ξ_φ are related as

$$\xi_\varphi = \beta\xi, \quad (4.16)$$

where β is of order unity.

Up to this point, we wrote the theory in the flavor frame in terms of an 8-spinor in real space. However, in Fourier space, the setup is reducible into two irreducible 4-spinor subsectors in the helicity representation. Therefore, it is more convenient to go to Fourier space and write it in the extended helicity frame which we introduce now.

In Fourier space, we expand $\tilde{\Psi}$ as

$$\tilde{\Psi}(\tau, \mathbf{x}) = \int d^3k e^{i\mathbf{k}\cdot\mathbf{x}}\tilde{\Psi}_{\mathbf{k}}. \quad (4.17)$$

For a given momentum, \mathbf{k} , the 8×8 helicity projection operators are

$$\tilde{P}_\pm(\mathbf{k}) = \mathbf{I}_2 \otimes \left(\frac{\mathbf{I}_4 \pm k^i\gamma^i}{2}\right), \quad (4.18)$$

which decompose $\tilde{\Psi}_{\mathbf{k}}$ into the plus and minus helicity states as

$$\tilde{\Psi}_{\mathbf{k}}^\pm = \tilde{P}_\pm(\mathbf{k})\tilde{\Psi}_{\mathbf{k}}, \quad (4.19)$$

where $\tilde{\Psi}_{\mathbf{k}} = \tilde{\Psi}_{\mathbf{k}}^+ + \tilde{\Psi}_{\mathbf{k}}^-$. The helicity representation decomposes the system of 8-spinor in real space in Eq. (4.13) into two subspaces of 4-spinors in real space

$$\tilde{\Psi} = \Psi^+ \oplus \Psi^- = \begin{pmatrix} \Psi^+ \\ \Psi^- \end{pmatrix}, \quad (4.20)$$

such that the theory is given as

$$S[\tilde{\Psi}] = S_+[\Psi^+] + S_-[\Psi^-].$$

More details of the setup is given in the Appendix of [56]. Here, we write the final theories for each of the 4-spinor subspaces in Fourier space ¹

$$S_+ = \int d\tau d^3k \bar{\Psi}_{\mathbf{k}}^+ \left[i\gamma^0 \partial_\tau - \gamma^3 k - \left(2\xi_\varphi - \frac{\xi_A}{2} \right) \mathcal{H} \lambda_4 - \mu_m \mathcal{H} I_4 \right] \Psi_{\mathbf{k}}^+, \quad (4.21)$$

$$S_- = \int d\tau d^3k \bar{\Psi}_{\mathbf{k}}^- \left[i\gamma^0 \partial_\tau + \gamma^3 k - \left(2\xi_\varphi + \frac{\xi_A}{2} \right) \mathcal{H} \lambda_4 - \mu_m \mathcal{H} I_4 + \gamma^1 \xi_A \mathcal{H} \right] \Psi_{\mathbf{k}}^-, \quad (4.22)$$

where

$$\gamma^0 = \begin{pmatrix} \mathbf{I}_2 & \mathbf{0} \\ \mathbf{0} & -\mathbf{I}_2 \end{pmatrix}, \quad \gamma^i = \begin{pmatrix} \mathbf{0} & \boldsymbol{\sigma}^i \\ -\boldsymbol{\sigma}^i & \mathbf{0} \end{pmatrix}, \quad \lambda_4 = \begin{pmatrix} \mathbf{0} & \mathbf{I}_2 \\ -\mathbf{I}_2 & \mathbf{0} \end{pmatrix}. \quad (4.23)$$

The field equations of $\Psi_{\mathbf{k}}^+$ and $\Psi_{\mathbf{k}}^-$ are

$$\left[i\gamma^0 \partial_\tau - \gamma^3 k - \left(2\xi_\varphi - \frac{\xi_A}{2} \right) \mathcal{H} \lambda_4 - \mu_m \mathcal{H} I_4 \right] \Psi_{\mathbf{k}}^+ = 0, \quad (4.24)$$

and

$$\left[i\gamma^0 \partial_\tau + \gamma^3 k - \left(2\xi_\varphi + \frac{\xi_A}{2} \right) \mathcal{H} \lambda_4 - \mu_m \mathcal{H} I_4 + \gamma^1 \xi_A \mathcal{H} \right] \Psi_{\mathbf{k}}^- = 0, \quad (4.25)$$

respectively. Therefore, we have two independent Dirac fermions, $\Psi_{\mathbf{k}}^\pm$. We solve them in the next section. Before that, let us take a closer look at the field equations to have a qualitative understanding of each field.

Our Dirac fields can be expanded as

$$\Psi_{\mathbf{k}}^\pm = \sum_{s=\pm} \begin{pmatrix} \psi_s^{\pm\uparrow}(\tau, k) \mathbf{E}_s \\ s \psi_s^{\pm\downarrow}(\tau, k) \mathbf{E}_s \end{pmatrix}, \quad (4.26)$$

where $\psi_s^{\pm\uparrow}(\tau, k)$ and $\psi_s^{\pm\downarrow}(\tau, k)$ are mode functions and \mathbf{E}_s with $s = \pm 1$ are the two-spinor polarization states

$$\mathbf{E}_+ = \begin{pmatrix} 1 \\ 0 \end{pmatrix} \quad \text{and} \quad \mathbf{E}_- = \begin{pmatrix} 0 \\ 1 \end{pmatrix}. \quad (4.27)$$

Since we are already in the helicity states of the given momentum \mathbf{k} , the 2-spinor polarization states are k -independent.

Using the above in the field equations (4.24) and (4.25), we find the following.

¹Note that the form of the S_+ is very similar to the action describing a *single* fermion derivatively coupled to an axion considered in [137]. There the authors make a local chiral transformation of the fermion basis to avoid unphysical behaviour of the Bogoliubov coefficients in the massless fermion. However, for sufficiently large masses ($\mu_m \gtrsim 1$) the transformation is not necessary. We do not follow this prescription for two reasons. First, the focus of the current study is limited to ($\mu_m \gtrsim 1$). Second, the transformation is not applicable in the presence of our non-abelian gauge field. In particular, it does not simplify the S_- action, because of the last term in the action.

- For the plus spinor field: the field is decoupled in terms of the polarization spinor \mathbf{E}_s . Thus, we have two pairs of coupled field equations for each polarization.
- For the minus spinor field: the field equation is not diagonalizable in terms of \mathbf{E}_s . That is because of the extra (time dependent) term proportional to γ^1 in the minus field equation (4.25). As a result, we have four coupled field equations. In the limit of either being well inside the horizon, i.e. $k \gg \mathcal{H}$, or $\xi_A \ll 1$, this term is negligible and the system reduces to two pairs of coupled field equations.

4.3 Fermion Production

We now calculate the evolution of the plus and minus fermionic fields, $\Psi_{\mathbf{k}}^{\pm}$. Since these 4-spinors are decoupled [see Eqs. (4.24) and (4.25)], we consider them separately.

4.3.1 Ψ^+ Spinors

We begin with the $\Psi_{\mathbf{k}}^+$ modes, described by the S_+ action given in Eq. (4.21). Since the modes are four-dimensional objects, their first order in time linear equation of motion, Eq. (4.24), should yield four linearly independent 4-spinor solutions, i.e.,

$$\Psi_{\mathbf{k}}^+ = \sum_{s=\pm} \left[U_{s,\mathbf{k}}^+(\tau) a_{s,\mathbf{k}}^+ + V_{s,-\mathbf{k}}^+(\tau) b_{s,-\mathbf{k}}^{+\dagger} \right], \quad (4.28)$$

where creation and annihilation operators satisfy

$$\begin{aligned} \{a_{s,\mathbf{k}}^+, a_{s',\mathbf{k}'}^{+\dagger}\} &= \delta_{ss'} \delta^{(3)}(\mathbf{k} - \mathbf{k}'), \\ \{b_{s,\mathbf{k}}^+, b_{s',\mathbf{k}'}^{+\dagger}\} &= \delta_{ss'} \delta^{(3)}(\mathbf{k} - \mathbf{k}'). \end{aligned} \quad (4.29)$$

We then decompose $U_{s,\mathbf{k}}^+$ and $V_{s,\mathbf{k}}^+$ as

$$U_{s,\mathbf{k}}^+(\tau) = \frac{1}{\sqrt{2}} \begin{pmatrix} \mathbf{E}_s u_s^\uparrow(k, \tau) \\ s \mathbf{E}_s u_s^\downarrow(k, \tau) \end{pmatrix}, \quad (4.30)$$

and

$$V_{s,-\mathbf{k}}^+(\tau) = \frac{1}{\sqrt{2}} \begin{pmatrix} \mathbf{E}_s v_s^\uparrow(k, \tau) \\ s \mathbf{E}_s v_s^\downarrow(k, \tau) \end{pmatrix}, \quad (4.31)$$

where \mathbf{E}_s are the 2-spinor polarization states defined in (4.27).

Using the procedure in that will be explained shortly we can derive the initial conditions,

$$u_s^\uparrow(k, \tau) = v_s^{\uparrow*}(k, \tau) \quad \text{and} \quad u_s^\downarrow(k, \tau) = -v_s^{\downarrow*}(k, \tau). \quad (4.32)$$

Since $u_s^{\uparrow\downarrow}$ and $v_s^{\uparrow\downarrow}$ depend on each other, we can first solve the field equations of $u_s^{\uparrow\downarrow}$, and then use (4.32) to find $v_s^{\uparrow\downarrow}$ and read $V_{s,-\mathbf{k}}^+(\tau)$ as

$$V_{s,-\mathbf{k}}^+(\tau) = \frac{1}{\sqrt{2}} \begin{pmatrix} \mathbf{E}_s u_s^{\uparrow*}(k, \tau) \\ -s \mathbf{E}_s u_s^{\downarrow*}(k, \tau) \end{pmatrix}. \quad (4.33)$$

Upon substituting the ansatz (4.28) and (4.30) into the field equation (4.24), we arrive at two sets of coupled field equations for each polarization:

$$(i\partial_\tau - \mu_m \mathcal{H})u_s^\uparrow - \left[k + s \left(2\xi_\varphi - \frac{\xi_A}{2} \right) \mathcal{H} \right] u_s^\downarrow = 0, \quad (4.34)$$

$$(i\partial_\tau + \mu_m \mathcal{H})u_s^\downarrow - \left[k + s \left(2\xi_\varphi - \frac{\xi_A}{2} \right) \mathcal{H} \right] u_s^\uparrow = 0. \quad (4.35)$$

To find analytical solutions we make the following decomposition

$$u_s^\uparrow = \frac{1}{\sqrt{2\tilde{\tau}}} (Y_s + Z_s) \quad \text{and} \quad u_s^\downarrow = \frac{1}{\sqrt{2\tilde{\tau}}} (Y_s - Z_s), \quad (4.36)$$

where $\tilde{\tau}$ is the physical momentum rescaled by H , i.e. ,

$$\tilde{\tau} \equiv \frac{k}{aH} = -k\tau. \quad (4.37)$$

The coupled set of first order differential Eqs. (4.34) and (4.35) can be decoupled into two second order differential equations for Y_s and Z_s as

$$\partial_{\tilde{\tau}}^2 Y_s + \left[1 - \frac{2i\kappa_s^+}{\tilde{\tau}} + \frac{1/4 - \mu^{+2}}{\tilde{\tau}^2} \right] Y_s = 0, \quad (4.38)$$

$$\partial_{\tilde{\tau}}^2 Z_s + \left[1 - \frac{2i\tilde{\kappa}_s^+}{\tilde{\tau}} + \frac{1/4 - \mu^{+2}}{\tilde{\tau}^2} \right] Z_s = 0, \quad (4.39)$$

where κ_s^+ , and $\tilde{\kappa}_s^+$ are

$$\kappa_s^+ = \frac{1}{2} + is \left(2\xi_\varphi - \frac{\xi_A}{2} \right), \quad (4.40)$$

and

$$\tilde{\kappa}_s^+ = -\frac{1}{2} + is \left(2\xi_\varphi - \frac{\xi_A}{2} \right), \quad (4.41)$$

while μ^+ is

$$\mu^+ = i \left[\mu_m^2 + \left(2\xi_\varphi - \frac{\xi_A}{2} \right)^2 \right]^{\frac{1}{2}}. \quad (4.42)$$

The general solutions for equations (4.38) and (4.39) are $W_{\kappa,\mu}(-2i\tilde{\tau})$ and $M_{\kappa,\mu}(-2i\tilde{\tau})$ Whittaker functions. Setting the Bunch-Davies vacuum as the initial condition for u_s^\uparrow and u_s^\downarrow ,

$$\lim_{\tau \rightarrow -\infty} u_s^\uparrow(\tau, k) = \frac{1}{(2\pi)^{\frac{3}{2}}} \frac{e^{-ik\tau}}{\sqrt{2k}}, \quad (4.43)$$

and

$$\lim_{\tau \rightarrow -\infty} u_s^\downarrow(\tau, k) = \frac{1}{(2\pi)^{\frac{3}{2}}} \frac{e^{-ik\tau}}{\sqrt{2k}}, \quad (4.44)$$

68 4. Fermions Production and Backreaction from Axion-SU(2) Gauge Fields

and using the asymptotic form of the W and M functions in (B.1), we find that Y_s and Z_s are given by

$$Y_s = b_{1s} W_{\tilde{\kappa}_s^+, \mu^+}(-2i\tilde{\tau}), \quad (4.45)$$

and

$$Z_s = b_{2s} W_{\tilde{\kappa}_s^+, \mu^+}(-2i\tilde{\tau}). \quad (4.46)$$

Therefore, in the asymptotic past limit, we have $Z_s = \frac{i}{2}(b_{2s}/b_{1s})\tilde{\tau}^{-1}Y_s \ll Y_s$. Combination of the Bunch-Davies vacuum condition in (4.43) and the asymptotic form of the W function in (B.1) gives $b_{1s} = \frac{1}{(2\pi)^{\frac{3}{2}}} e^{s(\xi_A/4 - \xi_\varphi)\pi}$. Moreover, subtracting (4.35) from (4.34) and keeping the dominant terms in the asymptotic past limit, we find $b_{2s} = -i\mu_m b_{1s}$. Finally, we have

$$\begin{aligned} Y_s &= \frac{1}{(2\pi)^{\frac{3}{2}}} e^{s(\xi_A/4 - \xi_\varphi)\pi} W_{\tilde{\kappa}_s^+, \mu^+}(-2i\tilde{\tau}), \\ Z_s &= -\frac{i\mu_m}{(2\pi)^{\frac{3}{2}}} e^{s(\xi_A/4 - \xi_\varphi)\pi} W_{\tilde{\kappa}_s^+, \mu^+}(-2i\tilde{\tau}). \end{aligned} \quad (4.47)$$

Note that the amplitudes and the relative phases of the Bunch-Davies vacuum modes are such that the corresponding Hamiltonian is diagonalized. We present the detailed calculation of the Hamiltonian here. We note that the Hamiltonian diagonalization leaves a residual freedom in choosing the initial conditions for the mode functions. The same applies to the computation in the next section. In both cases, we chose a set of initial conditions for which the Hamiltonian is diagonalized in the sub-horizon limit.

The Hamiltonian is derived from the actions, given in Eqs. (4.21) and (4.22), by defining the Lagrangian $S_\pm \equiv \int d\tau L_\pm$ and then carrying out a Legendre transformation. We derive the Hamiltonians for S_+ and S_- separately and diagonalize them afterwards. Before we calculate the Hamiltonian, we need to explain the quantization procedure for the fermions in S_+ and S_- .

4.3.2 Quantization of the S_+ fermions

The quantization procedure for the $\Psi_{\mathbf{k}}^+$ modes is the following. We first define the canonical conjugate momenta

$$\pi_{\mathbf{k},\alpha}^{\Psi_+} = \frac{\delta S_+}{\delta \partial_\tau \Psi_{\mathbf{k},\alpha}^+} = i\Psi_{+,\mathbf{k},\alpha}^*, \quad (4.48)$$

where α runs from 1 to 4. We then promote $\Psi_{\mathbf{k}}^+$ and $\pi_{\mathbf{k}}^{\Psi_+}$ to quantum operators, obeying the canonical equal-time anticommutation relations

$$\begin{aligned} \{\Psi_{\mathbf{k},\alpha}^+(\tau), \Psi_{\mathbf{k}',\beta}^+(\tau)\} &= 0, \\ \{\pi_{\mathbf{k},\alpha}^{\Psi_+}(\tau), \pi_{\mathbf{k}',\beta}^{\Psi_+}(\tau)\} &= 0, \\ \{\Psi_{\mathbf{k},\alpha}^+(\tau), \pi_{\mathbf{k}',\beta}^{\Psi_+}(\tau)\} &= i(2\pi)^{-3} \delta_{\alpha\beta} \delta^{(3)}(\mathbf{k} - \mathbf{k}'). \end{aligned} \quad (4.49)$$

We also impose that the time-independent coefficients in Eq. (4.28) are the standard anticommuting creation and annihilation operators, i.e.,

$$\begin{aligned} \{a_{s,\mathbf{k}}^+, a_{s',\mathbf{k}'}^{+\dagger}\} &= \delta_{ss'} \delta^{(3)}(\mathbf{k} - \mathbf{k}'), \\ \{b_{s,\mathbf{k}}^+, b_{s',\mathbf{k}'}^{+\dagger}\} &= \delta_{ss'} \delta^{(3)}(\mathbf{k} - \mathbf{k}'), \end{aligned} \quad (4.50)$$

with all other anticommutators vanishing. The canonical quantization expressions in Eqs. (4.49,4.50) yield the following normalization condition

$$\sum_{s=\pm} \left[(U_{s,k}^+(\tau))_\alpha (U_{s,k}^{+\dagger}(\tau))_\beta + (V_{s,k}^+(\tau))_\alpha (V_{s,k}^{+\dagger}(\tau))_\beta \right] = \delta_{\alpha\beta} (2\pi)^{-3}. \quad (4.51)$$

One can check that each term in the square brackets is indeed a constant, i.e., preserved by the equation of motion given in Eq. (4.24). In the following section each constant is determined after assuming that at very early times the modes are in the Bunch-Davies vacuum, i.e.,

$$\lim_{k\tau \rightarrow -\infty} U_{s,k}^+(\tau) \propto e^{-ik\tau}, \quad \lim_{k\tau \rightarrow -\infty} V_{s,k}^+(\tau) \propto e^{ik\tau}, \quad (4.52)$$

corresponding to the positive and negative frequency solutions, respectively. In addition to that, the amplitudes and the relative phases of the Bunch-Davies vacuum modes are such that the corresponding Hamiltonian is diagonalized.

4.3.3 S_+ Hamiltonian

For S_+ ,

$$\begin{aligned} H_+ &= \int d^3k \left(\pi_{\mathbf{k},\alpha}^{\Psi_+} \partial_\tau \Psi_{\mathbf{k},\alpha}^+ \right) - L_+ \\ &= \int d^3k \Psi_{\mathbf{k}}^{+\dagger} \gamma^0 \left[\gamma^3 k + \left(2\xi_\varphi - \frac{\xi_A}{2} \right) \mathcal{H} \lambda_4 + \mu_m \mathcal{H} I_4 \right] \Psi_{\mathbf{k}}^+. \end{aligned} \quad (4.53)$$

Using the mode function expansion from Eqs. (4.28) and (4.30) in the Hamiltonian, we arrive at

$$H_+ = \int d^3k \sum_{s=\pm} \frac{1}{2} (a_{s,\mathbf{k}}^{+\dagger}, b_{s,-\mathbf{k}}^+) \begin{pmatrix} E(u_s^\uparrow, u_s^\downarrow) & F^*(u_s^{\uparrow,\downarrow}, v_s^{\uparrow,\downarrow}) \\ F(u_s^{\uparrow,\downarrow}, v_s^{\uparrow,\downarrow}) & E(v_s^\uparrow, v_s^\downarrow) \end{pmatrix} \begin{pmatrix} a_{s,\mathbf{k}}^+ \\ b_{s,-\mathbf{k}}^+ \end{pmatrix}, \quad (4.54)$$

where

$$\begin{aligned} E(u_s^\uparrow, u_s^\downarrow) &= 2 \left[k + s \left(2\xi_\varphi - \frac{\xi_A}{2} \right) \mathcal{H} \right] \Re(u_s^{\uparrow*} u_s^\downarrow) + \mu_m \mathcal{H} (|u_s^\uparrow|^2 - |u_s^\downarrow|^2), \\ F(u_s^{\uparrow,\downarrow}, v_s^{\uparrow,\downarrow}) &= \left[k + s \left(2\xi_\varphi - \frac{\xi_A}{2} \right) \mathcal{H} \right] (u_s^\downarrow v_s^{\uparrow*} + u_s^\uparrow v_s^{\downarrow*}) + \mu_m \mathcal{H} (v_s^{\uparrow*} u_s^\uparrow - v_s^{\downarrow*} u_s^\downarrow). \end{aligned} \quad (4.55)$$

70 4. Fermions Production and Backreaction from Axion-SU(2) Gauge Fields

To bring the Hamiltonian into a diagonal form we make a time-dependent Bogoliubov transformation

$$\begin{pmatrix} \check{a}_{s,\mathbf{k}}^+(\tau) \\ \check{b}_{s,-\mathbf{k}}^{+\dagger}(\tau) \end{pmatrix} = \begin{pmatrix} \alpha_{s,k}(\tau) & \beta_{s,k}(\tau) \\ -\beta_{s,k}^*(\tau) & \alpha_{s,k}^*(\tau) \end{pmatrix} \begin{pmatrix} a_{s,\mathbf{k}}^+ \\ b_{s,-\mathbf{k}}^{+\dagger} \end{pmatrix}. \quad (4.56)$$

The new set of time-dependent creation and annihilation operators, $\check{a}_{s,\mathbf{k}}^+(\tau)$ and $\check{b}_{s,-\mathbf{k}}^{+\dagger}(\tau)$, respect the canonical anticommutation relations, given in Eq. (4.50), iff the Bogoliubov coefficients satisfy

$$|\alpha_{s,k}(\tau)|^2 + |\beta_{s,k}(\tau)|^2 = 1. \quad (4.57)$$

This condition is met and the Hamiltonian is diagonalized as

$$H_+ = \int d^3k \sum_{s=\pm} \left[\check{a}_{s,\mathbf{k}}^{+\dagger}(\tau) \check{a}_{s,\mathbf{k}}^+(\tau) - \check{b}_{s,-\mathbf{k}}^+ \check{b}_{s,-\mathbf{k}}^{+\dagger}(\tau) \right] \omega_{s,k}(\tau), \quad (4.58)$$

for

$$\begin{aligned} |\beta_{s,k}(\tau)|^2 &= \frac{1}{2} \left[1 - \frac{E(u_s^\uparrow, u_s^\downarrow) - E(v_s^\uparrow, v_s^\downarrow)}{\sqrt{4|F(u_s^{\uparrow,\downarrow}, v_s^{\uparrow,\downarrow})|^2 + (E(u_s^\uparrow, u_s^\downarrow) - E(v_s^\uparrow, v_s^\downarrow))^2}} \right], \\ |\alpha_{s,k}(\tau)|^2 &= \frac{1}{2} \left[1 + \frac{E(u_s^\uparrow, u_s^\downarrow) - E(v_s^\uparrow, v_s^\downarrow)}{\sqrt{4|F(u_s^{\uparrow,\downarrow}, v_s^{\uparrow,\downarrow})|^2 + (E(u_s^\uparrow, u_s^\downarrow) - E(v_s^\uparrow, v_s^\downarrow))^2}} \right], \end{aligned} \quad (4.59)$$

$$\alpha_{s,k}(\tau) = |\alpha_{s,k}(\tau)| e^{i\phi_F}, \quad \beta_{s,k}(\tau) = |\beta_{s,k}(\tau)| e^{-i\phi_F},$$

$$F(u_s^{\uparrow,\downarrow}, v_s^{\uparrow,\downarrow}) = |F(u_s^{\uparrow,\downarrow}, v_s^{\uparrow,\downarrow})| e^{2i\phi_F}.$$

The effective frequency is given by

$$\omega_{s,k}(\tau) = \frac{E(u_s^\uparrow, u_s^\downarrow) + E(v_s^\uparrow, v_s^\downarrow)}{4} + \frac{1}{4} \sqrt{4|F(u_s^{\uparrow,\downarrow}, v_s^{\uparrow,\downarrow})|^2 + (E(u_s^\uparrow, u_s^\downarrow) - E(v_s^\uparrow, v_s^\downarrow))^2}. \quad (4.60)$$

It is important to note that the amplitudes and the relative phases of the Bunch-Davies vacuum modes are such that the corresponding Hamiltonian is diagonalized. The following analysis will fix our initial conditions for the positive and negative frequency solutions.

The Bunch-Davies vacuum is defined as

$$a_{s,\mathbf{k}}^+ |0_{BD}\rangle = 0, \quad b_{s,\mathbf{k}}^+ |0_{BD}\rangle = 0, \quad (4.61)$$

whereas the instantaneous (or quasiparticle) vacuum as

$$\check{a}_{s,\mathbf{k}}^+(\tau) |0_\tau\rangle = 0, \quad \check{b}_{s,\mathbf{k}}^+(\tau) |0_\tau\rangle = 0. \quad (4.62)$$

We work in the Heisenberg picture and we assume that the Universe is in the Bunch-Davies vacuum. The expectation values of observables are calculated with respect to it, i.e., the expected particle number is given by

$$\begin{aligned} \check{N}_{s,\mathbf{k}}(\tau) &= \langle 0_{BD} | \check{n}_{s,\mathbf{k}}(\tau) | 0_{BD} \rangle \\ &= \langle 0_{BD} | \check{a}_{s,\mathbf{k}}^{+\dagger}(\tau) \check{a}_{s,\mathbf{k}}^+(\tau) | 0_{BD} \rangle = |\beta_{s,k}(\tau)|^2. \end{aligned} \quad (4.63)$$

Hence, $|\beta_{s,k}(\tau)|^2$ is the occupation number of particles with given s and \mathbf{k} at a time τ .

We assume that at very early times, $k\tau \rightarrow -\infty$, $\Psi_{\mathbf{k}}^+$ starts in the Bunch-Davies vacuum, i.e., its particle occupation numbers vanish:

$$\lim_{k\tau \rightarrow -\infty} \beta_{s,k}(\tau) = 0. \quad (4.64)$$

Then it follows from Eq. (4.59) that $\lim_{k\tau \rightarrow -\infty} F(u_s^{\uparrow,\downarrow}, v_s^{\uparrow,\downarrow}) = 0$, which is satisfied, according to Eq. (4.55), if $\lim_{k\tau \rightarrow -\infty} (u_s^{\uparrow}(k, \tau) - v_s^{\uparrow*}(k, \tau)) = 0$ and $\lim_{k\tau \rightarrow -\infty} (u_s^{\downarrow}(k, \tau) + v_s^{\downarrow*}(k, \tau)) = 0$. Note that there is some residual freedom in choosing the latter such that the Hamiltonian is diagonalized. One can show that the last two conditions are preserved by the equations of motion, i.e., if imposed initially they hold at later times (for arbitrary τ) as well:

$$u_s^{\uparrow}(k, \tau) = v_s^{\uparrow*}(k, \tau) \quad \text{and} \quad u_s^{\downarrow}(k, \tau) = -v_s^{\downarrow*}(k, \tau). \quad (4.65)$$

Eqs. (4.55), (4.59) and (4.60) then yield (for all τ)

$$\begin{aligned} E(u_s^{\uparrow}, u_s^{\downarrow}) &= -E(v_s^{\uparrow}, v_s^{\downarrow}), \\ |\beta_{s,k}(\tau)|^2 &= \frac{1}{2} \left[1 - \frac{E(u_s^{\uparrow}, u_s^{\downarrow})}{2\omega_{s,k}(\tau)} \right], \\ |\alpha_{s,k}(\tau)|^2 &= \frac{1}{2} \left[1 + \frac{E(u_s^{\uparrow}, u_s^{\downarrow})}{2\omega_{s,k}(\tau)} \right], \end{aligned} \quad (4.66)$$

where the effective frequency has been simplified to

$$\omega_{s,k}(\tau) = \frac{1}{2} \sqrt{|F|^2 + E(u_s^{\uparrow}, u_s^{\downarrow})^2}. \quad (4.67)$$

The last condition one has to impose for Eq. (4.64) to hold is $\lim_{k\tau \rightarrow -\infty} \Re(u_s^{\uparrow*}(k, \tau)u_s^{\downarrow}(k, \tau)) = 1$.

Note that then in the Bunch-Davies limit $\lim_{k\tau \rightarrow -\infty} \omega_{s,k} = k$.

Therefore, after applying Eqs. (4.51) and (4.52) and

$$\begin{aligned} \lim_{k\tau \rightarrow -\infty} (u_s^{\uparrow}(k, \tau) - v_s^{\uparrow*}(k, \tau)) &= 0, \\ \lim_{k\tau \rightarrow -\infty} (u_s^{\downarrow}(k, \tau) + v_s^{\downarrow*}(k, \tau)) &= 0, \\ \lim_{k\tau \rightarrow -\infty} \Re(u_s^{\uparrow*}(k, \tau)u_s^{\downarrow}(k, \tau)) &= 1, \end{aligned} \quad (4.68)$$

to Eqs. (4.36) and (4.45) we can completely fix the solutions for the $u_s^{\uparrow,\downarrow}(k, \tau)$ mode functions, whereas the solutions for $v_s^{\uparrow,\downarrow}(k, \tau)$ follow from Eq. (4.32). We also made use of the asymptotic form of the Whittaker function in (B.1) in Appendix B.

Before we go on further with our analysis, we should emphasize that as it was pointed out at the end of Appendix B in [137], the sudden transition and the final saturation of

72 4. Fermions Production and Backreaction from Axion-SU(2) Gauge Fields

the Bogoliubov coefficients $|\beta_{s,k}(\tau)|^2$ in the small mass regime shows unphysical behavior. As shown in the Figure 4.1, for the massless case ($\mu_m = 0$) (top row) and small mass case ($\mu_m = 0.01$) (middle row) the Bogoliubov coefficients behave nonphysically. That is the reason why we are only trusting our analysis for sufficiently larger masses ($\mu_m \gtrsim 1$) which are well behaved as it is shown in the bottom row of Fig. 4.1.

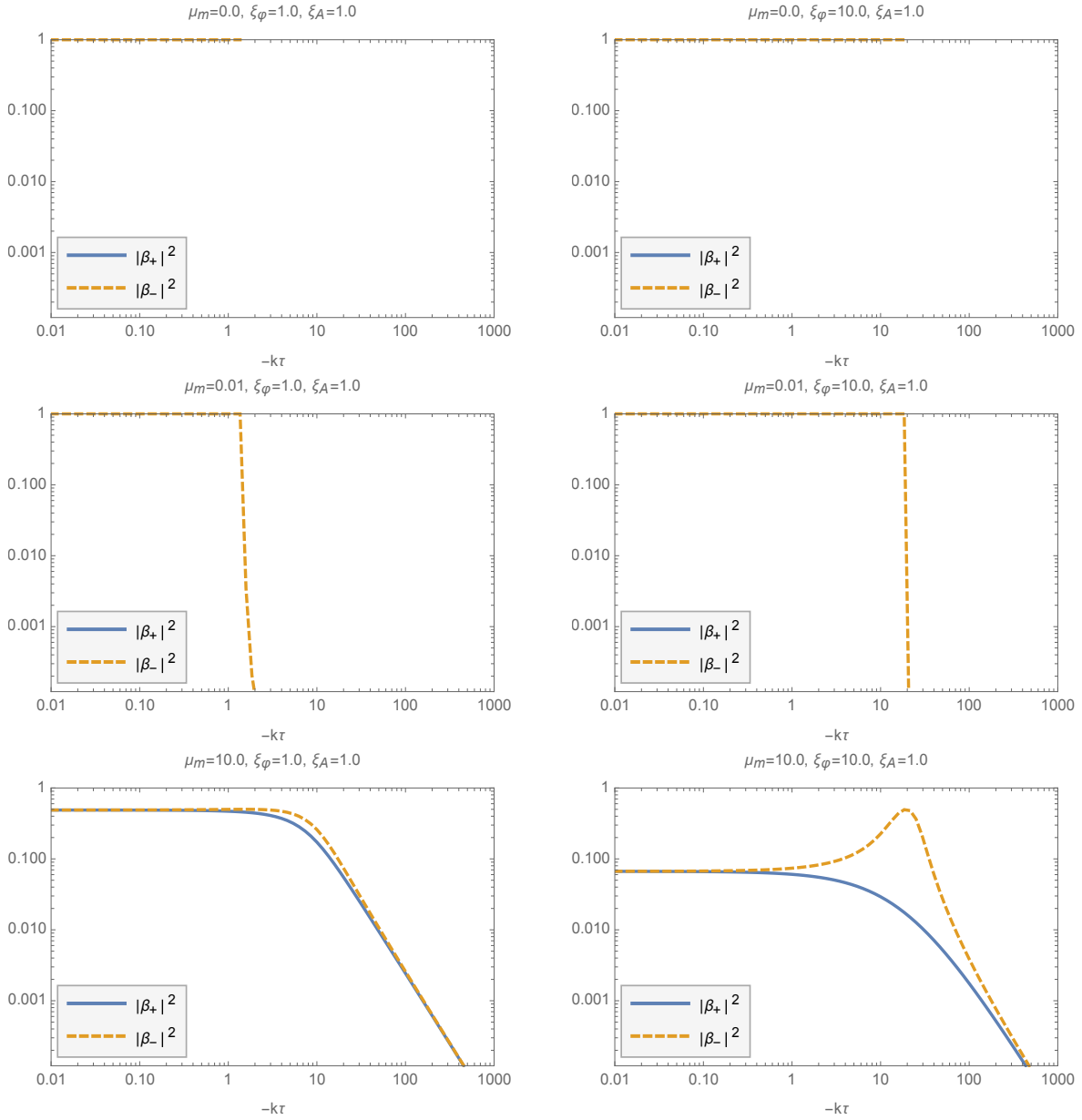


Figure 4.1: **(Top row)** The Bogoliubov coefficients $|\beta_{+,k}(\tau)|^2$ (solid blue) and $|\beta_{-,k}(\tau)|^2$ (dashed orange) is shown for the parameters $\{\mu_m, \xi_\varphi, \xi_A = 0, 1, 1\}$ (left panel) and $\{\mu_m, \xi_\varphi, \xi_A = 0, 10, 1\}$ (right panel). **(Middle row)** The same as first row but for the parameters $\{\mu_m, \xi_\varphi, \xi_A = 0.01, 1, 1\}$ (left panel) and $\{\mu_m, \xi_\varphi, \xi_A = 0.01, 10, 1\}$ (right panel). **(Bottom row)** The same as first row but for the parameters $\{\mu_m, \xi_\varphi, \xi_A = 10, 1, 1\}$ (left panel) and $\{\mu_m, \xi_\varphi, \xi_A = 10, 10, 1\}$ (right panel). For small masses (middle row) and the massless case (top row) the Bogoliubov coefficients shows unphysical behavior.

4.3.4 Ψ^- Spinors

Next, we calculate the $\Psi_{\mathbf{k}}^-$ modes, described by the S_- action given in Eq. (4.22). Since the modes are four-dimensional objects, their first order in time linear equation of motion, Eq. (4.25), should yield four linearly independent 4-spinor solutions, i.e.,

$$\Psi_{\mathbf{k}}^- = \sum_{s=\pm} \left[U_{s,\mathbf{k}}^-(\tau) a_{s,\mathbf{k}}^- + V_{s,-\mathbf{k}}^-(\tau) b_{s,-\mathbf{k}}^{-\dagger} \right], \quad (4.69)$$

where creation and annihilation operators satisfy

$$\begin{aligned} \{a_{s,\mathbf{k}}^-, a_{s',\mathbf{k}'}^{-\dagger}\} &= \delta_{ss'} \delta^{(3)}(\mathbf{k} - \mathbf{k}'), \\ \{b_{s,\mathbf{k}}^-, b_{s',\mathbf{k}'}^{-\dagger}\} &= \delta_{ss'} \delta^{(3)}(\mathbf{k} - \mathbf{k}'). \end{aligned} \quad (4.70)$$

The Lagrangian of the minus subspace is not diagonalizable in a time-independent frame. Hence, the helicity eigenstates are only the eigenstates of the Lagrangian in the asymptotic past limit. Therefore, we adopt a more general trial vector solution:

$$\begin{aligned} U_{s,k}^-(\tau) &= \frac{1}{\sqrt{2}} \begin{pmatrix} \mathbf{E}_s u_{s,+}^\uparrow(k, \tau) \\ s \mathbf{E}_s u_{s,+}^\downarrow(k, \tau) \end{pmatrix} + \frac{1}{\sqrt{2}} \begin{pmatrix} \mathbf{E}_{-s} u_{s,-}^\uparrow(k, \tau) \\ -s \mathbf{E}_{-s} u_{s,-}^\downarrow(k, \tau) \end{pmatrix}, \\ V_{s,k}^-(\tau) &= \frac{1}{\sqrt{2}} \begin{pmatrix} \mathbf{E}_s v_{s,+}^\uparrow(k, \tau) \\ s \mathbf{E}_s v_{s,+}^\downarrow(k, \tau) \end{pmatrix} + \frac{1}{\sqrt{2}} \begin{pmatrix} \mathbf{E}_{-s} v_{s,-}^\uparrow(k, \tau) \\ -s \mathbf{E}_{-s} v_{s,-}^\downarrow(k, \tau) \end{pmatrix}, \end{aligned} \quad (4.71)$$

where \mathbf{E}_s are the 2-spinor polarization states defined in (4.27). Since in the asymptotic past limit the system is diagonalized in this particular basis, we have

$$\begin{aligned} \lim_{\tilde{\tau} \rightarrow \infty} u_{s,-}^\uparrow(k\tau) &= \lim_{\tilde{\tau} \rightarrow \infty} u_{s,-}^\downarrow(k\tau) = 0, \\ \lim_{\tilde{\tau} \rightarrow \infty} v_{s,-}^\uparrow(k\tau) &= \lim_{\tilde{\tau} \rightarrow \infty} v_{s,-}^\downarrow(k\tau) = 0. \end{aligned} \quad (4.72)$$

Using the procedure that we will explain shortly, one can derive the initial conditions,

$$u_{s,+}^\uparrow(k, \tau) = v_{s,+}^{\uparrow*}(k, \tau), \quad u_{s,+}^\downarrow(k, \tau) = -v_{s,+}^{\downarrow*}(k, \tau). \quad (4.73)$$

Since $u_{s,p}^{\uparrow\downarrow}$ and $v_{s,p}^{\uparrow\downarrow}$ depend on each other, we can first solve the field equations of $u_{s,p}^{\uparrow\downarrow}$, and then, use (4.73) to read $v_{s,p}^{\uparrow\downarrow}$ from their corresponding $u_{s,p}^{\uparrow\downarrow}$.

After the substitution of the ansatz from Eq. (4.71) into the equation of motion (4.25), we arrive at

$$\begin{aligned} (i\partial_\tau - \mu_m \mathcal{H}) u_{s,p}^\uparrow + \left[k - sp \left(2\xi_\varphi + \frac{\xi_A}{2} \right) \mathcal{H} \right] u_{s,p}^\downarrow - sp \xi_A \mathcal{H} u_{s,-p}^\downarrow &= 0, \\ (i\partial_\tau + \mu_m \mathcal{H}) u_{s,p}^\downarrow + \left[k - sp \left(2\xi_\varphi + \frac{\xi_A}{2} \right) \mathcal{H} \right] u_{s,p}^\uparrow + sp \xi_A \mathcal{H} u_{s,-p}^\uparrow &= 0. \end{aligned} \quad (4.74)$$

Note also that for each given s and p , we have a pair of coupled equations between $p = +$ and $p = -$ fields.

Following our approach from the previous section, we make the decomposition

$$u_{s,p}^\uparrow = \frac{1}{\sqrt{2\tilde{\tau}}} (Y_{s,p} + Z_{s,p}) \quad (4.75)$$

and

$$u_{s,p}^\downarrow = \frac{1}{\sqrt{2\tilde{\tau}}} (Y_{s,p} - Z_{s,p}) , \quad (4.76)$$

yielding

$$\begin{aligned} i\partial_{\tilde{\tau}} Y_{s,p} - \left[1 - \frac{sp(4\xi_\varphi + \xi_A) - i}{2\tilde{\tau}} \right] Y_{s,p} + \frac{\mu_m}{\tilde{\tau}} Z_{s,p} - \frac{sp\xi_A}{\tilde{\tau}} Z_{s,-p} &= 0, \\ i\partial_{\tilde{\tau}} Z_{s,p} + \left[1 - \frac{sp(4\xi_\varphi + \xi_A) + i}{2\tilde{\tau}} \right] Z_{s,p} + \frac{\mu_m}{\tilde{\tau}} Y_{s,p} + \frac{sp\xi_A}{\tilde{\tau}} Y_{s,-p} &= 0. \end{aligned} \quad (4.77)$$

We can reduce the above coupled first order equations to pairs of coupled second order equations:

$$\begin{aligned} \partial_{\tilde{\tau}}^2 Y_{s,p} + \left[1 + \frac{i - 2sp(\xi_\varphi + \xi_A/2)}{\tilde{\tau}} + \frac{1/4 + \mu_m^2 + (\xi_\varphi + \xi_A/2)^2 + \xi_A^2}{\tilde{\tau}^2} \right] Y_{s,p} \\ - \frac{2\xi_A(\xi_\varphi + \xi_A/2)}{\tilde{\tau}^2} Z_{s,-p} &= 0, \end{aligned} \quad (4.78)$$

$$\begin{aligned} \partial_{\tilde{\tau}}^2 Z_{s,-p} + \left[1 - \frac{i - 2sp(\xi_\varphi + \xi_A/2)}{\tilde{\tau}} + \frac{1/4 + \mu_m^2 + (\xi_\varphi + \xi_A/2)^2 + \xi_A^2}{\tilde{\tau}^2} \right] Z_{s,-p} \\ - \frac{2\xi_A(\xi_\varphi + \xi_A/2)}{\tilde{\tau}^2} Y_{s,p} &= 0. \end{aligned} \quad (4.79)$$

Unlike before, the system cannot be solved analytically. Therefore, we solve them numerically. Furthermore, the amplitudes and the phases of the modes are adjusted to diagonalize the Hamiltonian.

4.3.5 Quantization of the S_- fermions

The quantization prescription for the $\Psi_{\mathbf{k}}^-$ modes remains unchanged. It begins with the definition of the canonical conjugate momenta,

$$\pi_{\mathbf{k},\alpha}^{\Psi^-} = \frac{\delta S_-}{\delta \partial_\tau \Psi_{\mathbf{k},\alpha}^-} = i\Psi_{\mathbf{k},\alpha}^{-,*}, \quad (4.80)$$

where α runs from 1 to 4. Then $\Psi_{\mathbf{k}}^-$ and $\pi_{\mathbf{k}}^{\Psi^-}$ are promoted to quantum operators, satisfying the canonical equal-time anticommutation relations

$$\begin{aligned} \{\Psi_{\mathbf{k},\alpha}^-(\tau), \Psi_{\mathbf{k}',\beta}^-(\tau)\} &= 0, \\ \{\pi_{\mathbf{k},\alpha}^{\Psi^-}(\tau), \pi_{\mathbf{k}',\beta}^{\Psi^-}(\tau)\} &= 0, \\ \{\Psi_{\mathbf{k},\alpha}^-(\tau), \pi_{\mathbf{k}',\beta}^{\Psi^-}(\tau)\} &= i(2\pi)^{-3} \delta_{\alpha\beta} \delta^{(3)}(\mathbf{k} - \mathbf{k}'). \end{aligned} \quad (4.81)$$

76 4. Fermions Production and Backreaction from Axion-SU(2) Gauge Fields

We again postulate that the time-independent coefficients in Eq. (4.69) are the standard anticommuting creation and annihilation operators, i.e.,

$$\begin{aligned} \{a_{s,\mathbf{k}}^-, a_{s',\mathbf{k}'}^{-\dagger}\} &= \delta_{ss'} \delta^{(3)}(\mathbf{k} - \mathbf{k}'), \\ \{b_{s,\mathbf{k}}^-, b_{s',\mathbf{k}'}^{-\dagger}\} &= \delta_{ss'} \delta^{(3)}(\mathbf{k} - \mathbf{k}'), \end{aligned} \quad (4.82)$$

with the rest of the anticommutators vanishing. Eqs. (4.81) and (4.82) then imply the normalization condition

$$\sum_{s=\pm} \left[(U_{s,k}^-(\tau))_\alpha (U_{s,k}^{-\dagger}(\tau))_\beta + (V_{s,k}^-(\tau))_\alpha (V_{s,k}^{-\dagger}(\tau))_\beta \right] = \delta_{\alpha\beta} (2\pi)^{-3}. \quad (4.83)$$

Every term in the square brackets is constant, according to the equation of motion given in Eq. (4.25). To find the constants, we again assume that the early-time modes are in the Bunch-Davies vacuum,

$$\lim_{k\tau \rightarrow -\infty} U_{s,k}^-(\tau) \propto e^{-ik\tau}, \quad \lim_{k\tau \rightarrow -\infty} V_{s,k}^-(\tau) \propto e^{ik\tau}. \quad (4.84)$$

Furthermore, the amplitudes and the phases of the modes are adjusted to diagonalize the Hamiltonian.

4.3.6 S_- Hamiltonian

For S_- ,

$$\begin{aligned} H_- &= \int d^3k \left(\pi_{\mathbf{k},\alpha}^{\Psi_-} \partial_\tau \Psi_{\mathbf{k},\alpha}^- \right) - L_- \\ &= \int d^3k \Psi_{\mathbf{k}}^{-\dagger} \gamma^0 \left[-\gamma^3 k - \gamma^1 \xi_A \mathcal{H} + \left(2\xi_\varphi + \frac{\xi_A}{2} \right) \mathcal{H} \lambda_4 + \mu_m \mathcal{H} \lambda_4 \right] \Psi_{\mathbf{k}}^-. \end{aligned} \quad (4.85)$$

After using the mode function expansion from Eqs. (4.69) and (4.71) in the Hamiltonian, we get

$$H_- = \int \frac{d^3k}{2} (\mathbf{a}_{\mathbf{k}}^{-\dagger}, \mathbf{b}_{-\mathbf{k}}^-) \begin{pmatrix} \mathbf{E}^u & \mathbf{F}^\dagger \\ \mathbf{F} & \mathbf{E}^v \end{pmatrix} \begin{pmatrix} \mathbf{a}_{\mathbf{k}}^- \\ \mathbf{b}_{-\mathbf{k}}^- \end{pmatrix}, \quad (4.86)$$

where

$$\begin{aligned} \mathbf{a}_{\mathbf{k}}^- &= \begin{pmatrix} a_{+,\mathbf{k}}^- \\ a_{-,\mathbf{k}}^- \end{pmatrix}, \quad \mathbf{b}_{-\mathbf{k}}^- = \begin{pmatrix} b_{+,-\mathbf{k}}^{-\dagger} \\ b_{-,-\mathbf{k}}^{-\dagger} \end{pmatrix}, \\ \mathbf{E}^u &= \begin{pmatrix} E_+^u & E_{\text{mix}}^{u*} \\ E_{\text{mix}}^u & E_-^u \end{pmatrix}, \quad \mathbf{F} = \begin{pmatrix} F_+ & F_{-, \text{mix}} \\ F_{+, \text{mix}} & F_- \end{pmatrix}, \end{aligned} \quad (4.87)$$

and

$$\begin{aligned}
E_s^u &= \sum_{p=\pm} \left\{ -2 \left[k + sp \left(2\xi_\varphi + \frac{\xi_A}{2} \right) \mathcal{H} \right] \Re(u_{s,p}^{\uparrow*} u_{s,p}^\downarrow) \right. \\
&\quad \left. + \mu_m \mathcal{H} (|u_{s,p}^\uparrow|^2 - |u_{s,p}^\downarrow|^2) + 2sp\xi_A \mathcal{H} \Re(u_{s,p}^{\uparrow*} u_{s,-p}^\downarrow) \right\}, \\
F_s &= \sum_{p=\pm} \left\{ - \left[k + sp \left(2\xi_\varphi + \frac{\xi_A}{2} \right) \mathcal{H} \right] (v_{s,p}^{\uparrow*} u_{s,p}^\downarrow + v_{s,p}^{\downarrow*} u_{s,p}^\uparrow) \right. \\
&\quad \left. + \mu_m \mathcal{H} (v_{s,p}^{\uparrow*} u_{s,p}^\uparrow - v_{s,p}^{\downarrow*} u_{s,p}^\downarrow) \right. \\
&\quad \left. + sp\xi_A \mathcal{H} (v_{s,p}^{\uparrow*} u_{s,-p}^\downarrow + u_{s,p}^\uparrow v_{s,-p}^{\downarrow*}) \right\}, \\
E_{\text{mix}}^u &= \sum_{p=\pm} \left\{ - \left[k + p \left(2\xi_\varphi + \frac{\xi_A}{2} \right) \mathcal{H} \right] (u_{-, -p}^{\uparrow*} u_{+, p}^\downarrow) \right. \\
&\quad \left. + u_{-, -p}^{\downarrow*} u_{+, p}^\uparrow) + \mu_m \mathcal{H} (u_{-, -p}^{\uparrow*} u_{+, p}^\uparrow - u_{-, -p}^{\downarrow*} u_{+, p}^\downarrow) \right. \\
&\quad \left. + p\xi_A \mathcal{H} (u_{-, -p}^{\uparrow*} u_{+, -p}^\downarrow + u_{+, p}^\uparrow u_{-, p}^{\downarrow*}) \right\}, \\
F_{s, \text{mix}} &= \sum_{p=\pm} \left\{ - \left[k + sp \left(2\xi_\varphi + \frac{\xi_A}{2} \right) \mathcal{H} \right] (v_{-, -p}^{\uparrow*} u_{s, p}^\downarrow) \right. \\
&\quad \left. + v_{-, -p}^{\downarrow*} u_{s, p}^\uparrow) + \mu_m \mathcal{H} (v_{-, -p}^{\uparrow*} u_{s, -p}^\uparrow - v_{-, -p}^{\downarrow*} u_{s, -p}^\downarrow) \right. \\
&\quad \left. + sp\xi_A \mathcal{H} (v_{-, -p}^{\uparrow*} u_{s, -p}^\downarrow + u_{s, p}^\uparrow v_{-, -p}^{\downarrow*}) \right\}.
\end{aligned} \tag{4.88}$$

The Hamiltonian can be diagonalized after making a time-dependent Bogoliubov transformation,

$$\begin{pmatrix} \check{\mathbf{a}}_{\mathbf{k}}^-(\tau) \\ \check{\mathbf{b}}_{-\mathbf{k}}^{-\dagger}(\tau) \end{pmatrix} = P_k(\tau) \begin{pmatrix} \mathbf{a}_{\mathbf{k}}^- \\ \mathbf{b}_{-\mathbf{k}}^{-\dagger} \end{pmatrix}. \tag{4.89}$$

The time-dependent creation and annihilation operators, $\check{\mathbf{a}}_{\mathbf{k}}^-(\tau)$ and $\check{\mathbf{b}}_{-\mathbf{k}}^{-\dagger}(\tau)$, obey the canonical anticommutation relations from Eq. (4.82), iff the transformation matrix is unitary:

$$P_k(\tau) P_k^\dagger(\tau) = I_4. \tag{4.90}$$

We then impose that

$$P_k(\tau) \begin{pmatrix} \mathbf{E}^u & \mathbf{F}^\dagger \\ \mathbf{F} & \mathbf{E}^v \end{pmatrix} P_k^\dagger(\tau), \tag{4.91}$$

is diagonal, implying that the eigenvectors of $\begin{pmatrix} \mathbf{E}^u & \mathbf{F}^\dagger \\ \mathbf{F} & \mathbf{E}^v \end{pmatrix}$ are the columns of $P_k^\dagger(\tau)$.

Due to the nature of the equations of motion in the S_- we cannot have analytical expressions for the effective frequency $\omega_{s,k}^-(\tau)$ as opposed to Eq. (4.60) in S_+ . Therefore, the

78 4. Fermions Production and Backreaction from Axion-SU(2) Gauge Fields

expectation values of observables are calculated numerically.

At early times all off-diagonal terms of the Hamiltonian should vanish for both $s = \pm$. In other words $P_k(\tau) = \mathbf{I}_4$, which is equivalent to having

$$H_- = \begin{pmatrix} \mathbf{I}_2 & 0 \\ 0 & -\mathbf{I}_2 \end{pmatrix}. \quad (4.92)$$

It follows from Eq. (4.88) that

$$\lim_{k\tau \rightarrow -\infty} F_s = 0, \quad \lim_{k\tau \rightarrow -\infty} E_{mix}^u = 0, \quad \lim_{k\tau \rightarrow -\infty} F_{s,mix} = 0. \quad (4.93)$$

The above conditions are met, if the following equations are satisfied:

$$1. \quad \lim_{k\tau \rightarrow -\infty} (u_{s,+}^\uparrow(k, \tau) - v_{s,+}^{\uparrow*}(k, \tau)) = 0, \quad \lim_{k\tau \rightarrow -\infty} (u_{s,+}^\downarrow(k, \tau) + v_{s,+}^{\downarrow*}(k, \tau)) = 0.$$

It can be shown that these conditions are preserved by the equations of motion, so if imposed once they hold for any arbitrary τ as well

$$u_{s,+}^\uparrow(k, \tau) = v_{s,+}^{\uparrow*}(k, \tau), \quad u_{s,+}^\downarrow(k, \tau) = -v_{s,+}^{\downarrow*}(k, \tau). \quad (4.94)$$

$$2. \quad \lim_{k\tau \rightarrow -\infty} \Re(u_{s,+}^{\uparrow*}(k, \tau)u_{s,+}^\downarrow(k, \tau)) = -1 \text{ and } \lim_{k\tau \rightarrow -\infty} \Re(v_{s,+}^{\uparrow*}(k, \tau)v_{s,+}^\downarrow(k, \tau)) = 1. \text{ This condition comes from Eq. (4.92).}$$

$$3. \quad \lim_{k\tau \rightarrow -\infty} u_{s,-}^{\uparrow,\downarrow}(k, \tau) = 0 \text{ and } \lim_{k\tau \rightarrow -\infty} v_{s,-}^{\uparrow,\downarrow}(k, \tau) = 0. \text{ This condition is imposed so that the particle occupation number vanishes at early times. Note that this is an arbitrary choice and one can make the mode functions vanish for, e.g., } p = +.$$

Using the above we can solve the equations of motion numerically.

4.4 Backreactions

The action (4.6) has a Noether current associated to the SU(2) isospin,

$$J^{\mu a} = \delta_\alpha^\mu \frac{g_A}{2a^4} \bar{\Psi} \sigma^a \otimes \gamma^\alpha \tilde{\Psi}, \quad (4.95)$$

and the axial vector current, J_5^μ , given in (4.10). Notice that $J^{\mu a} \equiv \frac{\delta S_{\text{fermion}}}{\sqrt{-g} \delta A_\mu^a}$ satisfies $\nabla_\mu J^{\mu a} \sigma^a = \mathbf{0}$. The Noether current and divergence of the chiral current induce backreactions on the background field equations of an axion-SU(2) setup. See [55] for details about a uniform presentation of the axion-SU(2) class of models and in particular its Sec. 2 for

the background equations. The Noether 4-current backreacts on the background equation of the gauge field as

$$\partial_\tau^2(a\psi) + 2\mathcal{H}\partial_\tau(a\psi) + (\partial_\tau\mathcal{H} + \mathcal{H}^2)(a\psi) + 2a^3g_A^2\psi^3 - \frac{g_A\lambda}{f}a^2\partial_\tau\varphi\psi^2 = -a^2\mathcal{J}, \quad (4.96)$$

where the spatially averaged component of the matter 3-current is

$$\mathcal{J} = \frac{1}{3a}\delta_b^j\langle J_j^b \rangle. \quad (4.97)$$

Moreover, the axial current backreacts on the axion background equation as

$$\partial_\tau^2\varphi + 2\mathcal{H}\partial_\tau\varphi + a^2\partial_\varphi V + 3\frac{g_A\lambda}{f}a\psi^2(\mathcal{H}\psi + \partial_\tau\psi) = a^2\mathcal{B}, \quad (4.98)$$

where the backreaction term is defined as

$$\mathcal{B} = \beta\frac{\lambda}{2f}\nabla_\mu J_5^\mu = -im\beta\frac{\lambda}{a^3f}\bar{\Psi}\gamma_5\Psi. \quad (4.99)$$

The last equality uses the field equations of the fermions.

We begin with an outline of our prescription for computing the VEVs of quadratic fermionic quantum operators such as \mathcal{J} and \mathcal{B} . We then calculate the fermionic backreaction on the gauge field and the axion backgrounds.

4.4.1 VEVs of Quadratic Fermionic Operators

In order to compute VEVs of quantum operators we follow [145, 67].

Consider a general four component fermionic field, similar to Ψ^+ and Ψ^- defined in section 4.2.

$$\begin{aligned} \eta_\alpha(\mathbf{x}, \tau) &= \int d^3k \eta_{\mathbf{k},\alpha}(\tau) e^{i\mathbf{k}\cdot\mathbf{x}}, \\ \eta_{\mathbf{k},\alpha}(\tau) &= \sum_{s=\pm} \left[U_{s,\mathbf{k},\alpha}(\tau) c_{s,\mathbf{k}} + V_{s,-\mathbf{k},\alpha}(\tau) d_{s,-\mathbf{k}}^\dagger \right], \end{aligned} \quad (4.100)$$

with a quadratic action

$$S_\eta = \int d\tau d^3k \left[i\eta_{\mathbf{k},\alpha}^\dagger \partial_\tau \eta_{\mathbf{k},\alpha} - \eta_{\mathbf{k},\alpha}^\dagger \Omega_{\alpha\beta}(k, \tau) \eta_{\mathbf{k},\beta} \right], \quad (4.101)$$

and a Hamiltonian

$$H_\eta = \int d^3k \eta_{\mathbf{k},\alpha}^\dagger \Omega_{\alpha\beta}(k, \tau) \eta_{\mathbf{k},\beta}, \quad (4.102)$$

where α and β run from 1 to 4, and $c_{s,\mathbf{k}}$ and $d_{s,-\mathbf{k}}$ are time-independent particle and antiparticle annihilation operators. Using Eq. (4.100) in the Hamiltonian, we obtain

$$H_\eta = \int d^3k (\mathbf{c}_\mathbf{k}^\dagger, \mathbf{d}_{-\mathbf{k}}) \begin{pmatrix} \mathcal{E}^U & \mathcal{F}^\dagger \\ \mathcal{F} & \mathcal{E}^V \end{pmatrix} \begin{pmatrix} \mathbf{c}_\mathbf{k} \\ \mathbf{d}_{-\mathbf{k}}^\dagger \end{pmatrix}, \quad (4.103)$$

80 4. Fermions Production and Backreaction from Axion-SU(2) Gauge Fields

where

$$\mathbf{c}_{\mathbf{k}} = [c_{+, \mathbf{k}} \quad c_{-, \mathbf{k}}]^T, \quad \mathbf{d}_{\mathbf{k}} = [d_{+, \mathbf{k}} \quad d_{-, \mathbf{k}}]^T, \quad (4.104)$$

and

$$\mathcal{E}_{ss'}^U = U_{s, \mathbf{k}, \alpha}^* \Omega_{\alpha\beta} U_{s', \mathbf{k}, \beta}, \quad \mathcal{F}_{ss'} = V_{s, \mathbf{k}, \alpha}^* \Omega_{\alpha\beta} V_{s', \mathbf{k}, \beta}. \quad (4.105)$$

In the ground state of a given k -mode of the fermionic field, i.e., in the Bunch-Davies vacuum (BD), the state vector is $|0_{\text{BD}}\rangle$

$$\mathbf{c}_{\mathbf{k}, s} |0_{\text{BD}}\rangle = 0, \quad \mathbf{d}_{\mathbf{k}, s} |0_{\text{BD}}\rangle = 0, \quad (4.106)$$

and

$$\text{BD vacuum : } \mathcal{E}_{ss'}^U = -\mathcal{E}_{ss'}^V = \omega_s \delta_{ss'}, \quad \mathcal{F}_{ss'} = 0. \quad (4.107)$$

When the mode is excited, its $\mathcal{E}_{ss'}^{U,V}$ can attain nonzero off-diagonal components and its $\mathcal{F}_{ss'}$ can also become nonvanishing. However, we can still diagonalize $\mathcal{E}_{ss'}^{U,V}$ with vanishing $\mathcal{F}_{ss'}$ by rewriting the Hamiltonian as

$$H_\eta = \int d^3k (\check{\mathbf{c}}_{\mathbf{k}}^\dagger, \check{\mathbf{d}}_{-\mathbf{k}}) \begin{pmatrix} \check{\mathcal{E}}^U & \check{\mathcal{F}}^\dagger \\ \check{\mathcal{F}} & \check{\mathcal{E}}^V \end{pmatrix} \begin{pmatrix} \check{\mathbf{c}}_{\mathbf{k}} \\ \check{\mathbf{d}}_{-\mathbf{k}}^\dagger \end{pmatrix}, \quad (4.108)$$

where

$$\begin{pmatrix} \check{\mathbf{c}}_{\mathbf{k}}^-(\tau) \\ \check{\mathbf{d}}_{-\mathbf{k}}^{\dagger}(\tau) \end{pmatrix} = P_k(\tau) \begin{pmatrix} \mathbf{c}_{\mathbf{k}}^- \\ \mathbf{d}_{-\mathbf{k}}^{\dagger} \end{pmatrix}, \quad (4.109)$$

and

$$P_k(\tau) P_k^\dagger(\tau) = \mathbb{I}_4. \quad (4.110)$$

We choose the eigenvectors of

$$\begin{pmatrix} \mathcal{E}^U & \mathcal{F}^\dagger \\ \mathcal{F} & \mathcal{E}^V \end{pmatrix}, \quad (4.111)$$

as the columns of $P_k^\dagger(\tau)$. Then,

$$\check{\mathcal{E}}_{ss'}^U = -\check{\mathcal{E}}_{ss'}^V = \check{\omega}_s \delta_{ss'}, \quad \check{\mathcal{F}}_{ss'} = 0, \quad (4.112)$$

as promised.

After the transformation in Eq. (4.109), a new state vector has the properties of the physical vacuum, $|0_\tau\rangle$, defined as

$$\check{\mathbf{c}}_{\mathbf{k}, s} |0_\tau\rangle = 0, \quad \check{\mathbf{d}}_{\mathbf{k}, s} |0_\tau\rangle = 0. \quad (4.113)$$

Note that we work in the Heisenberg picture in which the state vector is constant, i.e., it remains $|0_{\text{BD}}\rangle$ throughout.

The fermionic field can be rewritten as

$$\eta_{\mathbf{k}, \alpha}(\tau) = \sum_{s=\pm} \left[\check{U}_{s, \mathbf{k}, \alpha}(\tau) \check{c}_{s, \mathbf{k}} + \check{V}_{s, -\mathbf{k}, \alpha}(\tau) \check{d}_{s, -\mathbf{k}}^\dagger \right], \quad (4.114)$$

where

$$\begin{aligned}\check{U}_{s,\mathbf{k},\alpha} &= \sum_{s'=\pm} \left[U_{s',\mathbf{k},\alpha} P_{\frac{3-s'}{2}, \frac{3-s}{2}}^\dagger + V_{s',-\mathbf{k},\alpha} P_{\frac{7-s'}{2}, \frac{3-s}{2}}^\dagger \right], \\ \check{V}_{s,-\mathbf{k},\alpha} &= \sum_{s'=\pm} \left[V_{s',-\mathbf{k},\alpha} P_{\frac{7-s'}{2}, \frac{7-s}{2}}^\dagger + U_{s',\mathbf{k},\alpha} P_{\frac{3-s'}{2}, \frac{7-s}{2}}^\dagger \right].\end{aligned}\tag{4.115}$$

We wish to find the VEV of a Hermitian operator, which is quadratic in the fermionic field, of the general form

$$\mathcal{O}(\mathbf{x}, \tau) = \int d^3k d^3k' e^{i(\mathbf{k}-\mathbf{k}')\cdot\mathbf{x}} \eta_{\mathbf{k},\alpha}^\dagger(\tau) A_{\alpha,\beta}(\mathbf{k}, \mathbf{k}', \tau) \eta_{\mathbf{k}',\beta}(\tau),\tag{4.116}$$

with $A_{\alpha,\beta}^\dagger(\mathbf{k}, \mathbf{k}', \tau) = A_{\alpha,\beta}(\mathbf{k}', \mathbf{k}, \tau)$ by virtue of the Hermitian nature of the \mathcal{O} operator.

When computing the VEV, we need to make sure that

1. Particles and antiparticles are treated on equal footing.
2. Only physical field excitations, i.e., those on top of the physical vacuum, contribute to the VEV.

To address the first point, we follow [145] and define the antisymmetrized operator

$$\begin{aligned}\mathcal{O}_a(\mathbf{x}, \tau) &\equiv \int d^3k d^3k' e^{i(\mathbf{k}-\mathbf{k}')\cdot\mathbf{x}} A_{\alpha,\beta}(\mathbf{k}, \mathbf{k}', \tau) [\eta_{\mathbf{k},\alpha}^\dagger(\tau), \eta_{\mathbf{k}',\beta}(\tau)] \\ &= \int d^3k d^3k' e^{i(\mathbf{k}-\mathbf{k}')\cdot\mathbf{x}} A_{\alpha,\beta}(\mathbf{k}, \mathbf{k}', \tau) \frac{1}{2} \left(\eta_{\mathbf{k},\alpha}^\dagger(\tau) \eta_{\mathbf{k}',\beta}(\tau) - \eta_{\mathbf{k}',\beta}(\tau) \eta_{\mathbf{k},\alpha}^\dagger(\tau) \right),\end{aligned}\tag{4.117}$$

which has the same classical counterpart as \mathcal{O} . The difference is that when we take the BD VEV, \mathcal{O} receives only contributions from terms with $d_{s,-\mathbf{k}} d_{s,-\mathbf{k}}^\dagger$, i.e., the antiparticle creation and annihilation operators, whereas \mathcal{O}_a receives contributions from both $c_{s,\mathbf{k}} c_{s,\mathbf{k}}^\dagger$ and $d_{s,-\mathbf{k}} d_{s,-\mathbf{k}}^\dagger$.

To account for the second point, we follow [67] and we subtract from the BD VEV the expectation value with respect to $|0_\tau\rangle$. This way only nonvacuum field fluctuations contribute to the physical vacuum expectation value.

To sum up, the VEV of \mathcal{O} is defined as

$$\langle \mathcal{O}(\mathbf{x}, \tau) \rangle \equiv \langle 0_{\text{BD}} | \mathcal{O}_a(\mathbf{x}, \tau) | 0_{\text{BD}} \rangle - \langle 0_\tau | \mathcal{O}_a(\mathbf{x}, \tau) | 0_\tau \rangle,\tag{4.118}$$

which reduces to

$$\begin{aligned}\langle \mathcal{O}(\mathbf{x}, \tau) \rangle &= \int d^3k A_{\alpha,\beta}(\mathbf{k}, \mathbf{k}, \tau) \sum_{s=\pm} \frac{1}{2} \\ &\times \left[\left(V_{s,\mathbf{k},\alpha}^*(\tau) V_{s,\mathbf{k},\beta}(\tau) - U_{s,\mathbf{k},\beta}(\tau) U_{s,\mathbf{k},\alpha}^*(\tau) \right) \right. \\ &\left. - \left(\check{V}_{s,\mathbf{k},\alpha}^*(\tau) \check{V}_{s,\mathbf{k},\beta}(\tau) - \check{U}_{s,\mathbf{k},\beta}(\tau) \check{U}_{s,\mathbf{k},\alpha}^*(\tau) \right) \right].\end{aligned}\tag{4.119}$$

82 4. Fermions Production and Backreaction from Axion-SU(2) Gauge Fields

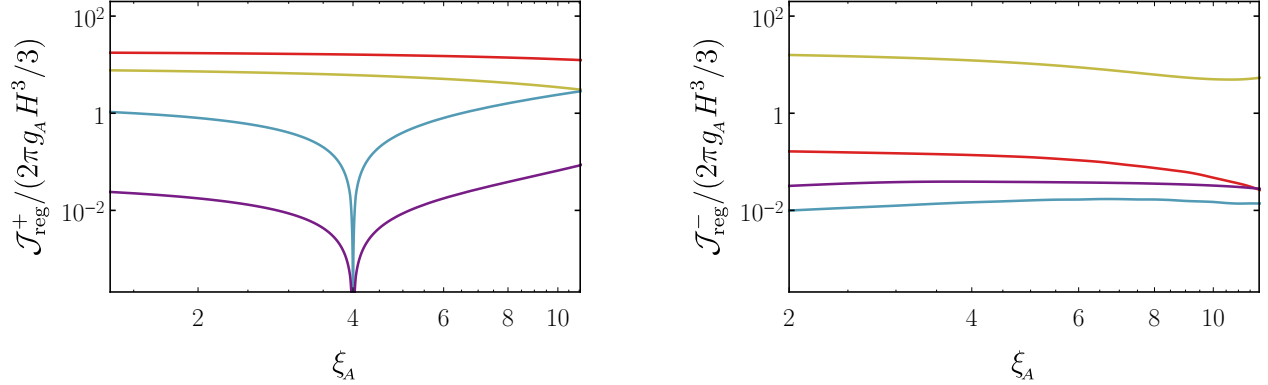


Figure 4.2: The expectation values of the backreaction currents of the + (**left panel**) and – (**right panel**) fermions as a function of ξ_A for $m = 10H$, $\xi_\varphi = 1$ (purple); $m = H$, $\xi_\varphi = 1$ (blue); $m = H$, $\xi_\varphi = 10$ (gold); $m = 10H$, $\xi_\varphi = 10$ (red). The prominent dip in the first panel at $2\xi_\varphi - \xi_A/2 = 0$ is due to an exact cancellation between the effective masses induced by the gauge field and the axion. Such a cancellation is not observed in the – fermions.

Here, we are interested in the backreaction of the fermion on the gauge field field equation, \mathcal{J}^\pm , and the axion field equation, \mathcal{B}^\pm , which can be computed by the above formula as

$$\begin{aligned} \langle \mathcal{J}^s \rangle &= \int d^3k A_{\alpha\beta}^{\mathcal{J}^s}(\mathbf{k}, \mathbf{k}, \tau) \frac{1}{2} \\ &\times \left[\left(V_{s,\mathbf{k},\alpha}^*(\tau) V_{s,\mathbf{k},\beta}(\tau) - U_{s,\mathbf{k},\beta}(\tau) U_{s,\mathbf{k},\alpha}^*(\tau) \right) \right. \\ &\left. - \left(\check{V}_{s,\mathbf{k},\alpha}^*(\tau) \check{V}_{s,\mathbf{k},\beta}(\tau) - \check{U}_{s,\mathbf{k},\beta}(\tau) \check{U}_{s,\mathbf{k},\alpha}^*(\tau) \right) \right], \end{aligned} \quad (4.120)$$

and

$$\begin{aligned} \langle \mathcal{B}^s \rangle &= \int d^3k A_{\alpha\beta}^{\mathcal{B}^s}(\mathbf{k}, \mathbf{k}, \tau) \frac{1}{2} \\ &\times \left[\left(V_{s,\mathbf{k},\alpha}^*(\tau) V_{s,\mathbf{k},\beta}(\tau) - U_{s,\mathbf{k},\beta}(\tau) U_{s,\mathbf{k},\alpha}^*(\tau) \right) \right. \\ &\left. - \left(\check{V}_{s,\mathbf{k},\alpha}^*(\tau) \check{V}_{s,\mathbf{k},\beta}(\tau) - \check{U}_{s,\mathbf{k},\beta}(\tau) \check{U}_{s,\mathbf{k},\alpha}^*(\tau) \right) \right], \end{aligned} \quad (4.121)$$

respectively.

4.4.2 Backreaction on the SU(2) Background

We now calculate the homogeneous and isotropic backreaction term on the SU(2) background, \mathcal{J} , defined in Eq. (4.97). It conveniently separates into two independent contributions from the + and – fermions:

$$\mathcal{J} = \mathcal{J}^+ + \mathcal{J}^-. \quad (4.122)$$

The expressions for \mathcal{J}^+ and \mathcal{J}^- take the form given in Eq. (4.120), with

$$\begin{aligned}
 A^{\mathcal{J}^+}(\mathbf{k}, \mathbf{k}, \tau) &= \frac{g_A}{3a^3} \begin{pmatrix} 0 & 0 & 1 & 0 \\ 0 & 0 & 0 & 1 \\ 1 & 0 & 0 & 0 \\ 0 & 1 & 0 & 0 \end{pmatrix}, \\
 A^{\mathcal{J}^-}(\mathbf{k}, \mathbf{k}, \tau) &= -\frac{g_A}{3a^3} \begin{pmatrix} 0 & 0 & 1 & -2 \\ 0 & 0 & -2 & 1 \\ 1 & -2 & 0 & 0 \\ -2 & 1 & 0 & 0 \end{pmatrix}.
 \end{aligned} \tag{4.123}$$

In Fig. 4.2, we show \mathcal{J}^+ (left) and \mathcal{J}^- (right) for different values of the parameters ξ_φ , m and ξ_A . We observe the following dependence:

- \mathcal{J}^+ has a prominent dip when $2\xi_\varphi - \xi_A/2 = 0$, which occurs because the axion and gauge field-induced effective mass terms cancel. Besides this feature, for a fixed mass, \mathcal{J}^+ increases monotonically with ξ_A . Otherwise when the “bare” mass of the fermion is the dominant scale, i.e., $m/H > \xi_A, \xi_\varphi$, we observe a decrease in particle production as the mass increases, as expected. In the opposite limit, $m/H < \xi_A, \xi_\varphi$, there is an increase in particle production as the mass increases, until the mass becomes the dominant scale.²
- \mathcal{J}^- exhibits a complex behavior with the parameters which we attribute to the additional couplings in this sector. Using the current regularization scheme and for the parameter region of interest, \mathcal{J}^- never exceeds \mathcal{J}^+ apart from the dips in \mathcal{J}^+ , so the dominant contribution to the backreaction considered in the next section comes from \mathcal{J}^+ .
- When compared to the scalar case considered in [54], the fermion model has an important new feature. Unlike scalars, fermion particles are copiously produced as ξ_A increases and dominate the other scales in the problem. Our setup provides a novel mechanism for efficient production of fermionic matter during inflation.
- The fermion Schwinger particle production by a homogeneous U(1) gauge field studied in [135] is different from our SU(2) case with the isotropic and homogeneous VEV. In the U(1) case the current decreases with the increase of the fermion mass. However, in both cases, the current increases like ξ_A^2 in the very strong gauge field limit.

Having computed \mathcal{J}^\pm , we can compute their backreaction on the SU(2) gauge field background, ψ , by following [55]. Assuming slow-roll evolution of the axion-SU(2), i.e.,

²A similar increase in particle production with the increase in mass was observed in [137]. In their setup, the fermion is not coupled to a gauge field but is derivatively coupled to an axion field.

84 4. Fermions Production and Backreaction from Axion-SU(2) Gauge Fields

$\frac{\ddot{\psi}}{H^2\psi} \ll \frac{\dot{\psi}}{H\psi} \ll 1$, the field equation of the gauge field given in (4.96) can be approximated as

$$3H\dot{\psi} + \dot{H}\psi + V_{\text{eff},\psi}(\psi) \simeq 0, \quad (4.124)$$

where a dot is a derivative with respect to cosmic time and the field derivative of the effective potential of ψ is

$$V_{\text{eff},\psi}(\psi) \simeq 2H^2\psi(1 + \xi_A^2) - \frac{g_A\lambda\dot{\psi}}{f}\psi^2. \quad (4.125)$$

Slow-roll demands $V_{\text{eff},\psi}(\psi) \ll 1$, while each of the terms in the right-hand side can be much larger, e.g., $\frac{g_A\lambda\dot{\psi}}{f}\psi^2/V_{\text{eff},\psi} \gg 1$. On the other hand, \mathcal{J} in the right-hand side of (4.96) should be at most on the order of the slow-roll suppressed terms, i.e.,

$$\frac{\mathcal{J}}{H^2\psi} \ll 1, \quad (4.126)$$

so that it does not break the slow-roll dynamics in the background and can be considered as a perturbation correction. Otherwise, the perturbative expansion and slow-roll dynamics are not trustable and the models should be studied numerically.

Therefore, we define the regime of strong backreaction as

$$\mathcal{J} < 10^{-2}H^2\psi. \quad (4.127)$$

We will use the above to explore the possible parameter space of one possible axion-SU(2) gauge field model in Sec. 4.4.4.

4.4.3 Backreaction on the Axion Background

We now turn to the homogeneous and isotropic backreaction term on the axion background, \mathcal{B} , defined in Eq. (4.99). It again splits into the sum of two independent + and – components:

$$\mathcal{B} = \mathcal{B}^+ + \mathcal{B}^-. \quad (4.128)$$

\mathcal{B}^+ and \mathcal{B}^- reduce to the form given in Eq. (4.121):

$$A^{\mathcal{B}^+}(\mathbf{k}, \mathbf{k}, \tau) = A^{\mathcal{B}^-}(\mathbf{k}, \mathbf{k}, \tau) = \beta \frac{\lambda m H^3}{2if} \begin{pmatrix} \mathbf{0} & -\mathbf{I}_2 \\ \mathbf{I}_2 & \mathbf{0} \end{pmatrix}. \quad (4.129)$$

From the axion field equation in the slow-roll regime, we have $\frac{\ddot{\varphi}}{H\dot{\varphi}} \ll 1$, and

$$3H\dot{\varphi} + V_{\varphi,\text{eff}} \simeq 0, \quad (4.130)$$

where $V_{\varphi,\text{eff}} = V_\varphi + \frac{3\lambda g_A}{f}\psi^2(\dot{\psi} + H\psi)$. The validity of the perturbation and slow-roll dynamics requires \mathcal{B} to be at most of the order of the slow-roll suppressed terms, e.g.

$$\mathcal{B} \ll H\dot{\varphi}. \quad (4.131)$$

Interestingly, however we find that our choice of initial conditions that makes the Hamiltonian diagonalized yields

$$A_{\alpha\beta}^{\mathcal{B}^s}(\mathbf{k}, \mathbf{k}, \tau) \left(V_{s,\mathbf{k},\alpha}^*(\tau) V_{s,\mathbf{k},\beta}(\tau) - U_{s,\mathbf{k},\beta}(\tau) U_{s,\mathbf{k},\alpha}^*(\tau) \right) = 0, \quad (4.132)$$

which implies that

$$\mathcal{B} = 0. \quad (4.133)$$

Therefore, the particle production does not lead to *any* backreaction on the axion background. Note that this is the direct result of our quantization skim based on diagonalization of the Hamiltonian. Setting the initial condition based on charge conjugation symmetry which does not diagonalize the Hamiltonian at asymptotic past, leads to a different and nonvanishing value for $\nabla_\mu J_5^\mu$, which is worked out in [57].

The computation so far has been done effectively at tree level. A one-loop effect, which has not been included consistently (see [58] for a related work with massless fermions), is the chiral anomaly, i.e., a quantum correction to the expectation value of $\nabla_\mu J^{\mu 5}$, equal to $g_A^2 \text{Tr}(\mathbf{F}_{\mu\nu} \tilde{\mathbf{F}}^{\mu\nu}) / (16\pi^2)$ [144] which is $\approx 3g_A^3 \psi^3 H / (4\pi^2)$. Since $\mathcal{B} = (\beta\lambda) / (2f) \nabla_\mu J^{\mu 5}$, using $g_A \lambda \partial_\tau \varphi / (af) \approx 2H(\xi_A + \xi_A^{-1})$, Eq. (4.131) yields

$$\left(\frac{f}{H} \right)^2 \gg \frac{3}{16\pi^2} \beta \xi_A^2 (\xi_A^2 + 1). \quad (4.134)$$

Since the right-hand side is always of the order of unity, the backreaction is never important when $f \gg H$.

4.4.4 Parameter Space of a Model

Our method applies to models in which inflation is driven by the axion-gauge field sector [28, 29, 30, 31], as well as to those in which the axion and gauge fields are in a spectator sector [66]. For concreteness, we consider the latter model and compare our results with observational bounds on the following spectator model:

$$S = S_{\text{EH}} + S_\phi + S_{\text{spec}} + S_{\text{fermion}} + S_{\text{int}},$$

$$S_{\text{spec}} = \int d^4x \sqrt{-g} \left[\frac{1}{2} \partial_\mu \varphi \partial^\mu \varphi - V(\varphi) - \frac{1}{2} \text{Tr}(\mathbf{F}_{\mu\nu} \mathbf{F}^{\mu\nu}) - \frac{\lambda \varphi}{2f} \text{Tr}(\mathbf{F}_{\mu\nu} \tilde{\mathbf{F}}^{\mu\nu}) \right], \quad (4.135)$$

where S_{EH} and S_ϕ are the Einstein-Hilbert and the inflaton actions, respectively, responsible for inflation of the universe, and S_{spec} is the action of the spectator sector. It contains the axion-gauge field sector, where φ is the axion with a potential $V(\varphi)$ and a decay constant f , and

$$\mathbf{F}_{\mu\nu} = \nabla_\mu \mathbf{A}_\nu - \nabla_\nu \mathbf{A}_\mu + ig_A (\mathbf{A}_\mu \mathbf{A}_\nu - \mathbf{A}_\nu \mathbf{A}_\mu), \quad (4.136)$$

is the field strength tensor of the SU(2) gauge fields. The last term in S_{spec} is the Chern-Simons interaction, where λ parametrizes its strength and $\tilde{\mathbf{F}}^{\mu\nu}$ is the dual of $\mathbf{F}_{\mu\nu}$.

86 4. Fermions Production and Backreaction from Axion-SU(2) Gauge Fields

For the bound on the backreaction of the gauge fields we use Eq. (4.127), which reduces to

$$\epsilon_B < \xi_A^3 \frac{10^2 \pi^2 A_s r_{\text{vac}}}{2} \frac{\mathcal{J}}{g_A H^3}, \quad (4.137)$$

where $\epsilon_B \equiv \xi_A^4 H^2 / (g_A^2 m_{\text{pl}}^2)$ is about 2 times the energy density fraction of the gauge field. We have also used the slow-roll relation $r_{\text{vac}} = 2H^2 / (A_s \pi^2 m_{\text{pl}}^2)$ to parametrize the Hubble scale of inflation, i.e., r_{vac} is the standard vacuum contribution to the tensor-to-scalar ratio in single-field slow-roll inflation. The amplitude of the curvature power spectrum is $A_s \approx 2.2 \times 10^{-9}$ [18].

In Figs. 4.3, 4.4, 4.5, 4.6, the orange solid line and the shaded area underneath it depict the inequality in Eq. (4.137), i.e., the regions where strong backreaction occurs due to the induced current. From these figures we can conclude that no additional constraint comes from the fermionic particle production.

Note that the contribution from chiral anomaly is small for the masses under consideration $\mu_m \gtrsim 1$, and also it is suppressed by a factor of g_A^2 , (see Page 65 for motivation behind this mass constraint, and see [58] for inclusion of one-loop effects for massless fermions).

4.5 Discussion

We have studied the evolution of a Dirac field doublet, which is covariantly coupled to an axion and an isotropic SU(2) gauge field background in de Sitter spacetime. We assumed the fermion field to have a Dirac mass term. Our work extends the previous work on fermion production from axion and Abelian U(1) gauge fields [135, 136, 137, 138], as well as on the simplest SU(2) case with massless fermions [58].

We discovered that the SU(2) background, in combination with the Dirac mass term, leads to nontrivial couplings between fermion components of different flavors and chirality. We then found a new convenient basis for the doublet of fermionic fields, given as a linear transformation in Fourier space of the original doublet, for which the action separates into two decoupled sectors. One of the subsystems is solvable analytically, whereas the other subsector is not and we solved it numerically.

Using these solutions, we computed the expectation values of the induced currents, which we used to estimate for what model parameters backreaction effects become important. More specifically, we considered the isotropic part of the SU(2) matter current, as well as the 4-divergence of the axial current, which can be used to estimate the fermionic backreaction on the gauge field and axion backgrounds, respectively.

To find the vacuum expectation values of bilinearies in fermionic fields, such as the currents, we had to deal with UV-divergent integrals. To this end, we extended the idea of an existing instantaneous vacuum subtraction scheme [67], which involves the subtraction of the contribution of zero-point fluctuations to the currents. We extended it to fermionic models with most generic Hamiltonians, which permit only a numerical treatment. We compared the results with an independent regularization scheme, i.e the point-splitting method and found an excellent agreement for S_+ (the details of the latter method is

studied in [57]). We find that the adiabatic vacuum subtraction scheme could not be utilized here, since there are instants where adiabatic modes are ill behaved. We also made a careful distinction between the contributions of particles and antiparticles to the vacuum expectation values, which played an important role in the computation of the tree-level backreaction on the axion.

We showed that the SU(2)-background experiences strong backreaction due to fermions only for model parameters which are already excluded on observational and/or theoretical grounds (see Figs. 2 – 5), similarly to the case of scalars [54]. The tree-level expectation value of the 4-divergence of the axial current vanishes. We then estimated when the chiral anomaly, which is a loop effect, becomes important for the backreaction on the axion background. We find that backreaction remains unimportant provided that $f \gg H$.

We conclude that the background dynamics of an axion-SU(2) gauge field spectator sector remains unaffected by the production of fermions.

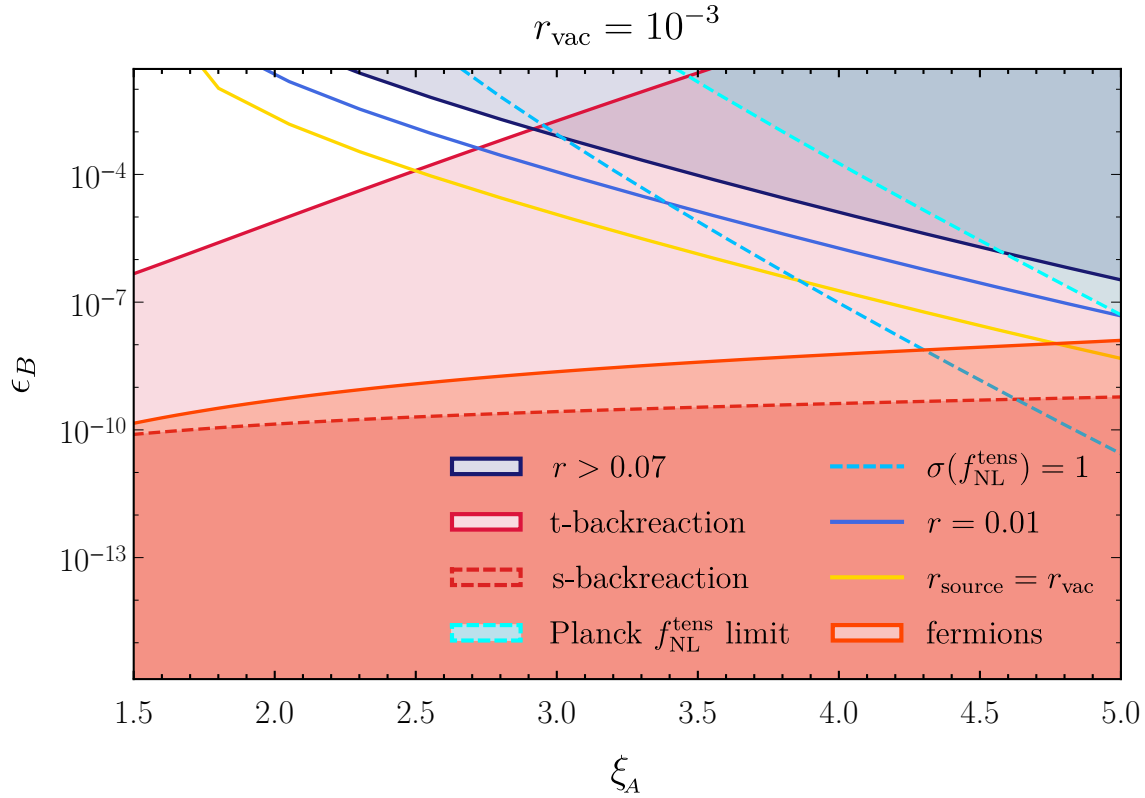


Figure 4.3: We plot the energy density fraction of the gauge field ϵ_B as a function of the effective mass of the gauge field, ξ_A . Excluded parameter space with $r_{vac} = 10^{-3}$. The blue shaded area is excluded by the tensor-to-scalar ratio, the light red area by the large tensor backreaction discussed in [55]. The cyan area by the tensor non-Gaussianity, and the dark red area by the Schwinger pair creation of scalar fields discussed in [54]. The blue and yellow lines show $r = 10^{-2}$ and $r_{source} = r_{vac}$, respectively, while the dashed cyan line shows $f_{NL}^{tens} = 1$. The bound from the fermion particle production, depicted by the orange solid line (for $m = H$ and $\xi_\varphi = 1$) and the area underneath, does not lead to additional bounds on the observationally relevant parameter space. The ξ_A on the horizontal axis is the same as m_Q in [66, 36, 37].

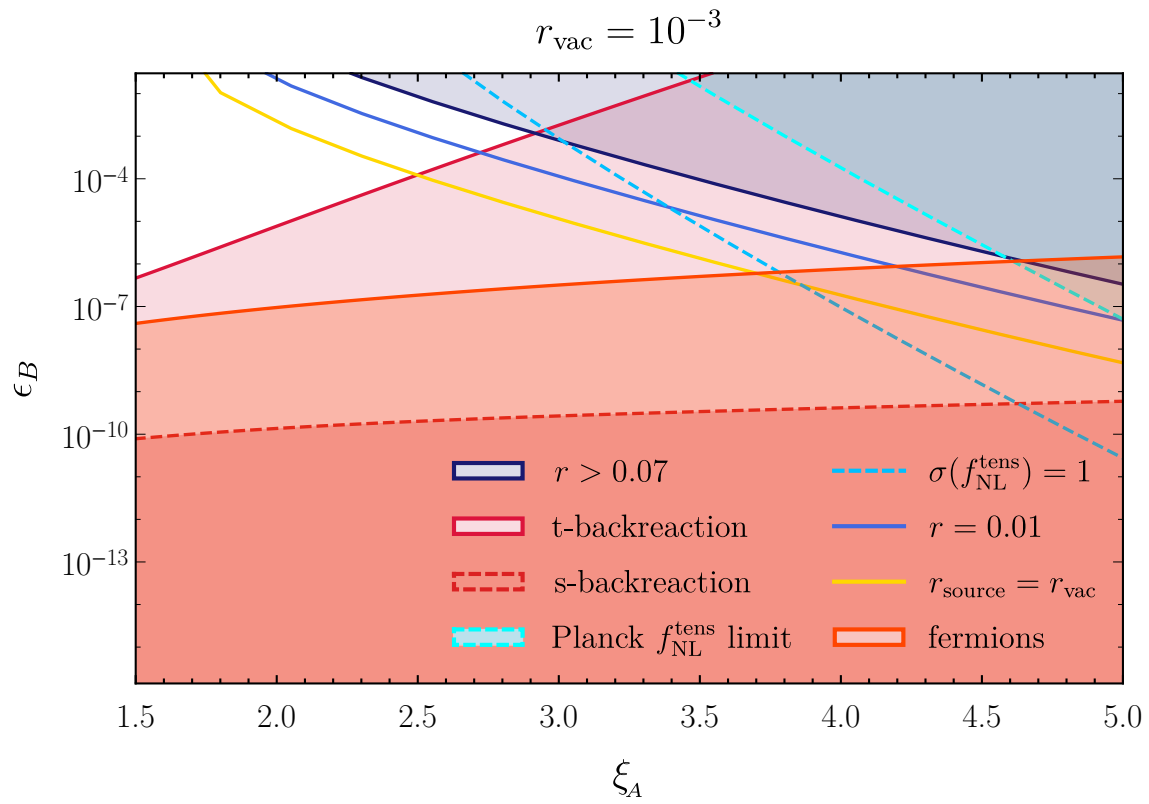


Figure 4.4: Same as Fig. 4.3, but for $m = 10H$ and $\xi_\varphi = 10$.

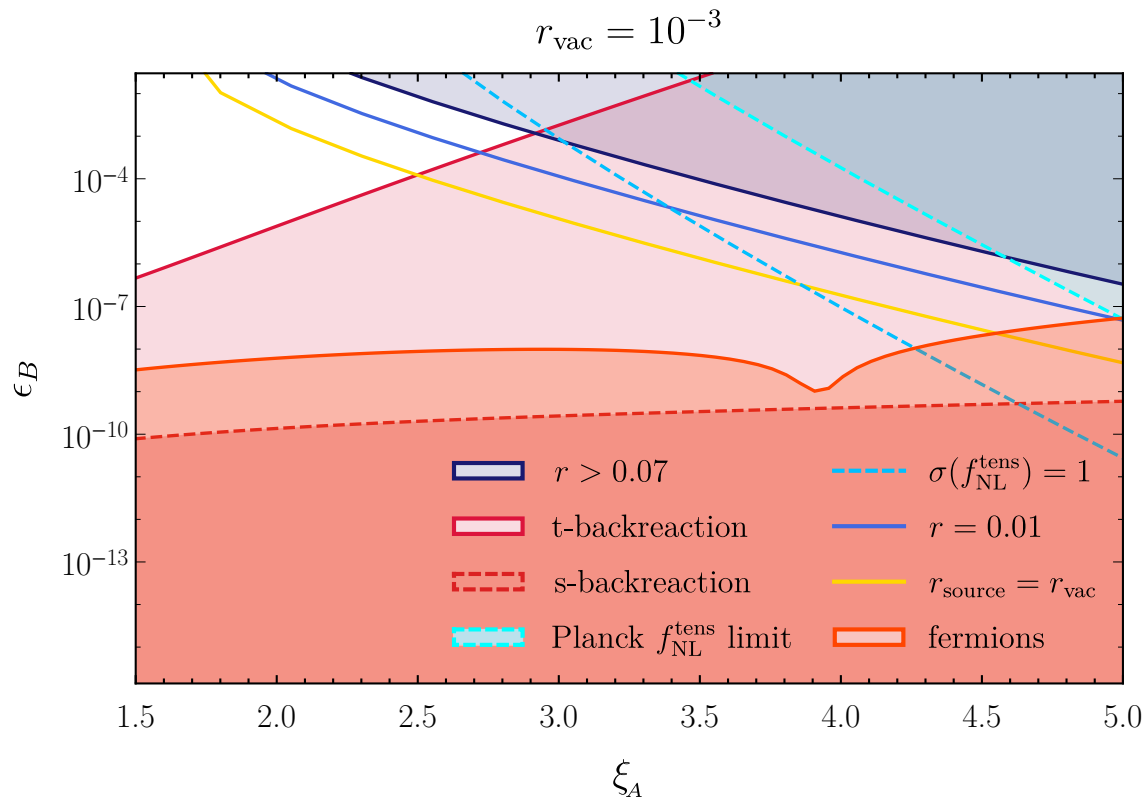


Figure 4.5: Same as Fig. 4.3, but for $m = 10H$ and $\xi_\varphi = 1$.

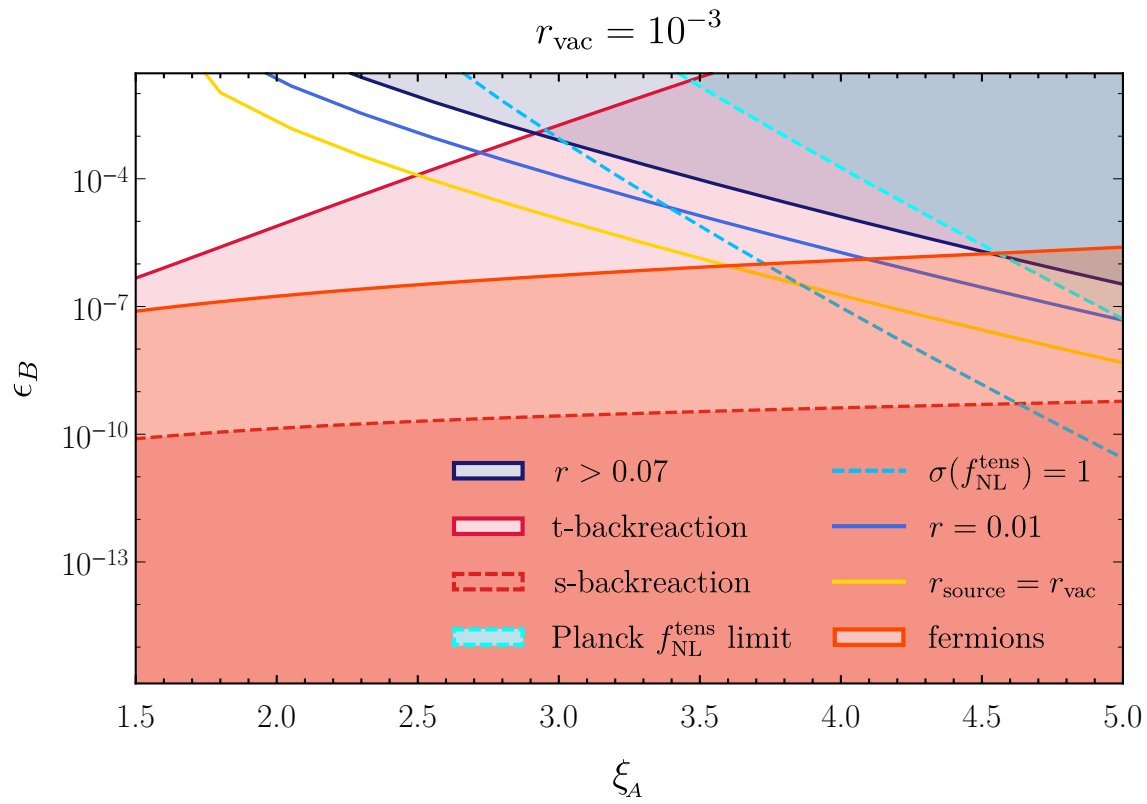


Figure 4.6: Same as Fig. 4.3, but for $m = H$ and $\xi_\varphi = 10$.

Chapter 5

Summary and Outlook

The two important experimental data that exist and can be used to constrain our early universe models are coming from big bang nucleosynthesis and CMB. Inflation as a theoretic model of the early stages of the universe satisfies the bounds coming from these data sets available so far and in light of this, presents itself as the most accepted model compared to the competing theories in explaining the primordial history of the universe. Nonetheless, one of the crucial predictions of all inflationary scenarios, namely the existence of a stochastic background of gravitational waves, has not yet been confirmed.

Furthermore, inflation provides us with a mechanism to generate the scalar and tensor perturbations from the so-called quantum vacuum fluctuation. The scalar perturbations seed the large scale structure in the universe. These scalar fluctuations have been detected in the CMB experiments and their observational signatures hint towards a quantum nature of these perturbations.

Consequently, to differentiate between models of inflation, it is very important to detect primordial gravitational waves. However, detection of primordial gravitational waves is not only beneficial for evaluating the relevance of inflation but can also open a new window into the microphysics of the very early universe and can be used to probe energies that are unlikely to be achieved by the colliders.

If the primordial gravitational waves are detected, the question about the quantum nature of the vacuum fluctuations during the early stages of the universe can be settled once and for all. One has to note that the mere detection of primordial gravitational waves does not necessarily yield insight into the quantum nature of these perturbations; more investigation is required to achieve this goal. One can announce the discovery of vacuum fluctuations of spacetime that are consistent with quantum mechanics if and only if the following conditions are satisfied: i) the CMB polarizations must be detected in multiple frequencies (the primordial gravitational waves imprint a signature in the B-mode polarization which is the most promising channel for a future detection currently), ii) they must have a scale invariant spectrum, iii) they must be non-Gaussian and, finally, iv) the TB/EB correlations must be zero for them meaning they have to be non-chiral.

However, to be on a secure footing regarding the detection and the proper interpretation of the signals, we need to be sure that we understand all relevant mechanisms that can

lead to the production of B-modes in the context of inflation. In light of this, the so-called axion-SU(2) gauge field model of inflation has been the focus of this thesis as one relevant generation mechanism, besides vacuum fluctuations. The advantage of this model is that the gravitational waves produced in this setup have completely different signatures compared to the one from the vacuum so they can be easily distinguished from the vacuum ones via higher order observables such as the bispectrum. However, before the predictions of these models are taken seriously, it is important to check if these models are viable both phenomenologically and theoretically.

Given these considerations, we can understand the importance of the two studies presented in this dissertation, which provide two important consistency checks on both the dynamics of the gravitational waves and the background dynamics in axion-SU(2) gauge field models of inflation. Based on both of these investigations, we conclude that the background dynamics of an axion-SU(2) sector remains unaffected and phenomenologically viable in the presence of the gravitational Chern-Simons term and massive fermions.

In the light of the future data coming from numerous ground-based experiments, space-borne experiments, pulsar timing arrays and direct detection experiments, we can understand a detailed characterization of the primordial gravitational waves and determine if the detected signal was sourced by the quantum vacuum fluctuations in the metric tensor, as in the single-field slow-roll scenario, or from alternative scenarios such as the axion-SU(2) gauge field model considered in this dissertation.

Appendix A

Spinor Covariant Derivative

The 8-spinor covariant derivative in (4.7) is defined as

$$D_\mu \otimes \gamma^\alpha \tilde{\Psi} \equiv (\mathbf{I}_2 \nabla_\mu - i g_A \mathbf{A}_\mu) \otimes \gamma^\alpha \tilde{\Psi}, \quad (\text{A.1})$$

where the spin covariant derivative is

$$\nabla_\mu \tilde{\Psi} = [\mathbf{I}_4 \partial_\mu + \omega_\mu] \tilde{\Psi}, \quad (\text{A.2})$$

ω_μ are the spin connections,

$$\omega_\mu = -\frac{i}{2} \omega_\mu^{\alpha\beta} \sigma_{\alpha\beta}, \quad (\text{A.3})$$

where the spinor generators of the algebra are $\sigma_{\alpha\beta} = \frac{i}{4} [\gamma_\alpha, \gamma_\beta]$.

Considering a FLRW metric

$$ds^2 = a^2(\tau)(-d\tau^2 + \delta_{ij} dx^i dx^j), \quad (\text{A.4})$$

where τ is the conformal time. The elements of the spin connection $\omega_\mu^{\alpha\beta}$ are given by

$$\omega_\mu^{\alpha\beta} = \mathbf{e}_\nu^\alpha \nabla_\mu \mathbf{e}^{\nu\beta}. \quad (\text{A.5})$$

the vierbeins are defined as

$$\mathbf{e}^\mu_\alpha = a(\tau)^{-1} \delta_\alpha^\mu, \quad (\text{A.6})$$

and the only nonzero components of the spin connection coefficients are

$$\omega_\mu^{i0} = -\omega_\mu^{0i} = -\mathcal{H} \delta_\mu^i. \quad (\text{A.7})$$

Appendix B

Whittaker Functions

Through out the thesis we have been using the following Whittaker function identities:

Considering the limit $|z| \rightarrow \infty$:

Whittaker functions $W_{\kappa,\mu}(z)$ and $M_{\kappa,\mu}(z)$ take the following asymptotic forms

$$\begin{aligned} W_{\kappa,\mu}(z) &\rightarrow z^\kappa e^{-z/2}, \\ M_{\kappa,\mu}(z) &\rightarrow \Gamma(2\mu + 1) \left(\frac{i(-1)^{\mu-\kappa} z^\kappa e^{-z/2}}{\Gamma(-\kappa + \mu + \frac{1}{2})} + \frac{z^{-\kappa} e^{z/2}}{\Gamma(-\kappa + \mu + \frac{1}{2})} \right), \end{aligned} \quad (\text{B.1})$$

where $|\arg z| < \frac{3}{2}\pi$.

In case κ is complex, we have

$$\lim_{\tau \rightarrow -\infty} \frac{(2\tilde{\tau})^{-\kappa_{\text{R}}}}{\sqrt{2k}} e^{-\kappa_{\text{I}}\pi/2} W_{\kappa,\mu}(-2i\tilde{\tau}) = \frac{1}{\sqrt{2k}} e^{-ik\tau}, \quad (\text{B.2})$$

where κ_{R} and κ_{I} are the real and imaginary parts of κ .

Hence, the positive frequency solutions in the asymptotic past or the so called Bunch-Davies vacuum is defined as

$$\frac{(2\tilde{\tau})^{-\kappa_{\text{R}}}}{(2\pi)^{3/2}\sqrt{2k}} e^{-\kappa_{\text{I}}\pi/2} W_{\kappa,\mu}(-2i\tilde{\tau}). \quad (\text{B.3})$$

Bibliography

- [1] A. H. Guth, *The Inflationary Universe: A Possible Solution to the Horizon and Flatness Problems*, *Phys. Rev.* **D23** (1981) 347.
- [2] K. Sato, *First Order Phase Transition of a Vacuum and Expansion of the Universe*, *Mon. Not. Roy. Astron. Soc.* **195** (1981) 467.
- [3] A. D. Linde, *A New Inflationary Universe Scenario: A Possible Solution of the Horizon, Flatness, Homogeneity, Isotropy and Primordial Monopole Problems*, *Phys. Lett.* **108B** (1982) 389.
- [4] A. Starobinsky, *A new type of isotropic cosmological models without singularity*, *Physics Letters B* **91** (1980) 99 .
- [5] V. F. Mukhanov and G. V. Chibisov, *Quantum Fluctuations and a Nonsingular Universe*, *JETP Lett.* **33** (1981) 532.
- [6] S. Hawking, *The Development of Irregularities in a Single Bubble Inflationary Universe*, *Phys. Lett. B* **115** (1982) 295.
- [7] A. H. Guth and S. Pi, *Fluctuations in the New Inflationary Universe*, *Phys. Rev. Lett.* **49** (1982) 1110.
- [8] A. A. Starobinsky, *Dynamics of Phase Transition in the New Inflationary Universe Scenario and Generation of Perturbations*, *Phys. Lett. B* **117** (1982) 175.
- [9] L. Grishchuk, *Amplification of gravitational waves in an isotropic universe*, *Sov. Phys. JETP* **40** (1975) 409.
- [10] A. A. Starobinsky, *Spectrum of relict gravitational radiation and the early state of the universe*, *JETP Lett.* **30** (1979) 682.
- [11] J. M. Bardeen, *Gauge-invariant cosmological perturbations*, *Phys. Rev. D* **22** (1980) 1882.
- [12] V. Mukhanov, H. Feldman and R. Brandenberger, *Theory of cosmological perturbations*, *Physics Reports* **215** (1992) 203 .

- [13] V. Mukhanov, *Physical Foundations of Cosmology*. Cambridge University Press, Oxford, 2005.
- [14] D. Baumann, *Primordial Cosmology*, *PoS TASI2017* (2018) 009 [1807.03098].
- [15] K. D. Lozanov, *Lectures on Reheating after Inflation*, 1907.04402.
- [16] S. Weinberg, *Cosmology*. 2008.
- [17] R. L. Arnowitt, S. Deser and C. W. Misner, *The Dynamics of general relativity*, *Gen. Rel. Grav.* **40** (2008) 1997 [gr-qc/0405109].
- [18] PLANCK collaboration, *Planck 2018 results. VI. Cosmological parameters*, 1807.06209.
- [19] PLANCK collaboration, *Planck 2018 results. IX. Constraints on primordial non-Gaussianity*, 1905.05697.
- [20] D. H. Lyth, *What would we learn by detecting a gravitational wave signal in the cosmic microwave background anisotropy?*, *Phys. Rev. Lett.* **78** (1997) 1861 [hep-ph/9606387].
- [21] BICEP2, KECK ARRAY collaboration, *BICEP2 / Keck Array x: Constraints on Primordial Gravitational Waves using Planck, WMAP, and New BICEP2/Keck Observations through the 2015 Season*, *Phys. Rev. Lett.* **121** (2018) 221301 [1810.05216].
- [22] J. L. Cook and L. Sorbo, *Particle production during inflation and gravitational waves detectable by ground-based interferometers*, *Phys. Rev. D* **85** (2012) 023534 [1109.0022].
- [23] D. Carney, W. Fischler, E. D. Kovetz, D. Lorzshbough and S. Paban, *Rapid field excursions and the inflationary tensor spectrum*, *JHEP* **11** (2012) 042 [1209.3848].
- [24] M. Biagetti, M. Fasiello and A. Riotto, *Enhancing Inflationary Tensor Modes through Spectator Fields*, *Phys. Rev. D* **88** (2013) 103518 [1305.7241].
- [25] L. Senatore, E. Silverstein and M. Zaldarriaga, *New Sources of Gravitational Waves during Inflation*, *JCAP* **08** (2014) 016 [1109.0542].
- [26] D. Green, B. Horn, L. Senatore and E. Silverstein, *Trapped Inflation*, *Phys. Rev. D* **80** (2009) 063533 [0902.1006].
- [27] S. Mukohyama, R. Namba, M. Peloso and G. Shiu, *Blue Tensor Spectrum from Particle Production during Inflation*, *JCAP* **08** (2014) 036 [1405.0346].
- [28] A. Maleknejad and M. M. Sheikh-Jabbari, *Gauge-flation: Inflation From Non-Abelian Gauge Fields*, *Phys. Lett.* **B723** (2013) 224 [1102.1513].

- [29] A. Maleknejad and M. M. Sheikh-Jabbari, *Non-Abelian Gauge Field Inflation*, *Phys. Rev.* **D84** (2011) 043515 [1102.1932].
- [30] P. Adshead and M. Wyman, *Chromo-Natural Inflation: Natural inflation on a steep potential with classical non-Abelian gauge fields*, *Phys. Rev. Lett.* **108** (2012) 261302 [1202.2366].
- [31] P. Adshead, E. Martinec and M. Wyman, *Perturbations in Chromo-Natural Inflation*, *JHEP* **09** (2013) 087 [1305.2930].
- [32] A. Maleknejad, M. M. Sheikh-Jabbari and J. Soda, *Gauge Fields and Inflation*, *Phys. Rept.* **528** (2013) 161 [1212.2921].
- [33] P. Adshead, E. Martinec and M. Wyman, *Gauge fields and inflation: Chiral gravitational waves, fluctuations, and the Lyth bound*, *Phys. Rev.* **D88** (2013) 021302 [1301.2598].
- [34] E. Dimastrogiovanni and M. Peloso, *Stability analysis of chromo-natural inflation and possible evasion of Lyth's bound*, *Phys. Rev.* **D87** (2013) 103501 [1212.5184].
- [35] A. Maleknejad, *Axion Inflation with an $SU(2)$ Gauge Field: Detectable Chiral Gravity Waves*, *JHEP* **07** (2016) 104 [1604.03327].
- [36] A. Agrawal, T. Fujita and E. Komatsu, *Large tensor non-Gaussianity from axion-gauge field dynamics*, *Phys. Rev.* **D97** (2018) 103526 [1707.03023].
- [37] A. Agrawal, T. Fujita and E. Komatsu, *Tensor Non-Gaussianity from Axion-Gauge-Fields Dynamics : Parameter Search*, *JCAP* **1806** (2018) 027 [1802.09284].
- [38] T. Fujita, R. Namba and I. Obata, *Mixed Non-Gaussianity from Axion-Gauge Field Dynamics*, *JCAP* **1904** (2019) 044 [1811.12371].
- [39] E. Dimastrogiovanni, M. Fasiello, R. J. Hardwick, H. Assadullahi, K. Koyama and D. Wands, *Non-Gaussianity from Axion-Gauge Fields Interactions during Inflation*, *JCAP* **1811** (2018) 029 [1806.05474].
- [40] S. H.-S. Alexander, M. E. Peskin and M. M. Sheikh-Jabbari, *Leptogenesis from gravity waves in models of inflation*, *Phys. Rev. Lett.* **96** (2006) 081301 [hep-th/0403069].
- [41] A. Maleknejad, *Gravitational leptogenesis in axion inflation with $SU(2)$ gauge field*, *JCAP* **1612** (2016) 027 [1604.06520].
- [42] P. Adshead, A. J. Long and E. I. Sfakianakis, *Gravitational Leptogenesis, Reheating, and Models of Neutrino Mass*, *Phys. Rev.* **D97** (2018) 043511 [1711.04800].

- [43] R. R. Caldwell and C. Devulder, *Axion Gauge Field Inflation and Gravitational Leptogenesis: A Lower Bound on B Modes from the Matter-Antimatter Asymmetry of the Universe*, *Phys. Rev.* **D97** (2018) 023532 [1706.03765].
- [44] A. Papageorgiou and M. Peloso, *Gravitational leptogenesis in Natural Inflation*, *JCAP* **1712** (2017) 007 [1708.08007].
- [45] P. Adshead, J. T. Giblin and Z. J. Weiner, *Gravitational waves from gauge preheating*, *Phys. Rev.* **D98** (2018) 043525 [1805.04550].
- [46] A. Maleknejad, M. Noorbala and M. M. Sheikh-Jabbari, *Leptogenesis in inflationary models with non-Abelian gauge fields*, *Gen. Rel. Grav.* **50** (2018) 110 [1208.2807].
- [47] A. Maleknejad, *Chiral Gravity Waves and Leptogenesis in Inflationary Models with non-Abelian Gauge Fields*, *Phys. Rev.* **D90** (2014) 023542 [1401.7628].
- [48] T. Matsumura, Y. Akiba, J. Borrill, Y. Chinone, M. Dobbs, H. Fuke et al., *Mission Design of LiteBIRD*, *Journal of Low Temperature Physics* **176** (2014) 733.
- [49] M. Hazumi et al., *LiteBIRD: A Satellite for the Studies of B-Mode Polarization and Inflation from Cosmic Background Radiation Detection*, *Journal of Low Temperature Physics* **194** (2019) 443.
- [50] CMB-S4 collaboration, *CMB-S4 Science Book, First Edition*, 1610.02743.
- [51] B. Thorne, T. Fujita, M. Hazumi, N. Katayama, E. Komatsu and M. Shiraishi, *Finding the chiral gravitational wave background of an axion-SU(2) inflationary model using CMB observations and laser interferometers*, *Phys. Rev.* **D97** (2018) 043506 [1707.03240].
- [52] S. Shandera et al., *Probing the origin of our Universe through cosmic microwave background constraints on gravitational waves*, *Bull. Am. Astron. Soc.* **51** (2019) 338 [1903.04700].
- [53] P. Campeti, E. Komatsu, D. Poletti and C. Baccigalupi, *Measuring the spectrum of primordial gravitational waves with CMB, PTA and Laser Interferometers*, 2007.04241.
- [54] K. D. Lozanov, A. Maleknejad and E. Komatsu, *Schwinger Effect by an SU(2) Gauge Field during Inflation*, *JHEP* **02** (2019) 041 [1805.09318].
- [55] A. Maleknejad and E. Komatsu, *Production and Backreaction of Spin-2 Particles of SU(2) Gauge Field during Inflation*, *JHEP* **05** (2019) 174 [1808.09076].
- [56] L. Mirzaghali, A. Maleknejad and K. D. Lozanov, *Production and backreaction of fermions from axion-su(2) gauge fields during inflation*, *Phys. Rev. D* **101** (2020) 083528.

- [57] A. Maleknejad, *Dark Fermions and Spontaneous CP violation in SU(2)-axion Inflation*, *JHEP* **07** (2020) 154 [1909.11545].
- [58] V. Domcke, Y. Ema, K. Mukaida and R. Sato, *Chiral Anomaly and Schwinger Effect in Non-Abelian Gauge Theories*, *JHEP* **03** (2019) 111 [1812.08021].
- [59] A. Papageorgiou, M. Peloso and C. Unal, *Nonlinear perturbations from the coupling of the inflaton to a non-Abelian gauge field, with a focus on Chromo-Natural Inflation*, *JCAP* **1809** (2018) 030 [1806.08313].
- [60] A. Papageorgiou, M. Peloso and C. Unal, *Nonlinear perturbations from axion-gauge fields dynamics during inflation*, *JCAP* **1907** (2019) 004 [1904.01488].
- [61] I. Wolfson, A. Maleknejad and E. Komatsu, *How attractive is the isotropic attractor solution of axion-SU(2) inflation?*, 2003.01617.
- [62] A. Lue, L.-M. Wang and M. Kamionkowski, *Cosmological signature of new parity violating interactions*, *Phys. Rev. Lett.* **83** (1999) 1506 [astro-ph/9812088].
- [63] E. Witten, *Some Properties of O(32) Superstrings*, *Phys. Lett.* **149B** (1984) 351.
- [64] K. Choi, *Axions and the strong CP problem in M theory*, *Phys. Rev.* **D56** (1997) 6588 [hep-th/9706171].
- [65] K. Choi, J.-c. Hwang and K. W. Hwang, *String theoretic axion coupling and the evolution of cosmic structures*, *Phys. Rev.* **D61** (2000) 084026 [hep-ph/9907244].
- [66] E. Dimastrogiovanni, M. Fasiello and T. Fujita, *Primordial Gravitational Waves from Axion-Gauge Fields Dynamics*, *JCAP* **1701** (2017) 019 [1608.04216].
- [67] D. G. Figueroa and T. Meriniemi, *Stochastic Background of Gravitational Waves from Fermions – Theory and Applications*, *JHEP* **10** (2013) 101 [1306.6911].
- [68] K. Freese, J. A. Frieman and A. V. Olinto, *Natural inflation with pseudo - Nambu-Goldstone bosons*, *Phys. Rev. Lett.* **65** (1990) 3233.
- [69] K. Freese and W. H. Kinney, *On: Natural inflation*, *Phys. Rev. D* **70** (2004) 083512 [hep-ph/0404012].
- [70] T. Banks, M. Dine, P. J. Fox and E. Gorbatov, *On the possibility of large axion decay constants*, *JCAP* **06** (2003) 001 [hep-th/0303252].
- [71] E. Silverstein and A. Westphal, *Monodromy in the CMB: Gravity Waves and String Inflation*, *Phys. Rev. D* **78** (2008) 106003 [0803.3085].
- [72] L. McAllister, E. Silverstein and A. Westphal, *Gravity Waves and Linear Inflation from Axion Monodromy*, *Phys. Rev. D* **82** (2010) 046003 [0808.0706].

- [73] N. Kaloper and L. Sorbo, *A Natural Framework for Chaotic Inflation*, *Phys. Rev. Lett.* **102** (2009) 121301 [0811.1989].
- [74] C. Germani and A. Kehagias, *UV-Protected Inflation*, *Phys. Rev. Lett.* **106** (2011) 161302 [1012.0853].
- [75] J. Ohashi and S. Tsujikawa, *Potential-driven Galileon inflation*, *JCAP* **10** (2012) 035 [1207.4879].
- [76] D. Maity, *Kinetic Gravity Braiding and axion inflation*, *Phys. Lett. B* **720** (2013) 389 [1209.6554].
- [77] M. M. Anber and L. Sorbo, *Naturally inflating on steep potentials through electromagnetic dissipation*, *Phys. Rev. D* **81** (2010) 043534 [0908.4089].
- [78] P. Adshead and M. Wyman, *Gauge-fflation trajectories in Chromo-Natural Inflation*, *Phys. Rev. D* **86** (2012) 043530 [1203.2264].
- [79] M. Sheikh-Jabbari, *Gauge-fflation Vs Chromo-Natural Inflation*, *Phys. Lett. B* **717** (2012) 6 [1203.2265].
- [80] R. Namba, E. Dimastrogiovanni and M. Peloso, *Gauge-fflation confronted with Planck*, *JCAP* **1311** (2013) 045 [1308.1366].
- [81] M. E. Peskin and D. V. Schroeder, *An Introduction to quantum field theory*. Addison-Wesley, Reading, USA, 1995.
- [82] P. Sikivie and N. Weiss, *Classical yang-mills theory in the presence of external sources*, *Phys. Rev. D* **18** (1978) 3809.
- [83] M. Henneaux, *REMARKS ON SPACE-TIME SYMMETRIES AND NONABELIAN GAUGE FIELDS*, *J. Math. Phys.* **23** (1982) 830.
- [84] Y. Hosotani, *Exact Solution to the Einstein Yang-Mills Equation*, *Phys. Lett. B* **147** (1984) 44.
- [85] P. Moniz and J. Mourao, *Homogeneous and isotropic closed cosmologies with a gauge sector*, *Class. Quant. Grav.* **8** (1991) 1815.
- [86] P. Moniz, J. Mourao and P. Sa, *The Dynamics of a flat Friedmann-Robertson-Walker inflationary model in the presence of gauge fields*, *Class. Quant. Grav.* **10** (1993) 517.
- [87] K. Bamba, S. Nojiri and S. D. Odintsov, *Inflationary cosmology and the late-time accelerated expansion of the universe in non-minimal Yang-Mills- $F(R)$ gravity and non-minimal vector- $F(R)$ gravity*, *Phys. Rev. D* **77** (2008) 123532 [0803.3384].

- [88] E. Elizalde and A. Lopez-Revelles, *Reconstructing cosmic acceleration from modified and non-minimal gravity: The Yang-Mills case*, *Phys. Rev. D* **82** (2010) 063504 [1004.5021].
- [89] A. Maleknejad and E. Erfani, *Chromo-Natural Model in Anisotropic Background*, *JCAP* **03** (2014) 016 [1311.3361].
- [90] V. Domcke, B. Mares, F. Muia and M. Pieroni, *Emerging chromo-natural inflation*, *JCAP* **04** (2019) 034 [1807.03358].
- [91] P. Adshead, E. Martinec, E. I. Sfakianakis and M. Wyman, *Higgsed Chromo-Natural Inflation*, *JHEP* **12** (2016) 137 [1609.04025].
- [92] P. Adshead and E. I. Sfakianakis, *Higgsed Gauge-flation*, *JHEP* **08** (2017) 130 [1705.03024].
- [93] Y. Watanabe and E. Komatsu, *Gravitational Wave from Axion-SU(2) Gauge Fields: Effective Field Theory for Kinetically Driven Inflation*, 2004.04350.
- [94] L. Sorbo, *Parity violation in the Cosmic Microwave Background from a pseudoscalar inflaton*, *JCAP* **06** (2011) 003 [1101.1525].
- [95] M. M. Anber and L. Sorbo, *Non-Gaussianities and chiral gravitational waves in natural steep inflation*, *Phys. Rev. D* **85** (2012) 123537 [1203.5849].
- [96] N. Barnaby and M. Peloso, *Large Nongaussianity in Axion Inflation*, *Phys. Rev. Lett.* **106** (2011) 181301 [1011.1500].
- [97] N. Barnaby, J. Moxon, R. Namba, M. Peloso, G. Shiu and P. Zhou, *Gravity waves and non-Gaussian features from particle production in a sector gravitationally coupled to the inflaton*, *Phys. Rev. D* **86** (2012) 103508 [1206.6117].
- [98] M. Peloso, L. Sorbo and C. Unal, *Rolling axions during inflation: perturbativity and signatures*, *JCAP* **09** (2016) 001 [1606.00459].
- [99] A. H. Chamseddine and V. Mukhanov, *Mimetic Dark Matter*, *JHEP* **1311** (2013) 135 [1308.5410].
- [100] L. Sebastiani, S. Vagnozzi and R. Myrzakulov, *Mimetic gravity: a review of recent developments and applications to cosmology and astrophysics*, *Adv. High Energy Phys.* **2017** (2017) 3156915 [1612.08661].
- [101] A. Golovnev, *On the recently proposed Mimetic Dark Matter*, *Phys.Lett.* **B728** (2014) 39 [1310.2790].
- [102] A. Barvinsky, *Dark matter as a ghost free conformal extension of Einstein theory*, *JCAP* **01** (2014) 014 [1311.3111].

- [103] A. H. Chamseddine, V. Mukhanov and A. Vikman, *Cosmology with Mimetic Matter*, *JCAP* **1406** (2014) 017 [1403.3961].
- [104] L. Mirzaghali and A. Vikman, *Imperfect Dark Matter*, *JCAP* **06** (2015) 028 [1412.7136].
- [105] F. Capela and S. Ramazanov, *Modified Dust and the Small Scale Crisis in CDM*, *JCAP* **04** (2015) 051 [1412.2051].
- [106] M. A. Gorji, S. Mukohyama, H. Firouzjahi and S. A. Hosseini Mansoori, *Gauge Field Mimetic Cosmology*, *JCAP* **1808** (2018) 047 [1807.06335].
- [107] M. A. Gorji, S. Mukohyama and H. Firouzjahi, *Cosmology in Mimetic $SU(2)$ Gauge Theory*, *JCAP* **1905** (2019) 019 [1903.04845].
- [108] K. Hammer, P. Jirousek and A. Vikman, *Axionic cosmological constant*, 2001.03169.
- [109] A. Agrawal, *Non Gaussianity of primordial gravitational waves and cosmic density and velocity fields*, Ph.D. thesis, Munich U., 6, 2018.
- [110] M. Kamionkowski and E. D. Kovetz, *The Quest for B Modes from Inflationary Gravitational Waves*, *Ann. Rev. Astron. Astrophys.* **54** (2016) 227 [1510.06042].
- [111] S. Saito, K. Ichiki and A. Taruya, *Probing polarization states of primordial gravitational waves with CMB anisotropies*, *JCAP* **0709** (2007) 002 [0705.3701].
- [112] R. Namba, M. Peloso, M. Shiraishi, L. Sorbo and C. Unal, *Scale-dependent gravitational waves from a rolling axion*, *JCAP* **01** (2016) 041 [1509.07521].
- [113] V. Gluscevic and M. Kamionkowski, *Testing parity-violating mechanisms with cosmic microwave background experiments*, *Phys. Rev. D* **81** (2010) 123529.
- [114] M. Gerbino, A. Gruppuso, P. Natoli, M. Shiraishi and A. Melchiorri, *Testing chirality of primordial gravitational waves with Planck and future CMB data: no hope from angular power spectra*, *JCAP* **07** (2016) 044 [1605.09357].
- [115] J. M. Maldacena, *Non-Gaussian features of primordial fluctuations in single field inflationary models*, *JHEP* **05** (2003) 013 [astro-ph/0210603].
- [116] J. M. Maldacena and G. L. Pimentel, *On graviton non-Gaussianities during inflation*, *JHEP* **09** (2011) 045 [1104.2846].
- [117] A. Sakharov, *Violation of CP Invariance, C asymmetry, and baryon asymmetry of the universe*, *Sov. Phys. Usp.* **34** (1991) 392.
- [118] L. Alvarez-Gaum and E. Witten, *Gravitational anomalies*, *Nuclear Physics B* **234** (1984) 269 .

- [119] L. Mirzaghali, E. Komatsu, K. D. Lozanov and Y. Watanabe, *Effects of Gravitational Chern-Simons during Axion-SU(2) Inflation*, *JCAP* **06** (2020) 024 [2003.05931].
- [120] R. Jackiw and S. Y. Pi, *Chern-Simons modification of general relativity*, *Phys. Rev.* **D68** (2003) 104012 [gr-qc/0308071].
- [121] S. Alexander and J. Martin, *Birefringent gravitational waves and the consistency check of inflation*, *Phys. Rev.* **D71** (2005) 063526 [hep-th/0410230].
- [122] D. H. Lyth, C. Quimbay and Y. Rodriguez, *Leptogenesis and tensor polarisation from a gravitational Chern-Simons term*, *JHEP* **03** (2005) 016 [hep-th/0501153].
- [123] M. Satoh, S. Kanno and J. Soda, *Circular Polarization of Primordial Gravitational Waves in String-inspired Inflationary Cosmology*, *Phys. Rev.* **D77** (2008) 023526 [0706.3585].
- [124] W. Fischler and S. Paban, *Leptogenesis from Pseudo-Scalar Driven Inflation*, *JHEP* **10** (2007) 066 [0708.3828].
- [125] S. Alexander and N. Yunes, *Chern-Simons Modified General Relativity*, *Phys. Rept.* **480** (2009) 1 [0907.2562].
- [126] S. Dyda, E. E. Flanagan and M. Kamionkowski, *Vacuum Instability in Chern-Simons Gravity*, *Phys. Rev.* **D86** (2012) 124031 [1208.4871].
- [127] N. Bartolo and G. Orlando, *Parity breaking signatures from a Chern-Simons coupling during inflation: the case of non-Gaussian gravitational waves*, *JCAP* **1707** (2017) 034 [1706.04627].
- [128] N. Bartolo, G. Orlando and M. Shiraishi, *Measuring chiral gravitational waves in Chern-Simons gravity with CMB bispectra*, *JCAP* **1901** (2019) 050 [1809.11170].
- [129] K. Kamada, J. Kume, Y. Yamada and J. Yokoyama, *Gravitational leptogenesis with kination and gravitational reheating*, *JCAP* **2001** (2020) 016 [1911.02657].
- [130] J. Qiao, T. Zhu, W. Zhao and A. Wang, *Polarized primordial gravitational waves in the ghost-free parity-violating gravity*, *Phys. Rev.* **D101** (2020) 043528 [1911.01580].
- [131] S. Basilakos, N. E. Mavromatos and J. Sol Peracaula, *Do we Come from a Quantum Anomaly?*, *Int. J. Mod. Phys.* **D28** (2019) 1944002 [1905.04685].
- [132] S. Basilakos, N. E. Mavromatos and J. Sol Peracaula, *Quantum Anomalies, Running Vacuum and Leptogenesis: an Interplay*, *PoS CORFU2018* (2019) 044 [1905.05685].

- [133] S. Basilakos, N. E. Mavromatos and J. Sol Peracaula, *Gravitational and Chiral Anomalies in the Running Vacuum Universe and Matter-Antimatter Asymmetry*, *Phys. Rev.* **D101** (2020) 045001 [1907.04890].
- [134] S. Basilakos, N. E. Mavromatos and J. Sol Peracaula, *Quantum Anomalies in String-Inspired Running Vacuum Universe: Inflation and Axion Dark Matter*, *Phys. Lett.* **B803** (2020) 135342 [2001.03465].
- [135] T. Hayashinaka, T. Fujita and J. Yokoyama, *Fermionic Schwinger effect and induced current in de Sitter space*, *JCAP* **1607** (2016) 010 [1603.04165].
- [136] P. Adshead and E. I. Sfakianakis, *Fermion production during and after axion inflation*, *JCAP* **1511** (2015) 021 [1508.00891].
- [137] P. Adshead, L. Pearce, M. Peloso, M. A. Roberts and L. Sorbo, *Phenomenology of fermion production during axion inflation*, *JCAP* **1806** (2018) 020 [1803.04501].
- [138] V. Domcke and K. Mukaida, *Gauge Field and Fermion Production during Axion Inflation*, *JCAP* **11** (2018) 020 [1806.08769].
- [139] M. B. Frob, J. Garriga, S. Kanno, M. Sasaki, J. Soda, T. Tanaka et al., *Schwinger effect in de Sitter space*, *JCAP* **1404** (2014) 009 [1401.4137].
- [140] T. Kobayashi and N. Afshordi, *Schwinger Effect in 4D de Sitter Space and Constraints on Magnetogenesis in the Early Universe*, *JHEP* **10** (2014) 166 [1408.4141].
- [141] R. Sharma and S. Singh, *Multifaceted Schwinger effect in de Sitter space*, *Phys. Rev.* **D96** (2017) 025012 [1704.05076].
- [142] H. Kitamoto, *Schwinger Effect in Inflaton-Driven Electric Field*, *Phys. Rev.* **D98** (2018) 103512 [1807.03753].
- [143] S. Shakeri, M. A. Gorji and H. Firouzjahi, *Schwinger Mechanism During Inflation*, *Phys. Rev. D* **99** (2019) 103525 [1903.05310].
- [144] S. Weinberg, *The quantum theory of fields. Vol. 2: Modern applications*. Cambridge University Press, 2013.
- [145] L. Parker and D. Toms, *Quantum Field Theory in Curved Spacetime: Quantized Fields and Gravity*, Cambridge Monographs on Mathematical Physics. Cambridge University Press, 2009.

Acknowledgement

First, I would like to say thanks to my supervisor Eiichiro Komatsu for all he has done for me during these years, for taking me as a refugee, his support and scientific guidance and above all for providing a very fun group and work environment. I continue to be grateful to Stefan Hofmann who introduced me to Eiichiro in the first place.

I am very grateful to Kaloian Lozanov, who is essentially my second supervisor. He thought me so much! I would like to thank him for his patience, letting me pick his brain on a daily basis and above all, all the fun we had during the last three years working together. I would like to thank my collaborator Yuki Watanabe, although he was only visiting for one year I learned a lot from him and really enjoyed discussing with him.

I would like to thank Elisa Ferreira, Laura Herold, Marta Monelli for their super helpful comments on the thesis and Fabian Schmidt for his help with this dissertation. I benefited a lot from discussing with him especially for the discussions during the book club. I would like to thank everyone in the the physical cosmology group at MPA for all the fun discussions at the Friday journal club and all the group dinners and events. I also would like to thank Sonja, Maria and Gabi. They really make life easier for everyone working at MPA.

I am very grateful to my friends whom I met at MPA and LMU through out these years, many many thanks to Elisa and Linda for their crucial wisdom, special thanks to Patrick, Mariana, Aoife, Alex, Kalo, Titouan, Aniket, Fuzzy, Giovanni, Marc and Chris for all the great discussions and fun times. Very special thanks to Mauro and Nanni for all their warmth, support and fun times in Munich and cheering me on through the writing process.

I would like to thank Ophelia and Bahador for providing me with a place to work during the pandemic at the Crowd Cognition and CVBE Lab and all the fun discussions.

I am also grateful to my long-distance friends Shima, Samira, Ghazaleh, Mehran, Hadi, Soheila and Negar for all their support and fun times.

There are not enough words in the world to adequately express my gratitude and love towards my family. Special thanks to my mamani, she was the best grandmother I could ever ask for. Deepest gratitude to my mother Kobra and my father Farhad who introduced me to science, read to me everyday during my childhood and their great warmth and support. Hugest appreciation and love to my sister Mina who has always been there for me, the quality of my life really changed after she moved to Germany. Finally, unending thanks and love to my *sine quo non*, Amir Ahmad.